ATTACHMENT 2

WCAP-16636-NP, "Structural Integrity Evaluation of Reactor Vessel Upper Head Penetrations to Support Continued Operation: South Texas Units 1 & 2 (Non-Proprietary)

WCAP-16636-NP
Revision 0

September 2006

Structural Integrity Evaluation of Reactor Vessel Upper Head Penetrations to Support Continued Operation: South Texas Units 1 & 2

Westinghouse

WCAP-16636-NP
Revision 0

Structural Integrity Evaluation of Reactor Vessel Upper Head Penetrations to Support Continued Operation: South Texas Units 1 & 2

B.A. Leber*

September 2006

Verifier: C. K. Ng*
A. Udyawar*
Piping Analysis & Fracture Mechanics

Approved: S. A. Swamy*
Manager, Piping Analysis & Fracture Mechanics

Electronically approved records are authenticated in the Electronic Document Management System.

TABLE OF CONTENTS

LIST OF TABLES

LIST OF FIGURES

1   INTRODUCTION

In September of 1991, a leak was discovered in the Reactor Vessel Control Rod Drive Mechanism (CRDM) head penetration region of an operating plant. This has led to the question of whether such a leak could occur at the CRDM, head vent, or gas vent nozzle penetrations of South Texas Units 1 & 2 (STP). It shall be noted that the term "CRDM" is used generically in this report for any of the reactor vessel upper head penetrations which includes the control rod mechanism, instrumentation penetrations, and spare penetrations as applicable. The typical geometry of interest for a CRDM penetration nozzle is shown in Figure 1-1. Throughout this report, the penetration rows have been identified by their angle of intersection with the head. The locations of the head penetrations for STP are shown in Figure 1-2 [1A] and the angles of intersection for each penetration are identified in Table 1-1 [1B, 1C].

The CRDM leak resulted from cracking in Alloy 600 base metal, which occurred in the penetrations of a number of operating plants as discussed in Section 2. The outermost CRDM location, as well as a number of intermediate CRDM locations, head vent, and the gas vent nozzles were chosen for fracture mechanics analyses to support continued safe operation of STP if such cracking were to be found. It should be noted that the internal support housing nozzles (Penetration No. 74, 80 & 81) were not made of Alloy 600 material and are not subjected to Primary Water Stress Corrosion Cracking (PWSCC), therefore analysis for these three nozzles are not included. The dimensions of all the CRDM penetrations are identical, with a 4.00 inch Outside Diameter (OD) and a wall thickness of 0.625 inches [1D]. For the head vent, the OD is 1.315 inches and the wall thickness is 0.250 inches [1E]. For the gas vent, the OD is 3.490 inches and the wall thickness is 0.433 inches [1E]. All of these dimensions are summarized in Table 6-2.

The basis of the analysis was a detailed three-dimensional elastic-plastic finite element stress analysis of several penetration locations, as described in detail in Section 5, and a fracture analysis, as described in Section 6. The fracture analysis was carried out using crack growth rates recommended by the EPRI (Electric Power Research Institute) Materials Reliability Program (MRP)[8]. These rates are consistent with service experience. The results are presented in the form of flaw tolerance charts. If indications are found, the charts can then be used to determine the allowable service life of safe operation. The service life calculated in the flaw tolerance charts are all in Effective Full Power Years (EFPYs).

The objectives of this report can be summarized as follows:

- Provide technical support for continued operation of South Texas Units 1 and 2 if flaws are detected in the reactor vessel head penetration nozzles during the inspection

- Provide a simple tool for determining how long a detected flaw can remain in-service without repair

- Provide technical support to facilitate the submittal of relaxation request in the event that the inspection coverage below the J-groove weld required by the NRC order EA-03-009 cannot be met.

Note that there are several locations in this report where proprietary information has been identified and bracketed. For each of the bracketed locations, reasons for proprietary classifications are given using a standardized system. The proprietary brackets are labeled with three different letters to provide this information. The explanation for each letter is given below:

a.   The information reveals the distinguishing aspects of a process or component, structure, tool, method, etc., and the prevention of its use by Westinghouse's competitors, without license from Westinghouse, gives Westinghouse a competitive economic advantage.

c.   The information, if used by a competitor, would reduce the competitor's expenditure of resources or improve the competitor's advantage in the design, manufacture, shipment, installation, assurance of quality, or licensing of a similar product.

e.   The information reveals aspects of past, present, or future Westinghouse or customer funded development plans and programs of potential commercial value to Westinghouse.

Table 1-1 STP Head Penetration Nozzles with Intersection Angles Identified [1B, 1C]					
Nozzle No.	Angle (Degrees)	Nozzle No.	Angle (Degrees)	Nozzle No.	Angle (Degrees)
1	0.0	31	30.2	57	38.6
2	11.4	32	30.2	58	38.6
3	11.4	33	30.2	59	38.6
4	11.4	34	30.2	60	38.6
5	11.4	35	30.2	61	38.6
6	16.2	36	30.2	62	44.3
7	16.2	37	30.2	63	44.3
8	16.2	38	33.9	64	44.3
9	16.2	39	33.9	65	44.3
14	23.3	40	33.9	66	45.4
15	23.3	41	33.9	67	45.4
16	23.3	42	35.1	68	45.4
17	23.3	43	35.1	69	45.4
18	24.8	44	35.1	70	45.4
19	24.8	45	35.1	71	45.4
20	24.8	46	35.1	72	45.4
21	24.8	47	35.1	73	45.4
22	26.2	48	35.1	75	48.7
23	26.2	49	35.1	76	48.7
24	26.2	50	36.3	77	48.7
25	26.2	51	36.3	78	48.7
26	26.2	52	36.3	79	48.7
27	26.2	53	36.3		
28	26.2	54	38.6		
29	26.2	55	38.6		
30	30.2	56	38.6		

Note : The internal support housing nozzles (Penetration No. 74, 80 & 81) are not made of Alloy 600 material and are not subjected to PWSCC, therefore analysis for these three nozzles are not necessary.
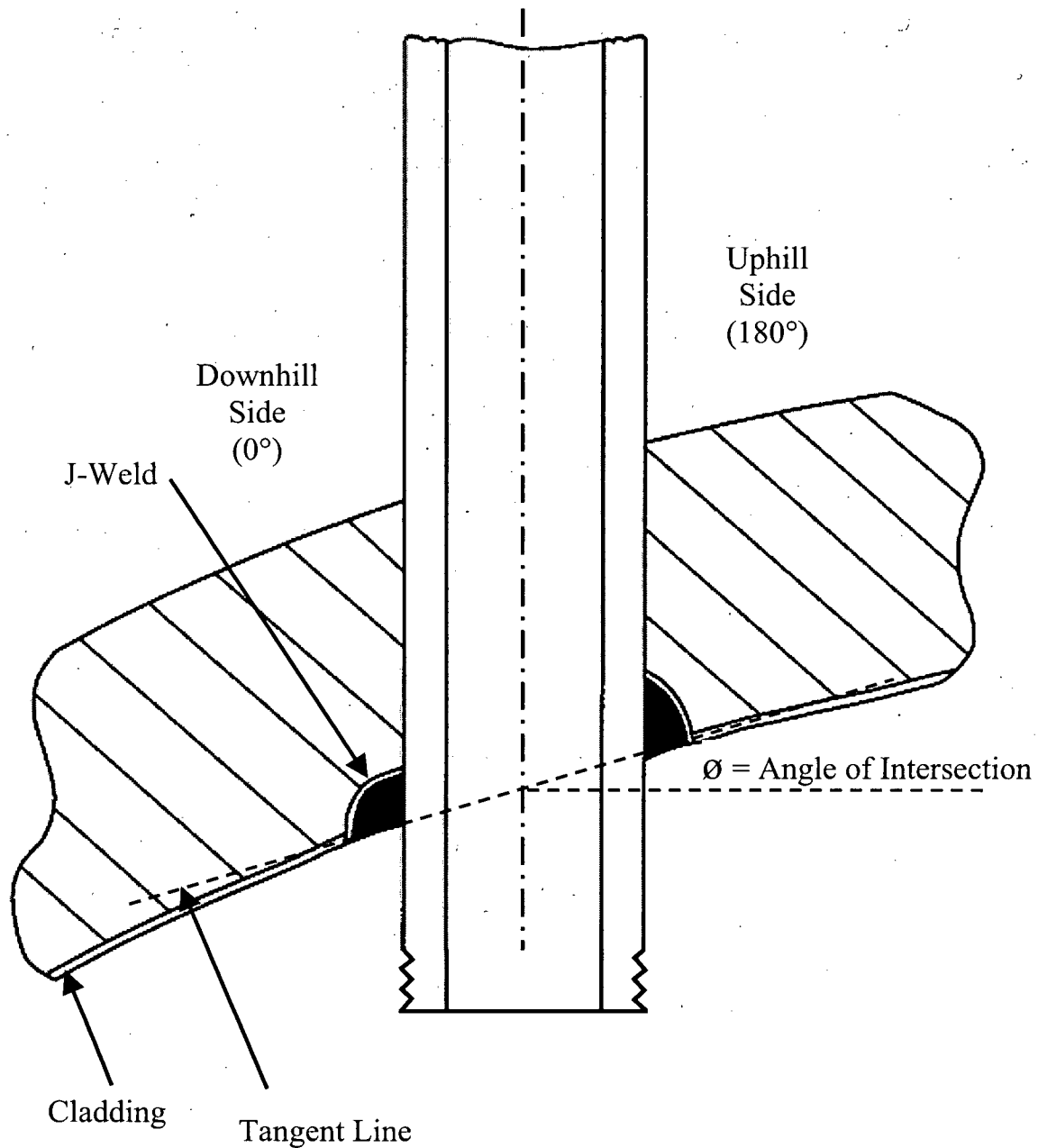
Figure 1-1 **Typical Reactor Vessel Control Rod Drive Mechanism (CRDM) Penetration**
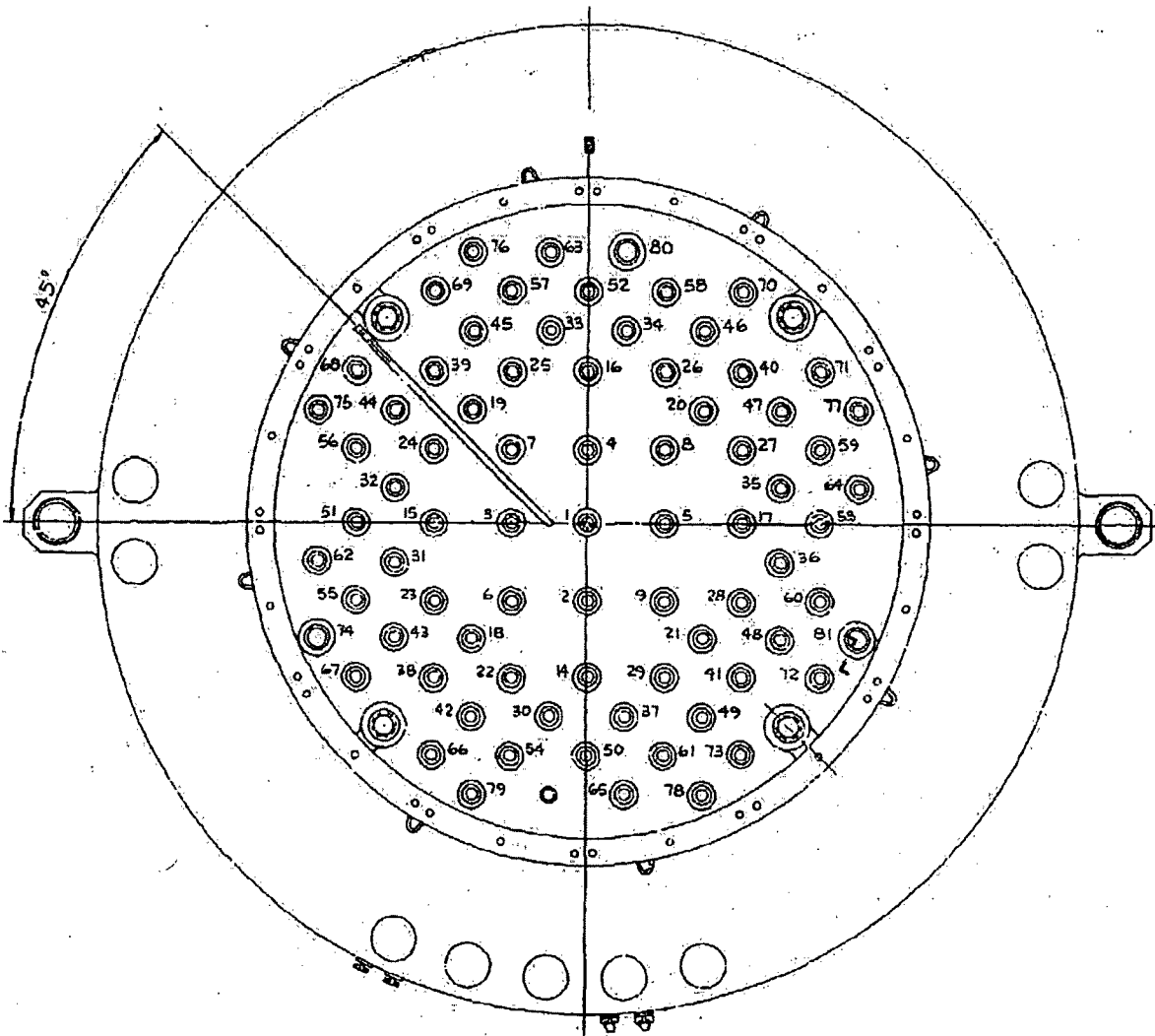
Figure 1-2   Location of Head Penetrations for STP [1A]

2   HISTORY OF CRACKING IN HEAD PENETRATIONS

In September of 1991, leakage was reported from the reactor vessel CRDM head penetration region of a French plant, Bugey Unit 3. Bugey 3 is a 920 megawatt three-loop Pressurized Water Reactor (PWR) plant which had just completed its tenth fuel cycle. The leak occurred during a post ten year hydrotest conducted at a pressure of approximately 3000 psi (204 bar) and a temperature of 194°F (90°C). The leak rate was estimated to be approximately 0.7 liter/hour. The location of the leak was subsequently established on a peripheral penetration with an active control rod (H-54), as seen in Figure 2-1.

The control rod drive mechanism and thermal sleeve were removed from this location to allow further examination. A study of the head penetration revealed the presence of longitudinal cracks near the head penetration attachment weld. Penetrant and ultrasonic testing confirmed the cracks. The cracked penetration was fabricated from Alloy 600 bar stock (SB-166), and has an outside diameter of 4 inches (10.16 cm) and an inside diameter of 2.75 inches (7.0 cm). As a result of the finding, all of the control rod drive mechanisms and thermal sleeves at Bugey 3 were removed for inspection of the head penetrations. Only two penetrations were found to have cracks, as shown in Figure 2-1.

An inspection of a sample of penetrations at three additional plants were planned and conducted during the winter of 1991-92. These plants were Bugey 4, Fessenheim 1, and Paluel 3. The three outermost rows of penetrations at each of these plants were examined, and further cracking was found in two of the three plants: At Bugey 4, eight of the 64 penetrations examined were found to contain axial cracks, while only one of the 26 penetrations examined at Fessenheim 1 was cracked. The locations of all the cracked penetrations are shown in Figure 2-1. At the time, none of the 17 CRDM penetrations inspected at Paluel 3 showed indications of cracking, however subsequent inspections of the French plants have confirmed at least one crack in each operating plant.

Thus far, the cracking in reactor vessel heads not designed by Babcock and Wilcox (B&W) has been consistent in both its location and extent. All cracks discovered by nondestructive examination have been oriented axially, and have been located in the bottom portion of the penetration in the vicinity of the partial penetration attachment weld to the vessel head as shown schematically in Figure 1-1.

One small, outside diameter initiated, circumferential flaw was found during destructive examination at Bugey 3. The flaw was found to have resulted from Primary Water Stress Corrosion Cracking (PWSCC) as a consequence of leakage of the PWR water from an axial through-wall crack into the annulus between the penetration and head.

Leaks were also discovered at seven Babcock & Wilcox designed plants:

- Oconee 1 (1 leaking nozzle)
- Oconee 2 (4 leaking nozzles)
- Oconee 3 (9 leaking nozzles)
- ANO-1 (1 leaking nozzle)

- Crystal River Unit 3 (1 leaking nozzle)
- Three Mile Island 1 (5 leaking nozzles)
- Davis-Besse (8 leaking nozzles)

In addition, five of the eight smaller diameter thermocouple nozzles at Oconee 1, and all eight at Three Mile Island 1, were discovered to have leaks. All of these leaks were first detected during visual inspections of the top surface of the vessel heads for boric acid crystal deposits. In all cases, except Davis-Besse, the quantity of boric acid crystals at each nozzle location was small (<1 in^3).

Destructive examinations of several specimens from cracked Oconee 1 and 3 nozzles showed that the leaks were the result of PWSCC. Non-destructive examinations of the leaking CRDM nozzles showed that most of the cracks were axially oriented, originating on the outside surface of the nozzles below the J-groove weld and propagating primarily in the nozzle base material to an elevation above the top of the J-groove weld. Leakage could then pass through the annulus to the top of the head where it was detected by visual inspection. In some cases the cracks initiated in the weld metal or propagated into the weld metal, and in a few cases the cracks propagated through the nozzle wall thickness to the inside surface.

In addition to the predominantly axial cracks, several nozzles had cracks on the outside surface of the nozzle approximately following the weld contour above or below the J-groove weld. At least eight of these nozzles (three in Oconee 3, one in Oconee 2, one in Crystal River 3, and three in Davis-Besse) were found to have cracks approximately following the weld contour just above the J-groove weld. Two of the nozzles had relatively short and shallow cracks. Two of these nozzles had cracks either through-wall or essentially through-wall over an arc length of about 165° around the nozzle centered approximately about the nozzle uphill side. Cracks which follow the weld contour are a greater concern than axial cracks in that they raise the potential for a nozzle to be ejected if a through-wall crack extends more than about [

]^{a,c,e}

Seventeen additional non-leaking Oconee 1 and nine non-leaking Oconee 3 CRDM nozzles were inspected by eddy current, ultrasonic testing, or eddy current and ultrasonic testing to assess the extent of the condition of non-leaking nozzles in the vessel head. No significant cracking was found in any of these additional nozzles.

The experience at Oconee, Three Mile Island, Crystal River, Davis-Besse, and ANO-1 differs from previous industry experience in that the cracking appears to initiate primarily on the outside surface of the nozzle below the weld rather than on the nozzle Inside Diameter (ID) surface. Five of the nozzles had also developed OD-initiated flaws approximately following the contour of the top of the J-groove weld. These CRDM tubes have shown no pattern of cracking, whereas the previous CRDM tubes were cracking only in the outermost three rows.

The cracking has now been confirmed to be primary water stress corrosion cracking. Relatively high residual stresses are produced in the outermost CRDM penetrations due to the welding process. Other important factors which affect this process are temperature and time, with higher temperatures and longer times being more detrimental.

All three Nuclear Steam Supply System (NSSS) Owners Groups submitted safety assessments to the USNRC between 1993 and 1994 in response to the leakage observed in Bugey Unit 3. The analyses demonstrated that CRDM nozzles are capable of accommodating long through-wall axial flaws and the resulting leakage. The analyses also demonstrated that the CRDM nozzles are capable of accommodating significant circumferential flaws above the J-groove weld. After reviewing the safety assessment submitted by the industry and examining international inspection findings, the USNRC concluded that CRDM nozzle and weld cracking observed to that time in Pressurized Water Reactor (PWR) facilities was not an immediate safety concern.

USNRC issued Generic Letter (GL) 97-01, "Degradation of Control Rod Drive Mechanism Nozzle and Other Vessel Closure Head Penetrations." on April 1, 1997. Responses to GL 97-01 were predicated on the development of susceptibility ranking models to relate the operating conditions for each plant to the plant's relative susceptibility to PWSCC. The industry committed to surface examinations (i.e., eddy current) of the vessel head penetration nozzles for plants with the highest relative susceptibility ranking.

In response to the inspection findings at Oconee in November 2000 and because existing requirements in the ASME Code and NRC regulations do not adequately address inspections of RPV head penetrations for degradation due to PWSCC, the NRC then issued Bulletin 2001-01, "Circumferential Cracking of Reactor Pressure Vessel Head Penetration Nozzles," dated August 3, 2001. In response to the bulletin, plans for inspecting the vessel head penetration nozzles and/or the outside surface of the reactor vessel head to determine whether the nozzles were leaking were provided by the industry.

On March 18, 2002, the NRC issued Bulletin 2002-01 in response to the head degradation found at Davis-Besse Nuclear Power Station, "Reactor Pressure Vessel Head Degradation and Reactor Coolant Pressure Boundary Integrity," which requested that information be provided on the reactor vessel head inspection and maintenance programs, the material condition of the reactor vessel heads, and the boric acid inspection programs.

NRC Bulletin 2002-02 "Reactor Pressure Vessel Head and Vessel Head Penetration Nozzle Inspection Programs," was issued later on August 9, 2002. This bulletin requested that information on the inspection programs and any plans to supplement existing visual inspections with additional measures (e.g., volumetric and surface examinations) be provided. The need to issue this bulletin and the associated objectives are stated clearly in the Bulletin: "As a result of the circumferential cracking of Vessel Head Penetration (VHP) nozzles at Oconee Nuclear Station 3 and other PWR facilities, the RPV head material degradation at Davis-Besse, and the staff's review of the responses to NRC Bulletins 2001-01 and 2002-01, the NRC staff has a number of concerns about the inspection requirements and programs for RPV head and VHP nozzles. Based on the experience and information currently available concerning cracking and degradation, it may be necessary for inspection programs that rely on visual examinations to be supplemented with additional measures (e.g., volumetric and surface examinations) to demonstrate compliance with applicable regulations."

On February 11, 2003, NRC issued Order EA-03-009 to establish a minimum set of RPV head inspection requirements, as a supplement to the existing inspection and other requirements in the

ASME Code and NRC regulations. The issuance of the Order was prompted by the plant inspection findings and the inadequate inspection requirements in the ASME Code and related NRC regulations. As discussed in EA-03-009, revising the ASME Code and subsequently the NRC regulations will take several years. In addition, it was stated that the resulting inspection plans and responses to the NRC bulletins have provided reasonable assurance of adequate protection of public health and safety for the near term operating cycles, but cannot be relied upon to do so for the entire interim period until NRC regulations are revised.

After the Order was issued in 2003, the first revised Order EA-03-009 was issued on February 20, 2004 to revise certain aspects of the original order in response to some of the common issues emerging from the numerous relaxation requests from the original order.
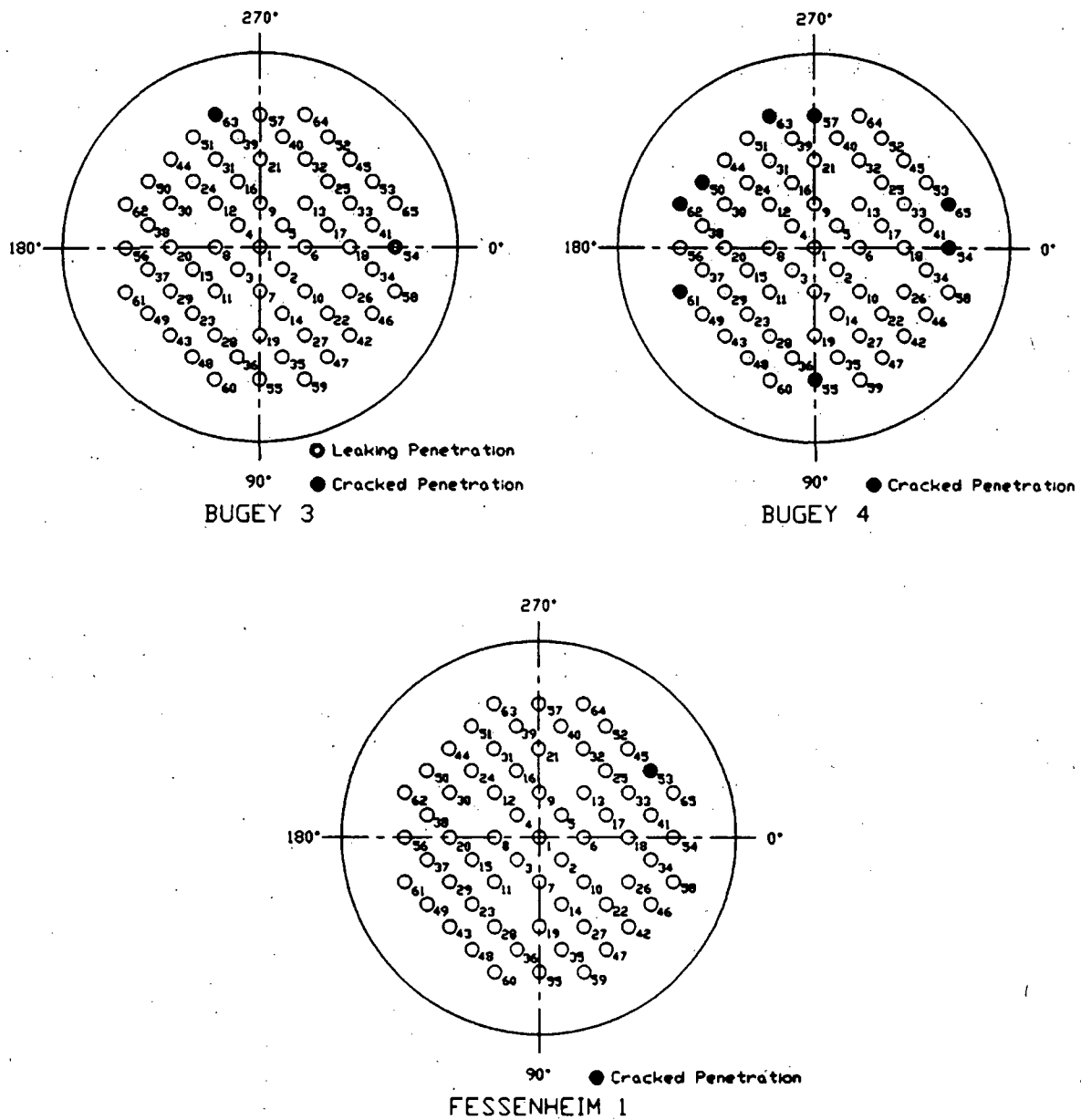
Figure 2-1   Électricité de France (EDF) Plant R/V Closure Head CRDM Penetrations

3 OVERALL TECHNICAL APPROACH

The primary objective of this work is to provide technical justification for the continued safe operation of South Texas Units 1 & 2 in the event that cracking is discovered during in-service inspections of the Alloy 600 reactor vessel upper head penetrations.

3.1 PENETRATION STRESS ANALYSIS

Three-dimensional elastic-plastic finite element stress analyses applicable to STP were performed in [3]. The results from these analyses were used to determine the stresses in the head penetration region for STP. The analyses considered the pressure loads associated with steady state operation, as well as the residual stresses that are produced by the fabrication process.

A number of rows of penetrations, including those nearest the head flange, which is the region where cracking has been discovered in other non-B&W design plants, were analyzed using the finite element analysis method. In addition, several other rows of penetrations and the center CRDM penetrations were analyzed to provide additional results, so a trend can be established as a function of radial location. The head vent and gas vent nozzles were also analyzed. The calculated stresses as well as field-measured deformation have been found to be more severe at the outermost location. The stress analysis will be used to provide input directly to the crack growth analysis.

The stress analysis provides the key input to the flaw tolerance evaluation, which is described below.

3.2 FLAW TOLERANCE APPROACH

A flaw tolerance approach has been developed to allow continued safe operation until an appropriate time for repair, or the end of plant life. The approach is based on the prediction of future growth of detected flaws, to ensure that such flaws will remain acceptable.

If an indication is discovered during in-service inspection, its size can be compared with the flaw size considered as allowable for continued service. This "allowable" flaw size is determined from the actual loading (including mechanical and residual loads) on the head penetration for STP. Acceptance criteria are discussed in Section 6.5. The time for the observed crack to reach the allowable crack size determines the length of time the plant can remain online before repair, if required. For the crack growth calculation, a best estimate is needed and no additional margins are necessary.

The results of the evaluation are presented in terms of simple flaw tolerance charts. The charts graphically show the time required to reach the allowable length or depth, which represents additional service life before repair. This result is a function of the loading on the particular head penetration as well as the circumferential location of the crack in the penetration nozzle.

Schematic drawings of the head penetration flaw tolerance charts are presented as Figure 3-1. This type of chart can be used to provide estimates of the remaining service life before a leak

would develop from an observed crack. For example, if a part-through flaw was discovered, the user would refer to Figure 3-1, to determine the allowable service life (t_P) which would be remaining before the crack would penetrate the wall or reach the allowable depth (t_a) (e.g. a/t = 0.75).
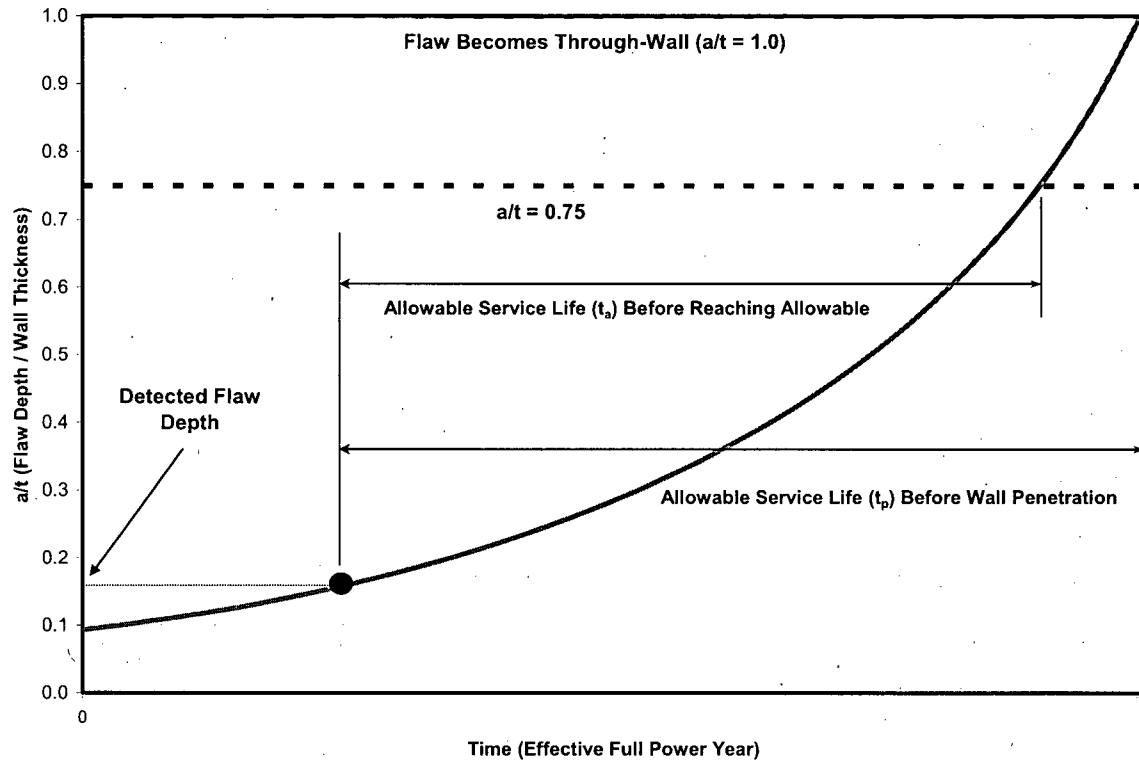
Figure 3-1   Schematic of a Head Penetration Flaw Growth Chart for Part-Through Wall Flaws

4 MATERIAL PROPERTIES, FABRICATION HISTORY AND CRACK GROWTH PREDICTION

4.1 MATERIALS AND FABRICATION

The reactor vessel head penetration nozzles for South Texas Units 1 & 2 were constructed from material supplied by Huntington Alloys USA. The carbon content and mechanical properties of the Alloy 600 material used to fabricate the STP vessel head penetration nozzles are provided in Table 4-1 [4]. The materials were annealed for 1.5 hours at a temperature of 1725°F and air cooled. Figures 4-1 and 4-2 illustrate the yield strengths and carbon content, based on percent of heats, of the head adapter penetrations in the STP vessel. The general trend for the head adapter penetrations in STP are of a higher carbon content, higher mill annealing temperature and in general lower yield strength relative to those on the French vessels. These factors should all have a beneficial effect on the material resistance to PWSCC in the head penetrations.

4.2 CRACK GROWTH PREDICTION

The cracks in the penetration region have been determined to result from primary water stress corrosion cracking in the Alloy 600 base metal and, in some cases, the Alloy 182 weld metal. There are a number of available measurements of static load crack growth rates in primary water environment, and in this section the available results will be compared and a representative growth rate will be established.

Direct measurements of Stress Corrosion Cracking (SCC) growth rates in Alloy 600 are relatively rare. Also, care should be used when interpreting the results because the materials may be excessively cold worked, or the loading applied may be near or exceeding the limit load of the penetration nozzle, meaning there will be an interaction between tearing and crack growth. In these cases the crack growth rates may not be representative of service conditions.

The effort to develop a reliable crack growth rate model for Alloy 600 began in the spring of 1992, when the Westinghouse Owners Group began to develop a safety case to support continued operation of plants. At the time, there was no available crack growth rate data for head penetration materials, and only a few publications existed on growth rates of Alloy 600 in any product form.

The best available publication at that time was that of Peter Scott of Framatome, who had developed a growth rate model for PWR steam generator materials [5]. His model was based on a study of results obtained by McIlree, Rebak and Smialowska [6] who had tested short steam generator tubes which had been flattened into thin compact specimens.

An equation was fitted to the data of reference [6] for the results obtained in water chemistries that fell within the standard specification for PWR primary water. Results for chemistries outside the specification were not used. The following equation was fitted to the data at 330°C (626°F):

$$\frac{da}{dt} = 2.8 \times 10^{-11} (K - 9)^{1.16} \, m/sec \qquad (4-1)$$

where:

K is in MPa$\sqrt{m}$

The next step was to correct these results for the effects of cold work. Based on work by Cassagne and Gelpi [7], Scott concluded that dividing the above equation by a factor of 10 would be appropriate for material that has not been cold-worked. The crack growth law for 330°C (626°F) then becomes:

$$\frac{da}{dt} = 2.8 \times 10^{-12} (K - 9)^{1.16} \, m/sec \qquad (4-2)$$

Scott further corrected this law for the effects of temperature. This forms the basis for the PWR Materials Reliability Program (MRP) recommended Crack Growth Rate (CGR) curve for the evaluation of SCC where a power-law dependence on stress intensity factor was assumed [8]. The MRP-recommended CGR curve was used in this report for determining the primary water stress corrosion crack growth rate and a brief discussion on this recommended curve is as follows:

The EPRI-MRP crack growth review team, an international panel of experts in the area of SCC crack growth, provided input to the MRP in its development of the recommended CGR curve. This group met to review the available worldwide data on October 2-4, 2001, in Airlie, Virginia. The PWR MRP has developed a recommended CGR curve for PWSCC of Alloy 600 materials.

[

]^{a,c,e}

The MRP is continuing its review of the available data regarding SCC crack growth in Alloy 600 components exposed to the primary water environment, and revised recommendations will be provided to the industry in the future as warranted.

There is a general agreement that crack growth in Alloy 600 materials in the primary water environment can be modeled using a power-law dependence on stress intensity factor with differences in temperature accounted for by an activation energy (Arrhenius) model for thermally controlled processes. Figure 4-3 shows the recommended CGR curve along with the laboratory data from Huntington materials used to develop the curve.

[

]^{a,c,e}

[

]]ᵃ,ᶜ,ᵉ

The MRP crack growth curve was structured to bound 75 percent of the 26 heats for which test results were available. Fits were done on the results for each heat, and the constant term was determined for each heat. This was done to eliminate the concern that the curve might be biased from a large number of results from a single heat. The 75th percentile was then determined from these results. The MRP expert panel on crack growth endorsed the resulting curve unanimously in a meeting on March 6th and 7th, 2002. This approach is consistent with the ASME Section XI flaw evaluation philosophy, which is to make a best estimate prediction of future growth of a flaw. Margins are incorporated in the allowable flaw sizes. The entire data set is shown in Figure 4-3, where the data have been adjusted to a single temperature of 325°C.

The applicability of the MRP recommended model to head penetrations was confirmed by two independent approaches. The first was a collection of all available data from Standard Steel and Huntington Alloys materials tested over the past ten years [8]. The results are shown in Figure 4-3, along with the Scott model for the test temperature.

A second independent set of data were used to validate the model, and these data were obtained from the two inspections carried out on penetration no. 75 of D. C. Cook Unit 2, which was first found to be cracked in 1994 [20]. The plant operated for one fuel cycle before the penetration was repaired in 1996 and the flaw was measured again before being repaired. These results were used to estimate the PWSCC growth rate for both the length of the flaw and its depth. These two points are also shown in Figure 4-4, and are consistent with the laboratory data for Huntington materials. In fact, Figure 4-4 demonstrates that the MRP model is nearly an upper bound for these materials. The D. C. Cook Unit 2 penetrations were made from Huntington materials.

The operating head temperature for South Texas Units 1 & 2 is 297°C (567°F) [21]. A temperature adjustment on the crack growth rate is necessary since the crack growth rate is strongly affected by the temperature. The temperature correction was obtained from study of both laboratory and field data for stress corrosion crack growth rates for Alloy 600 in primary water environments. The available data showing the effect of temperature are summarized in Figure 4-5. Most of the results shown here are from steam generator tube materials, with several sets of data from operating plants, and results from two heats of materials tested in a laboratory [9].

Study of the data shown in Figure 4-5 results in an activation energy of 31-33 kcal/mole, which can then be used to adjust for the lower operating temperature. This value is slightly lower than the generally accepted activation energy of 44-50 kcal/mole used to characterize the effect of temperature on crack initiation, but the trend of the actual data from many different sources is unmistakable.

[

$]^{a,c,e}$ Therefore, the following crack growth rate model was used in the crack growth calculation for STP head penetrations.

$$\frac{da}{dt} = 7.489 \times 10^{-13} \, (K - 9)^{1.16} \text{ m/sec}$$

where:

K = applied stress intensity factor, in $MPa\sqrt{m}$

This equation implies a threshold for cracking susceptibility, $K_{ISCC} = 9 \, MPa\sqrt{m}$. The crack growth rate is applicable to propagation in both axial and circumferential directions.

Table 4-1   STP Reactor Vessel Head Adapter Material Information [4]

a,c,e
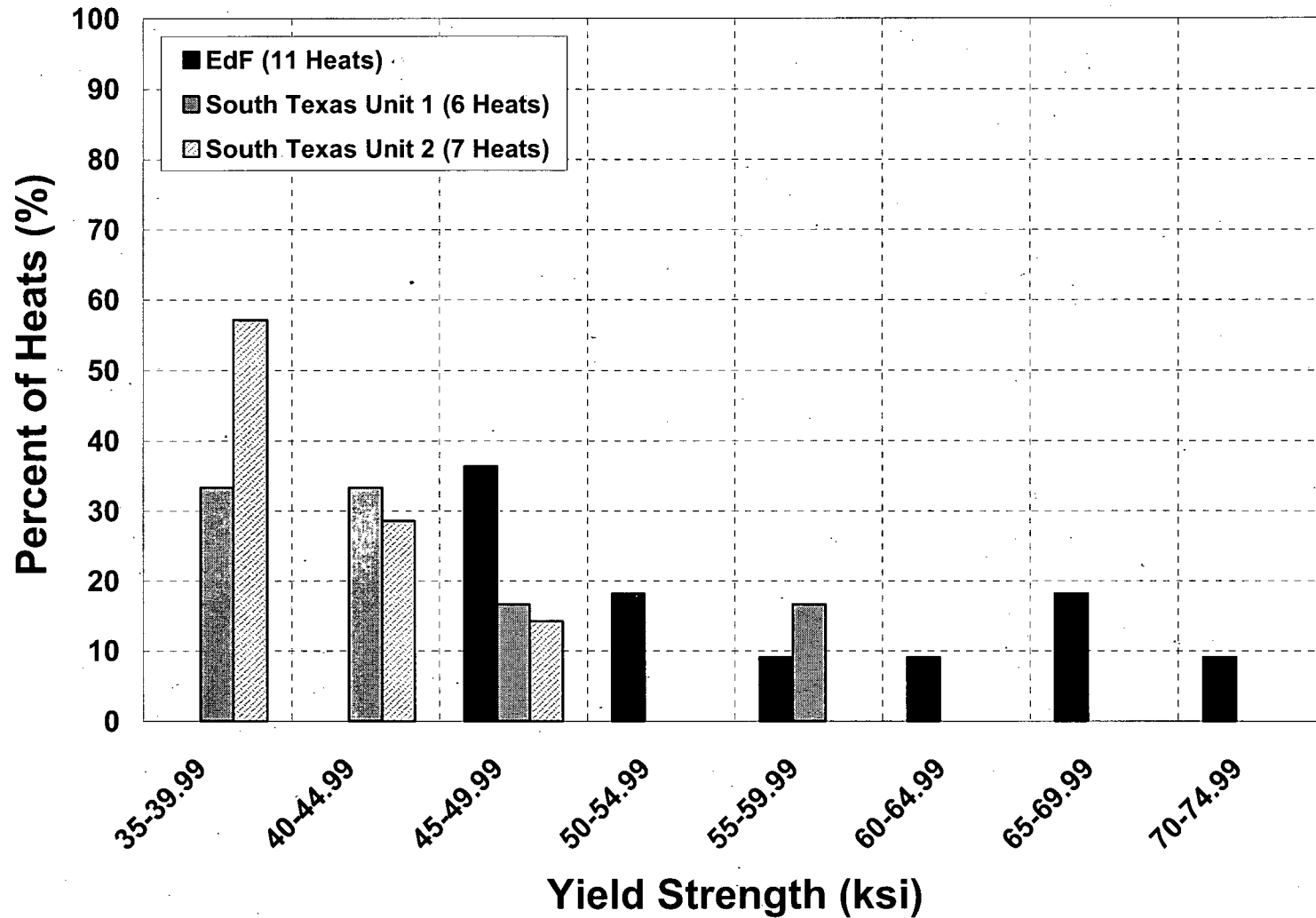
Figure 4-1   Yield Strength of the Various Heats of Alloy 600 Used in Fabricating the STP and French Head Penetrations
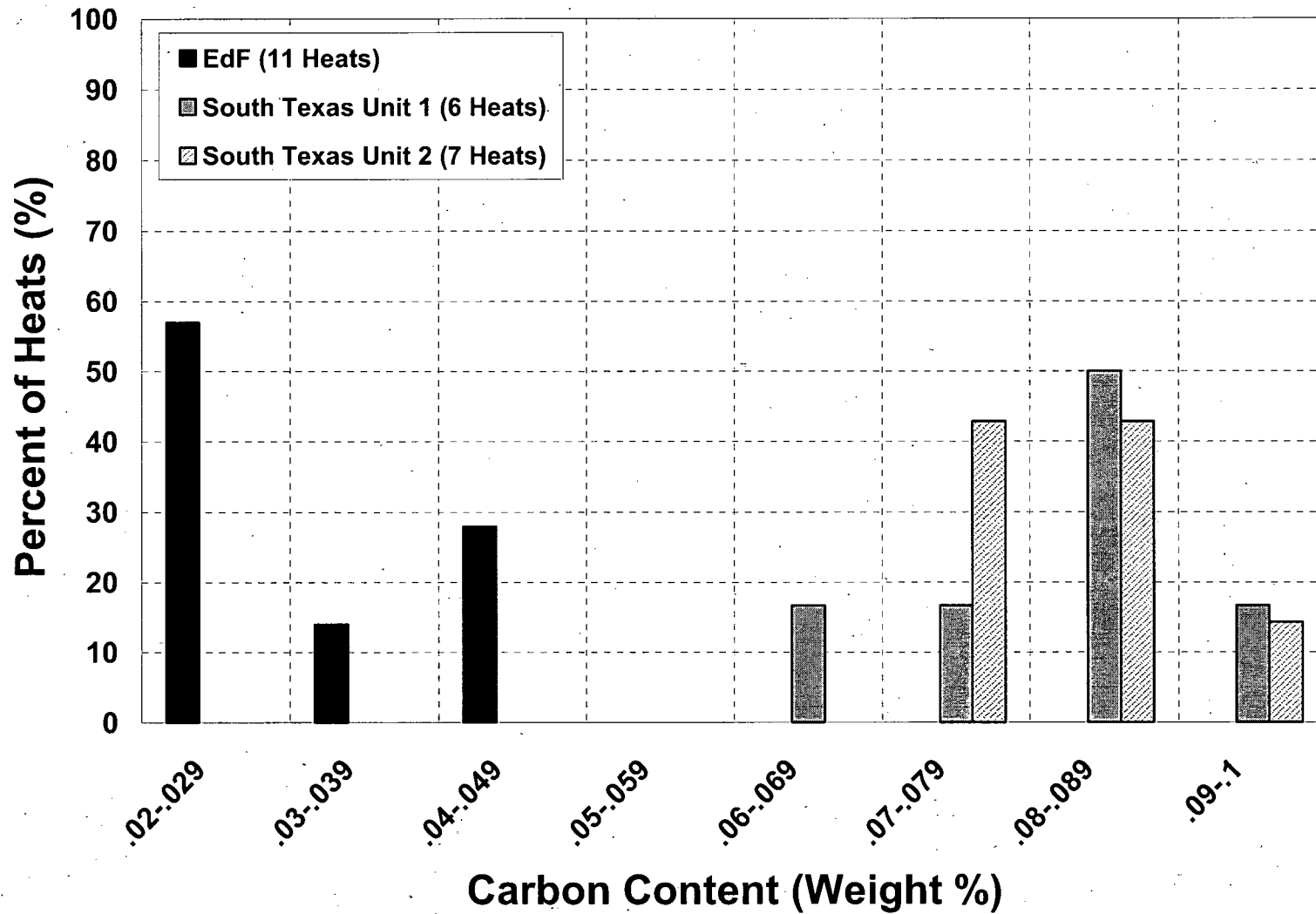
Figure 4-2   Carbon Content of the Various Heats of Alloy 600 Used in Fabricating the STP and French Head Penetrations

a,c,e

Figure 4-3   Screened Laboratory Data for Alloy 600 with the MRP Recommended Curve
(Note that the Modified Scott Model is also shown)

a,c,e
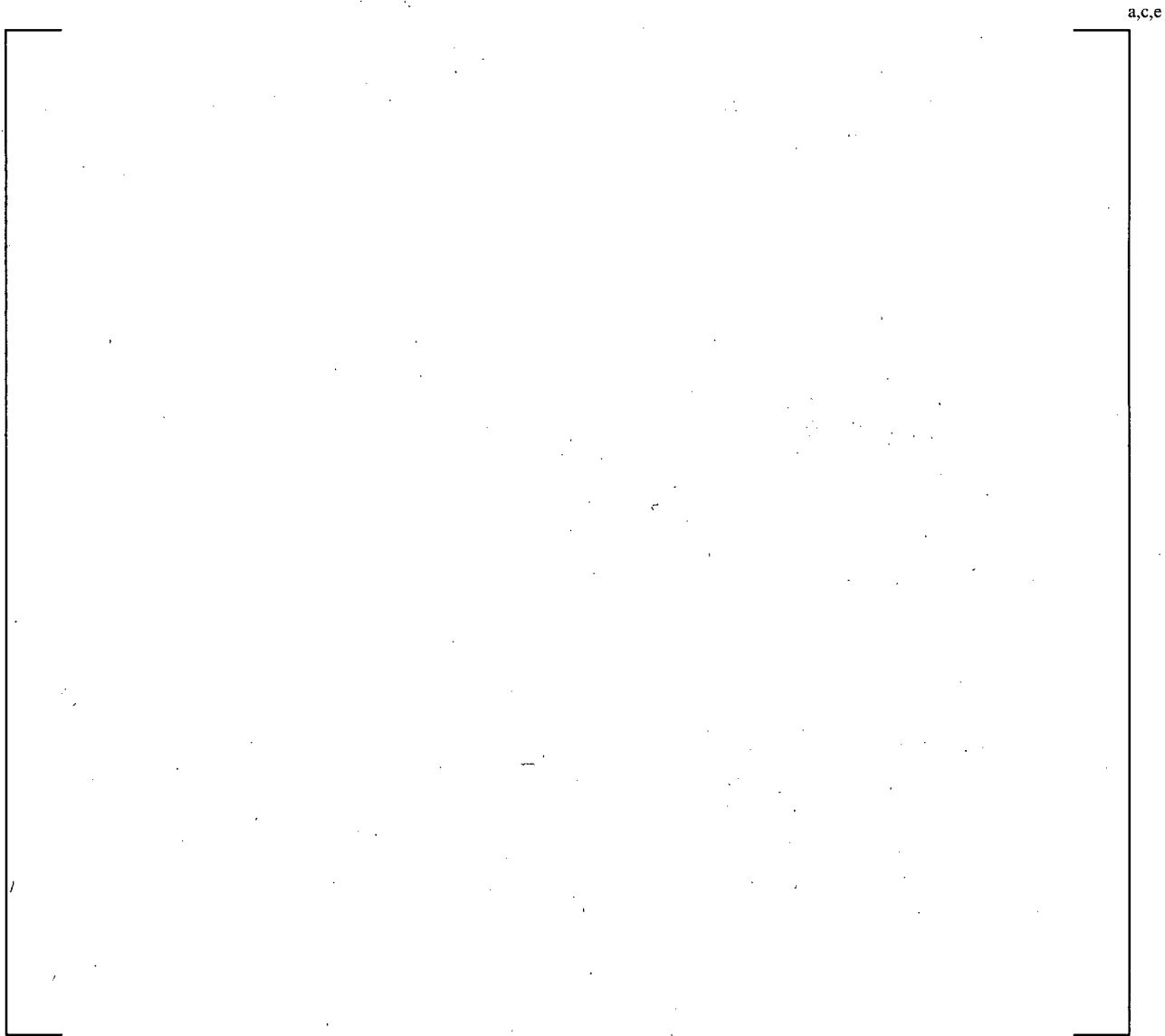
Figure 4-4   Model for PWSCC Growth Rates in Alloy 600 in Primary Water Environments
(325°C), With Supporting Data from Standard Steel, Huntington, and Sandvik
Materials

Note that the data have been normalized to a temperature of 325°C (617°F). The actual test temperatures are listed
in parenthesis after the caption. For example, the Huntington data were obtained at temperature ranging from 315°C
to 331°C (599°F to 628°F).
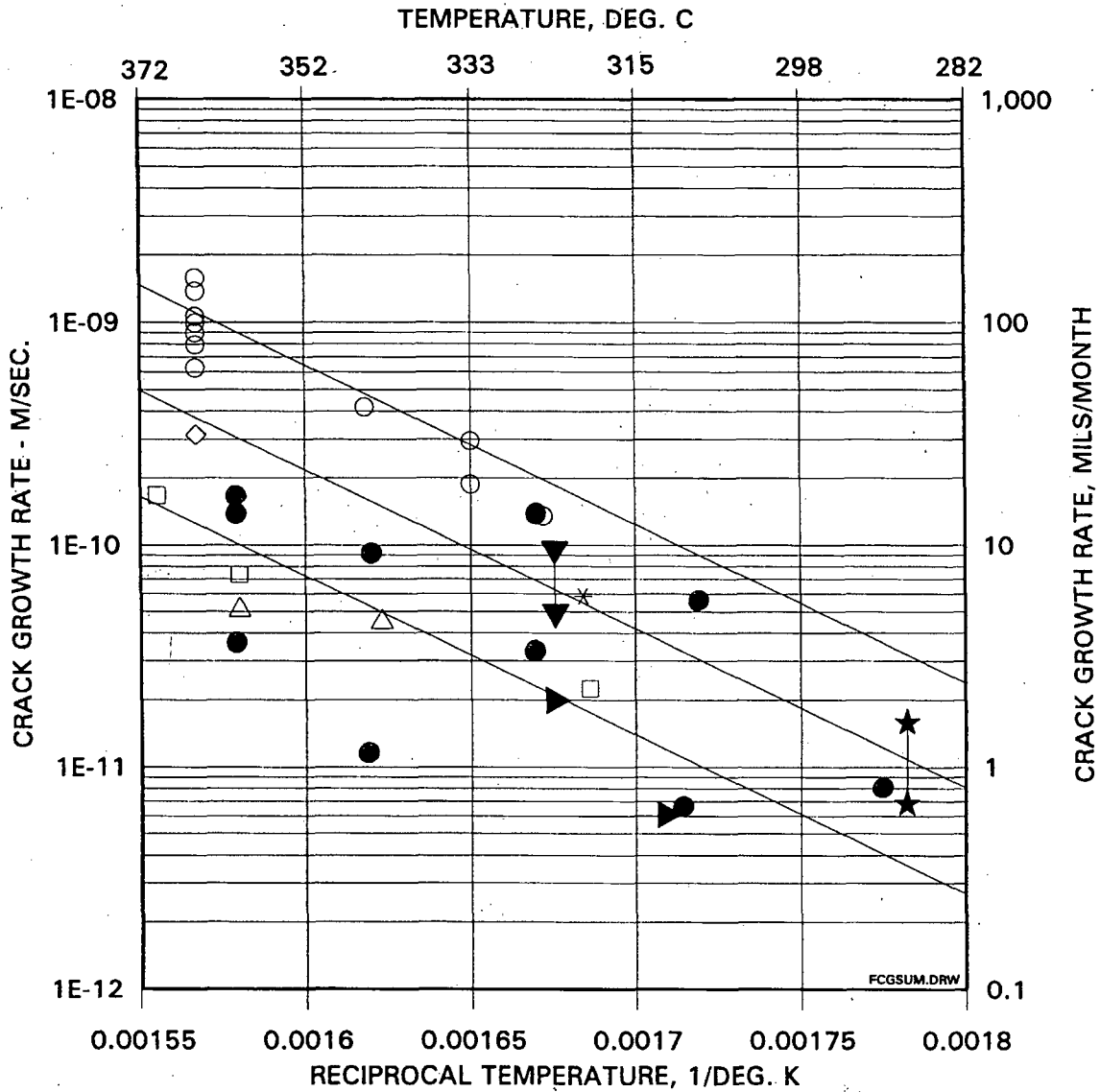
Figure 4-5 Summary of Temperature Effect on PWSCC Growth Rates for Alloy 600 in Primary Water

Note: All symbols are for steam generator materials, except the solid circles, which are head penetration laboratory data.

5 STRESS ANALYSIS

5.1 OBJECTIVES OF THE ANALYSIS

The objective of this analysis was to obtain accurate stresses in the CRDM, head vent, gas vent and their immediate vicinity. To do so requires a three dimensional finite element analysis which considers all the pertinent loadings on the penetrations [3]. Five CRDM locations were considered: 0 degree (Penetration No. 1), 26.2 degrees (Penetration Nos. 22 through 29), 44.3 degrees (Penetration Nos. 62 through 65), 45.4 degrees (Penetration Nos. 66 through 73), and 48.7 degrees (Penetration Nos. 75 through 79). In addition, the head vent and gas vent nozzles were also analyzed.

The analyses were used to provide information for the flaw tolerance evaluation, which follows in Section 6. Also, the results of the stress analysis were compared to the findings from service experience, to help assess the causes of the cracking which has been observed.

5.2 MODEL

A three-dimensional finite element model comprised of isoparametric brick and wedge elements was used to obtain the stresses and deflections. Taking advantage of the symmetry of the vessel head, only half of a CRDM penetration nozzle and half of the head vent and gas vent nozzles were modeled. Views of CRDM, head vent and gas vent nozzle models are shown in Figures 5-1, 5-2, and 5-3 respectively.

In the models, the lower portion of the Control Rod Drive Mechanism (CRDM) penetration nozzle, the head vent, the gas vent, the adjacent section of the vessel closure head, and the joining weld were modeled. The vessel to penetration nozzle weld as well as the head vent and the gas vent nozzle welds were simulated with two weld passes. The penetration nozzle, weld metal, cladding and the vessel head shell were modeled in accordance with the relevant materials.

The only loads used in the analysis are the steady state operating loads. External loads, such as seismic loads, have been studied and have no impact since the penetration nozzles are captured by the full thickness of the reactor vessel. In addition, the duration of the seismic loading is very short and will not have any significant impact on the overall PWSCC growth. The area of interest is in the penetration near the attachment weld, which is unaffected by these external loads.

## 5.3 STRESS ANALYSIS RESULTS – OUTERMOST CRDM PENETRATION (48.7°)

Figure 5-4 presents the hoop and axial stresses for the steady state condition for the outermost CRDM penetration.

The hoop stresses for steady state operation are much greater than the axial stresses. This is consistent with the field findings, where the cracks discovered are generally oriented axially. Typically, in-service cracks will orient themselves perpendicular to the largest stress component. Also it should be noted from Figure 5-4 that the highest tensile hoop stresses are at the uphill side and downhill side locations rather than midway around the penetration, where they are

compressive. This is consistent with finding the axial cracks only at the uphill side and downhill side locations. It is these steady state stresses that will be used to predict crack extension in the penetrations, as will be discussed further in Section 6.

These stress findings also support the safety argument that cracks are unlikely to propagate in the circumferential direction, because the axial stresses are relatively low. This is illustrated in a cut taken along the plane of the top of the attachment weld, as shown in Figure 5-11. Note that the stresses at the mid-wall are compressive or mildly tensile.

5.4 STRESS ANALYSIS RESULTS – INTERMEDIATE CRDM PENETRATIONS

The stresses in these penetrations are similar in character. Figures 5-5, 5-6, and 5-7 show the results for the 45.4 degrees, 44.3 degrees, and 26.2 degrees CRDM penetrations, respectively. As with the outermost housing, the hoop stresses for steady state operation are greater than the axial stresses.

5.5 STRESS ANALYSIS RESULTS – CENTER CRDM PENETRATION (0°)

Figure 5-8 shows the hoop and axial stresses at steady state for the center CRDM penetration. The hoop stresses near the weld are generally lower than the hoop stresses at the downhill side or uphill side locations of the outer head penetration.

5.6 STRESS ANALYSIS RESULTS – HEAD VENT

The head vent nozzle is a smaller penetration than the CRDM head penetration, but is also constructed of Alloy 600 material, with a partial penetration weld at the inside of the reactor vessel head. The head vent was evaluated using a three-dimensional finite element model as shown in Figure 5-2.

The critical stress location in the head vent is in the vicinity of the attachment weld, where residual and pressure stresses have the most impact. As with the CRDM penetrations, the residual stresses dominate. Also similar to the CRDM head penetrations, the stresses in the pipe decrease quickly as a function of distance up the pipe away from the weld. The hoop and axial stresses are shown as contours in Figure 5-9.

5.7 STRESS ANALYSIS RESULTS – GAS VENT

The gas vent nozzle is similar in size to the CRDM head penetration, and is also constructed of Alloy 600 material, with a partial penetration weld at the inside of the reactor vessel head. The gas vent was evaluated using a three-dimensional finite element model as shown in Figure 5-3.

The critical stress location in the gas vent is in the vicinity of the attachment weld, where residual and pressure stresses have the most impact. As with the CRDM penetrations, the residual stresses dominate. Also similar to the CRDM head penetrations, the stresses in the pipe decrease quickly as a function of distance up the pipe away from the weld. The hoop and axial stresses are shown as contours in Figure 5-10.
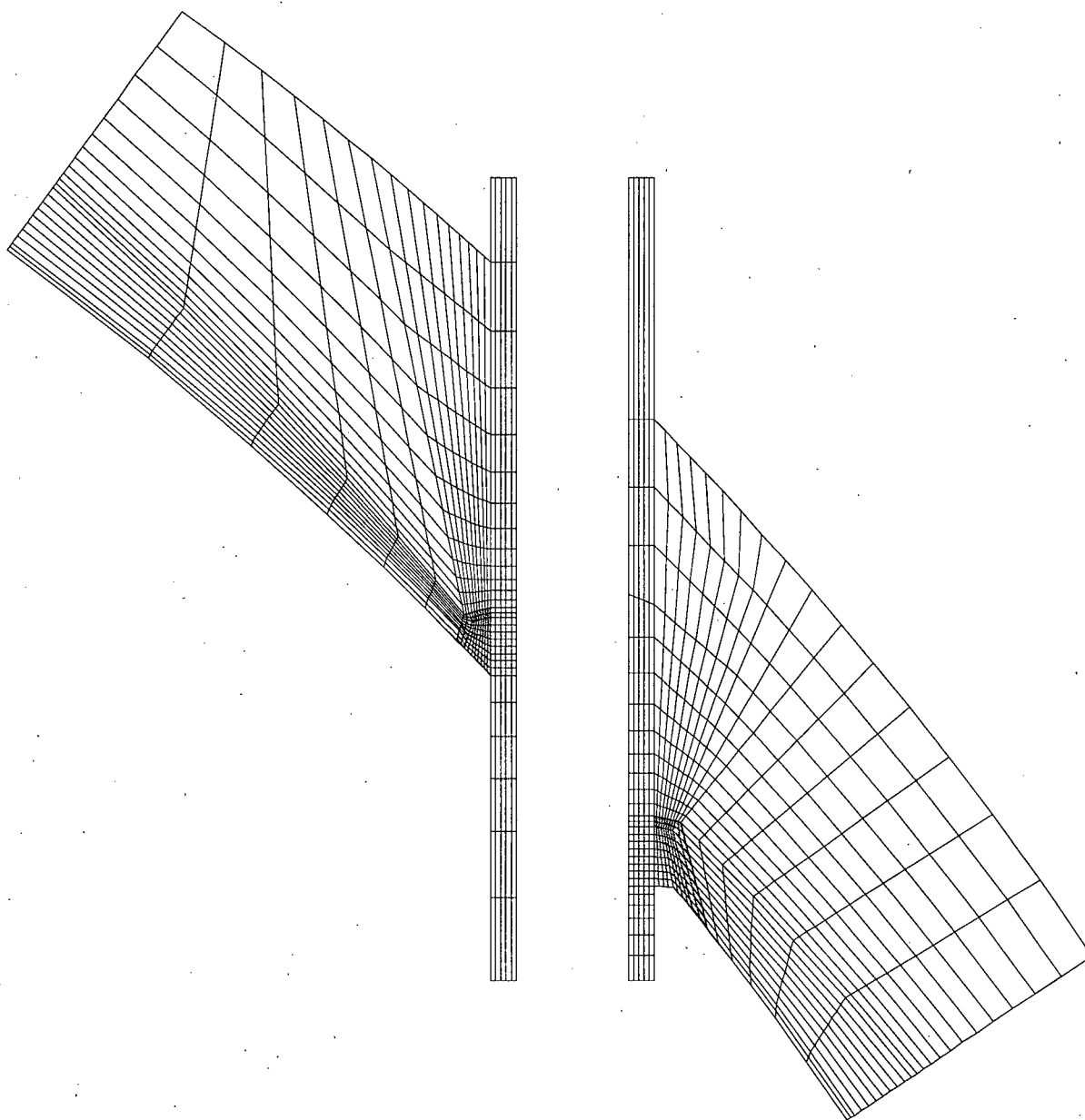
Figure 5-1 Finite Element Model of CRDM Penetration
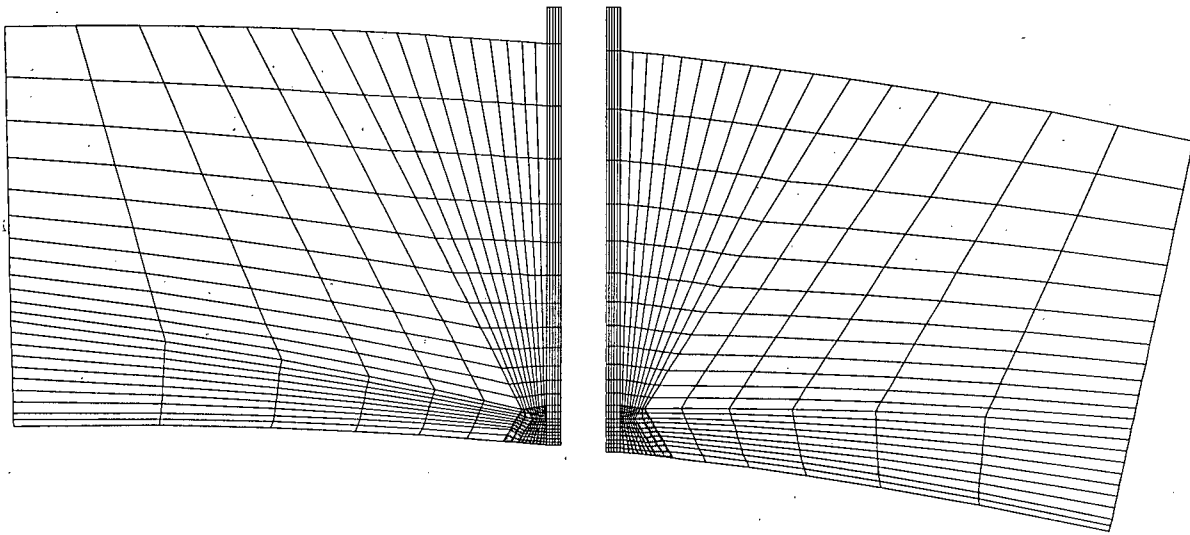
Figure 5-2 Finite Element Model of Head Vent Pipe
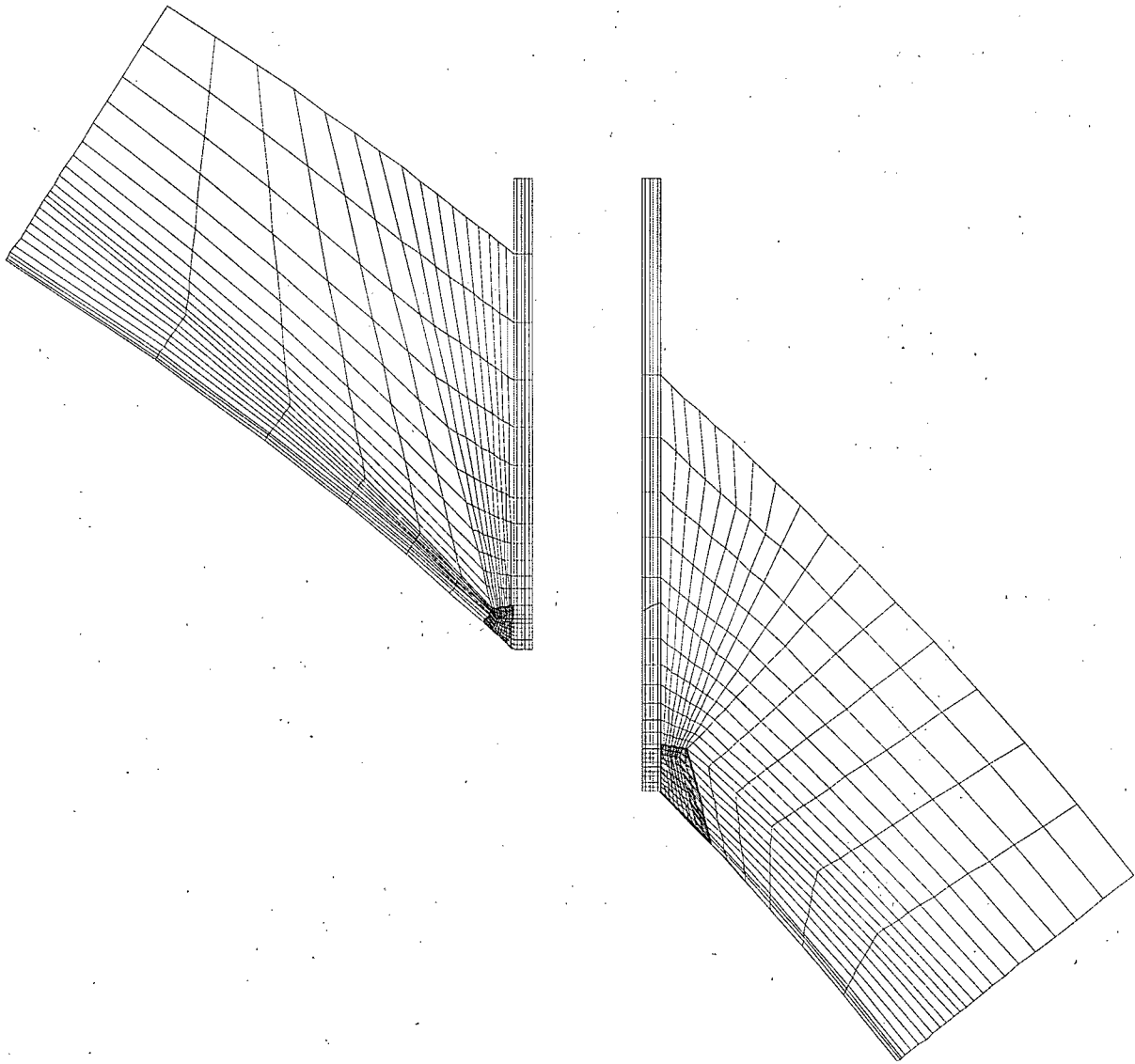
Figure 5-3 Finite Element Model of Gas Vent Pipe
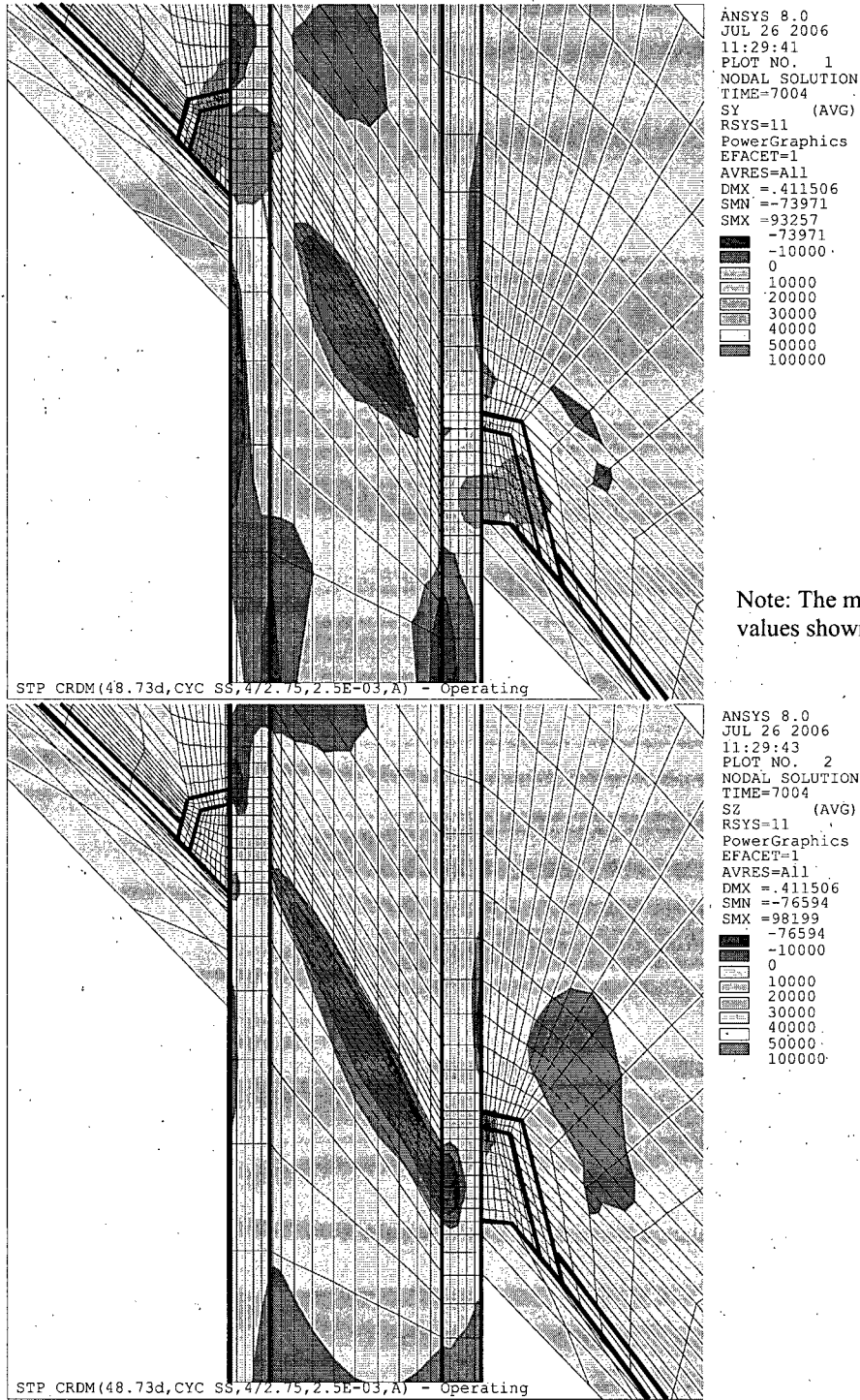
Note: The magnitude of the stress values shown is in psi.

Figure 5-4   Stress Distribution at Steady State Conditions: Outermost CRDM Penetration Nozzle (48.7 Degrees) (Hoop Stress is the Top Figure, Axial Stress is the Bottom Figure)
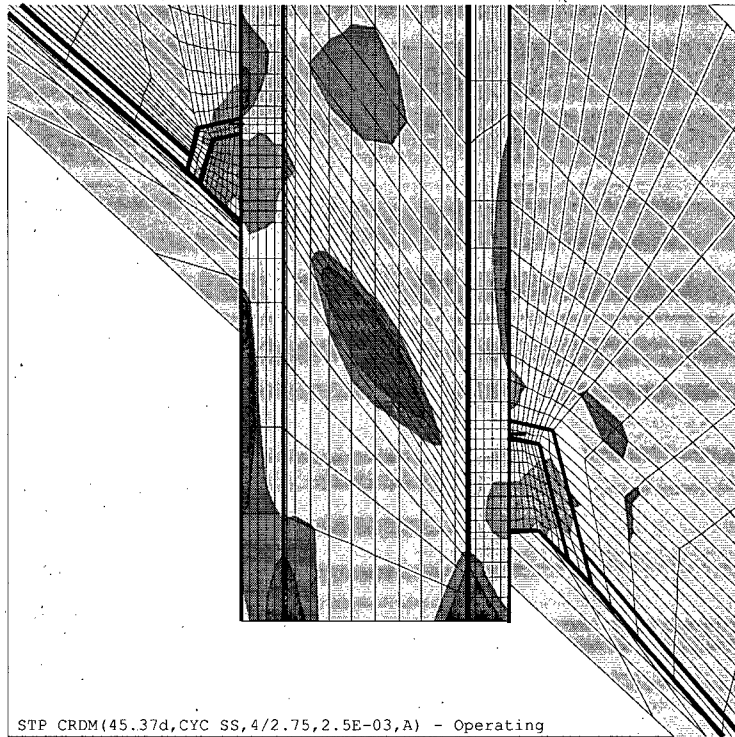
Note: The magnitude of the stress values shown is in psi.
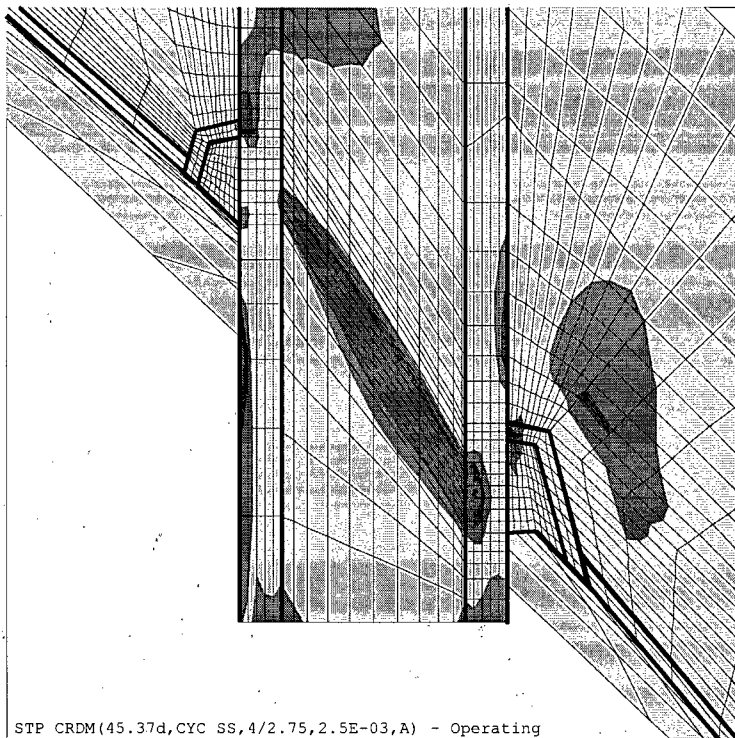
Figure 5-5 **Stress Distribution at Steady State Conditions for the 45.4 Degrees CRDM Penetration (Hoop Stress is the Top Figure; Axial Stress is the Bottom Figure)**
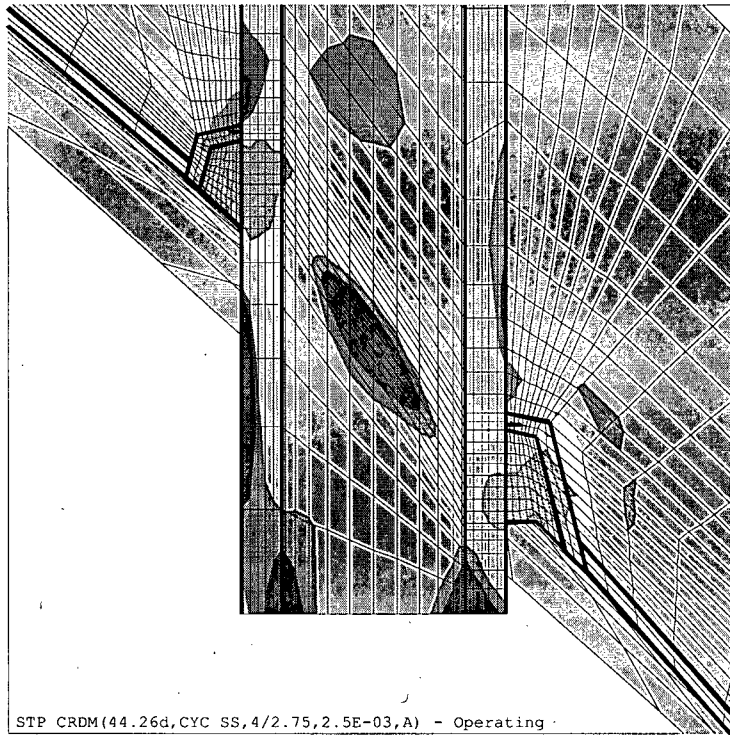
Note: The magnitude of the stress values shown is in psi.
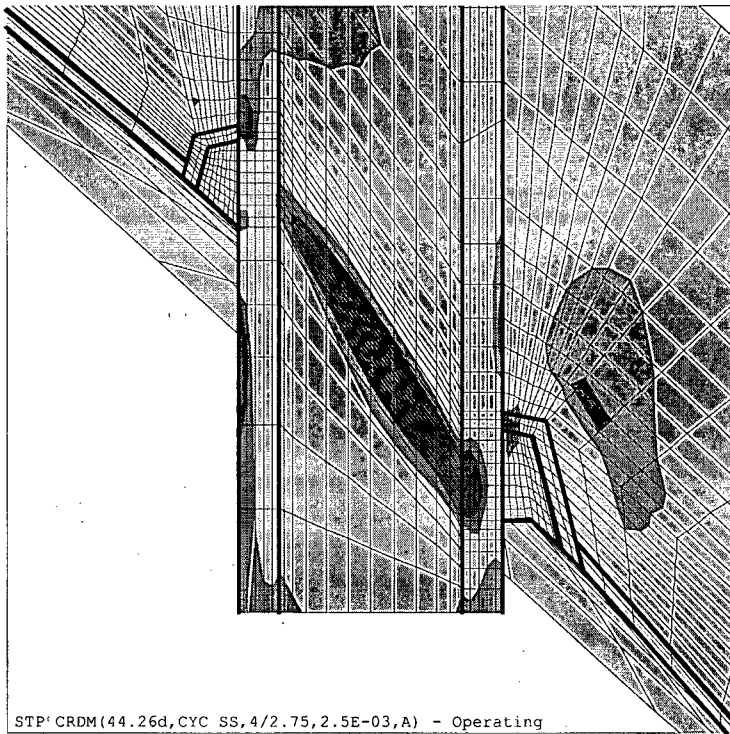
Figure 5-6   Stress Distribution at Steady State Conditions for the 44.3 Degrees CRDM Penetration (Hoop Stress is the Top Figure; Axial Stress is the Bottom Figure)
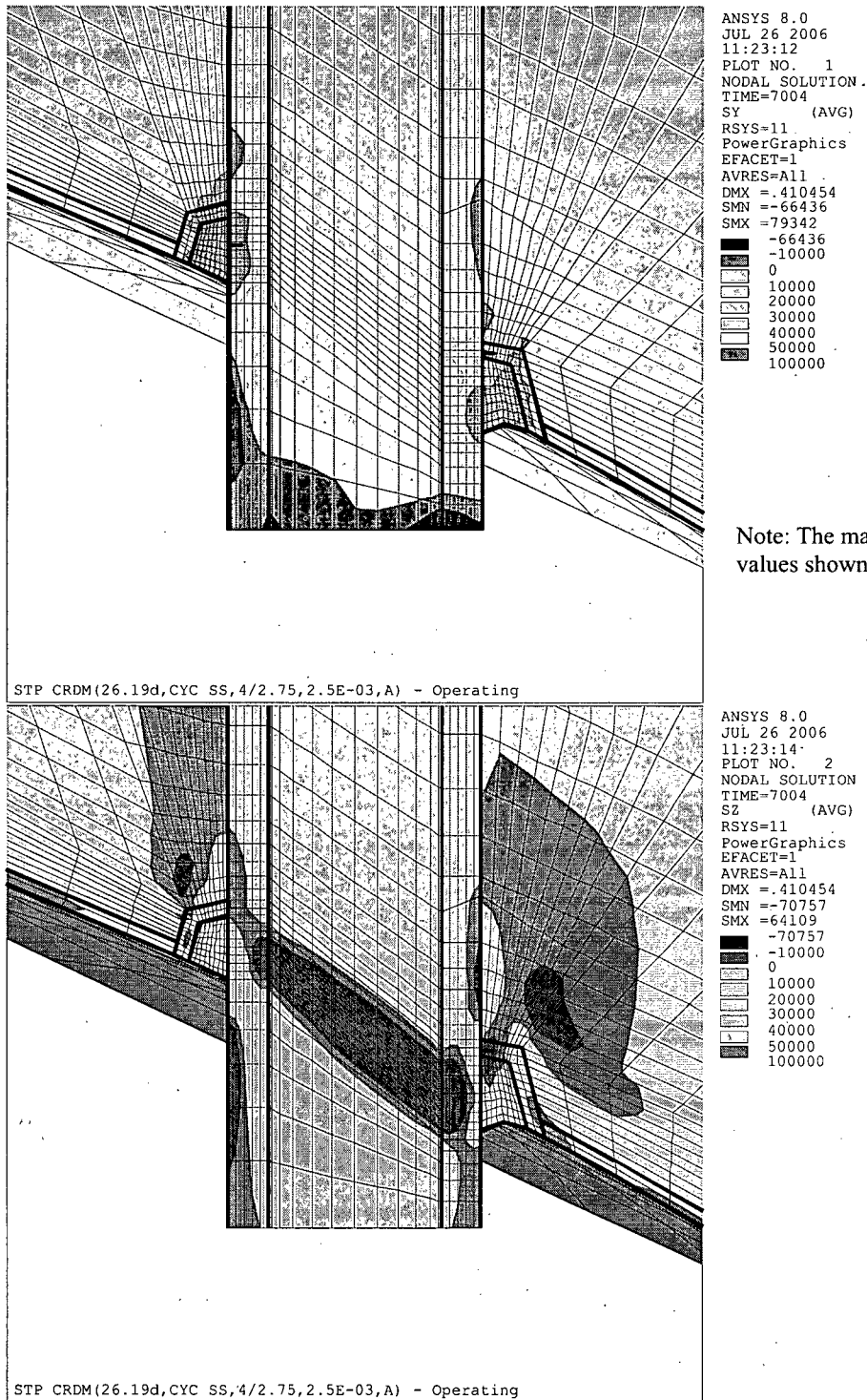
Note: The magnitude of the stress values shown is in psi.

Figure 5-7   Stress Distribution at Steady State Conditions for the 26.2 Degrees CRDM Penetration (Hoop Stress is the Top Figure; Axial Stress is the Bottom Figure)

```
ANSYS 8.0
JUL 26 2006
11:16:30
PLOT NO.   1
NODAL SOLUTION
TIME=7004
SY        (AVG)
RSYS=11
PowerGraphics
EFACET=1
AVRES=All
DMX =.408709
SMN =-47746
SMX =74928
    -47746
    -10000
    0
    10000
    20000
    30000
    40000
    50000
    100000
```

Note: The magnitude of the stress values shown is in psi.

STP CRDM(0d,CYC SS,4/2.75,0,A) - Operating

```
ANSYS 8.0
JUL 26 2006
11:16:32
PLOT NO.   2
NODAL SOLUTION
TIME=7004
SZ        (AVG)
RSYS=11
PowerGraphics
EFACET=1
AVRES=All
DMX =.408709
SMN =-67977
SMX =55631
    -67977
    -10000
    0
    10000
    20000
    30000
    40000
    50000
    100000
```

STP CRDM(0d,CYC SS,4/2.75,0,A) - Operating
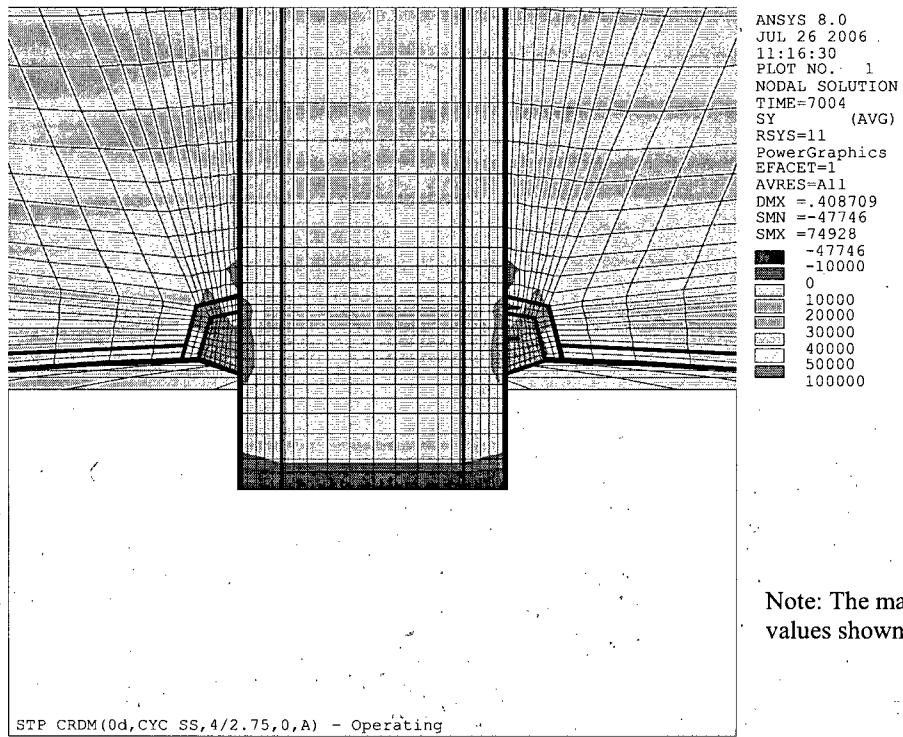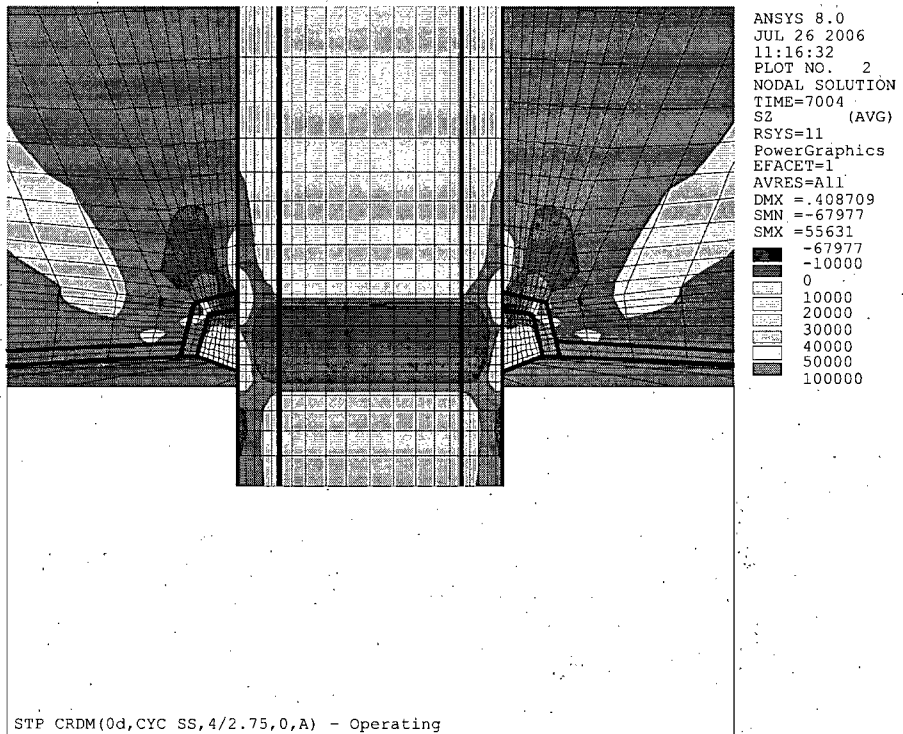
Figure 5-8   Stress Distribution at Steady State Conditions for the Center CRDM Penetration (Hoop Stress is the Top Figure; Axial Stress is the Bottom Figure)

```
ANSYS 8.0
JUL 26 2006
11:17:14
PLOT NO.    1
NODAL SOLUTION
TIME=7004
SY          (AVG)
RSYS=11
PowerGraphics
EFACET=1
AVRES=All
DMX =.395962
SMN =-11039
SMX =76590
        -11039
        -10000
        0
        10000
        20000
        30000
        40000
        50000
        100000
```

Note: The magnitude of the stress values shown is in psi.

STP HV(5.66d,CYC SS,1.315/0.815,0,A) - Operating

```
ANSYS 8.0
JUL 26 2006
11:17:16
PLOT NO.    2
NODAL SOLUTION
TIME=7004
SZ          (AVG)
RSYS=11
PowerGraphics
EFACET=1
AVRES=All
DMX =.395962
SMN =-41984
SMX =48300
        -41984
        -10000
        0
        10000
        20000
        30000
        40000
        50000
        100000
```

STP HV(5.66d,CYC SS,1.315/0.815,0,A) - Operating
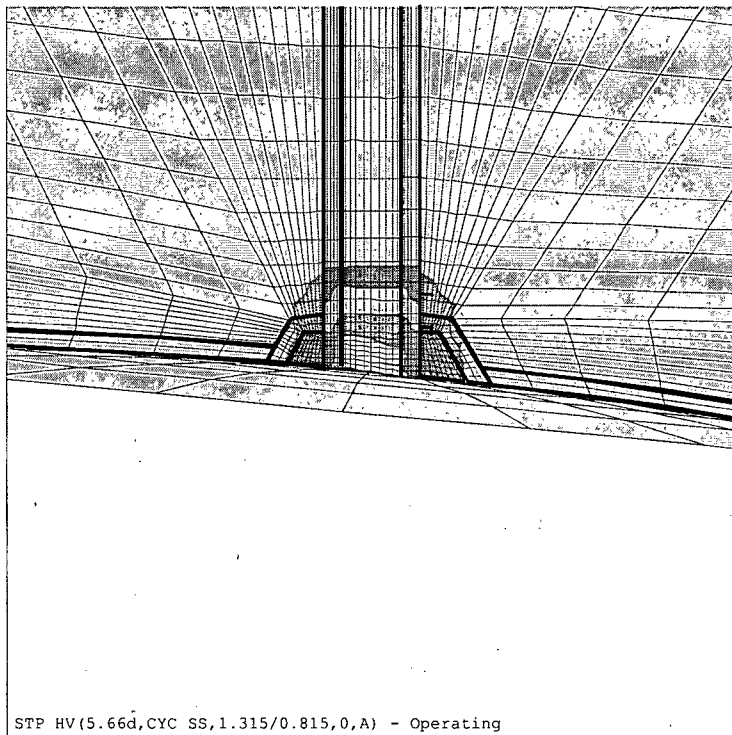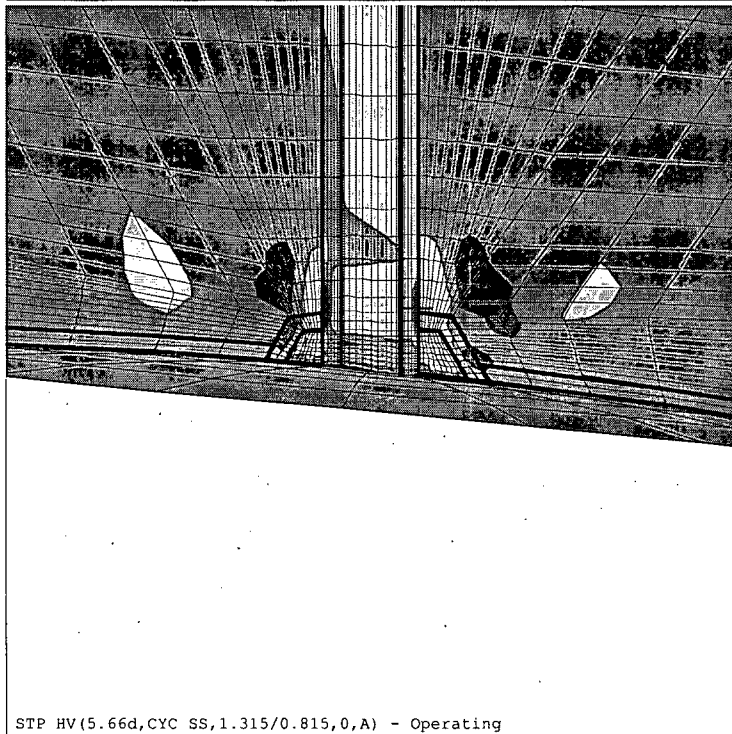
Figure 5-9   Stress Contours in the Head Vent Nozzle as a Result of Residual Stresses and Operating Pressure (Hoop Stress is the Top Figure; Axial Stress is the Bottom Figure)

```
ANSYS 8.0
JUL 27 2006
13:51:09
PLOT NO.   1
NODAL SOLUTION
TIME=7004
SY        (AVG)
RSYS=11
PowerGraphics
EFACET=1
AVRES=All
DMX =.413035
SMN =-21969
SMX =92359
        -21969
        -10000
        0
        10000
        20000
        30000
        40000
        50000
        100000
```

Note: The magnitude of the stress values shown is in psi.

STP GV(44.26d,CYC SS,3.49/2.624,4.E-03,A) - Operating

```
ANSYS 8.0
JUL 27 2006
13:51:12
PLOT NO.   2
NODAL SOLUTION
TIME=7004
SZ        (AVG)
RSYS=11
PowerGraphics
EFACET=1
AVRES=All
DMX =.413035
SMN =-50997
SMX =88170
        -50997
        -10000
        0
        10000
        20000
        30000
        40000
        50000
        100000
```

STP GV(44.26d,CYC SS,3.49/2.624,4.E-03,A) - Operating
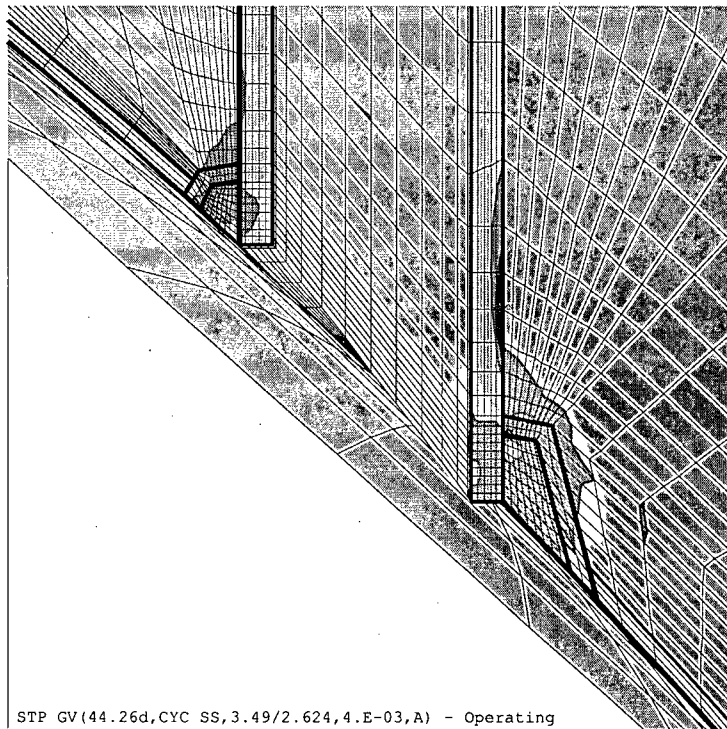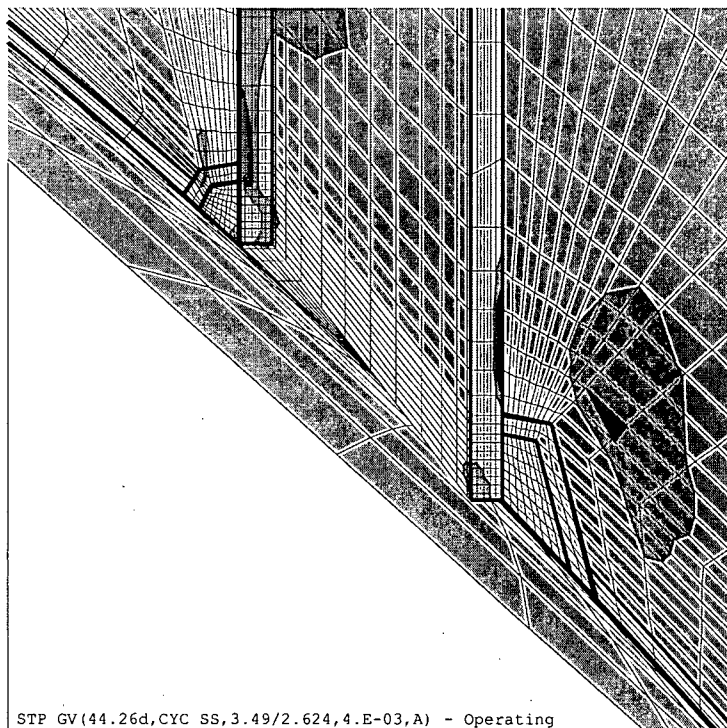
Figure 5-10   Stress Contours in the Gas Vent Nozzle as a Result of Residual Stresses and Operating Pressure (Hoop Stress is the Top Figure; Axial Stress is the Bottom Figure)

```
ANSYS 8.0
JUL 26 2006
11:29:46
PLOT NO.   5
DISPLACEMENT
TIME=7004
RSYS=SOLU
DMX =.411506

*DSCA=10
XV   =-1
ZV   =2
DIST=8.426
XF   =-.204284
YF   =63.636
ZF   =63.587
VUP  =Z
PRECISE HIDDEN

NODAL SOLUTION
TIME=7004
SZ          (AVG)
RSYS=SOLU
DMX =.378274
SMN =-23543
SMX =42112
      -23543
      -10000
      0
      10000
      20000
      30000
      40000
      50000
      100000
```

STP CRDM(48.73d,CYC SS,4/2.75,2.5E-03,A) - Operating
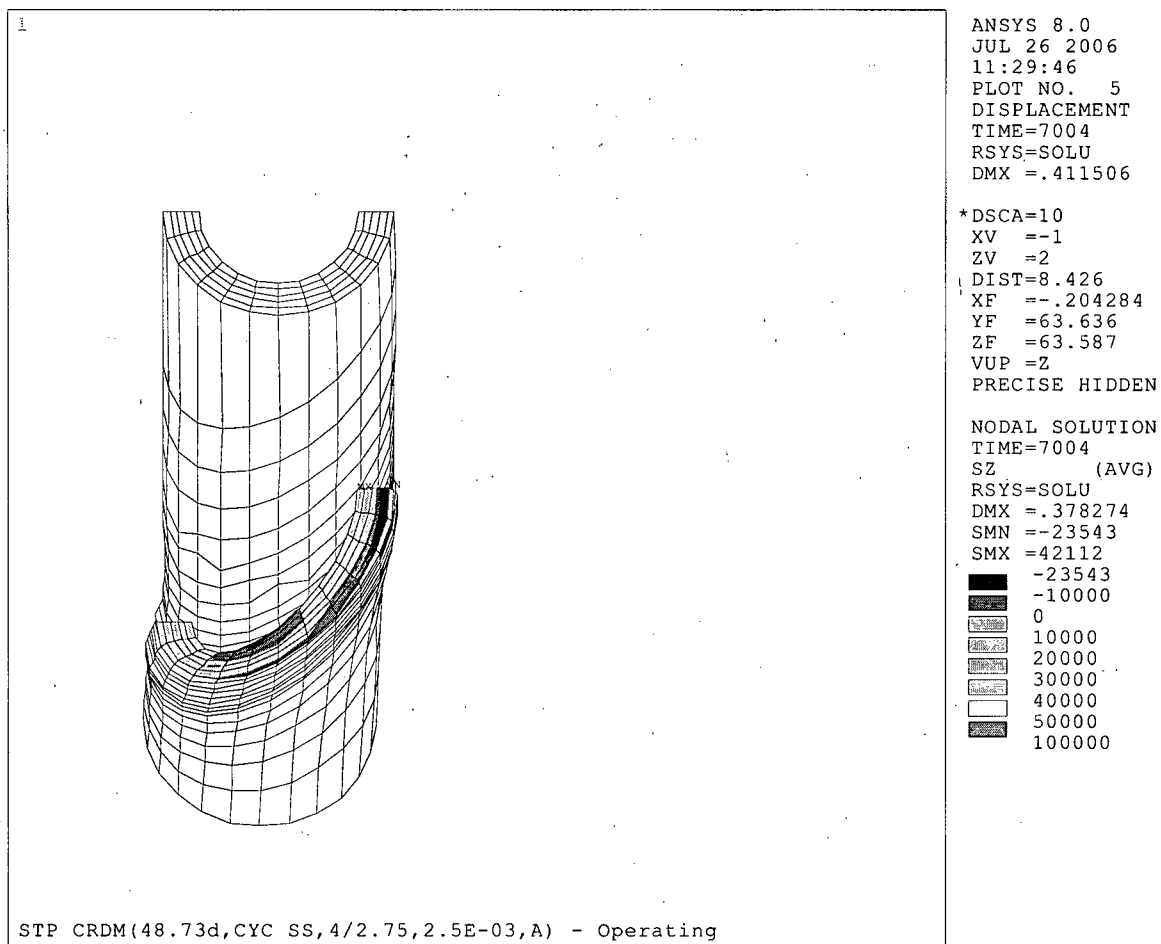
Note: The magnitude of the stress values shown is in psi.

Figure 5-11   Axial Stress Distribution at Steady State Conditions for the Outermost CRDM Penetration (48.7 Degrees), Along a Plane Oriented Parallel to, and Just Above, the Attachment Weld

6 FLAW TOLERANCE CHARTS

6.1 INTRODUCTION

The flaw tolerance charts were developed using the stress analysis of each of the penetration locations as discussed in Section 5. The crack growth rate used for STP is discussed in Section 4.2, and several flaw tolerance charts were developed for each penetration location. The first series of charts characterizes the growth of a partial through-wall (i.e. surface) flaw and is used in predicting remaining service life of the penetration nozzle. The second series of charts, which characterizes the growth of a through-wall flaw below the J-groove weld, can be used to determine the minimum required inspection coverage to ensure that any flaws initiated below the weld in the region of the penetration nozzle not being inspected would not reach the bottom of the weld before the next inspection. All service lives resulting from these calculations are in EFPYs, since crack growth will only occur at operating temperatures.

6.2 OVERALL APPROACH

The results of the three-dimensional stress analyses of the penetration locations were used directly in the flaw tolerance evaluation.

The crack growth evaluation for the partial through-wall flaws was based on the worst stress distribution through the penetration wall at the location of interest of the penetration. The location of interest, i.e., the highest stressed location, was found to be in the immediate vicinity of the weld for both the center and outermost penetrations.

The stress profile was represented by a cubic polynomial:

$$\sigma(x) = A_0 + A_1 x + A_2 x^2 + A_3 x^3 \tag{6-1}$$

where:

x = the coordinate distance into the nozzle wall
σ = stress perpendicular to the plane of the crack
A_I = coefficients of the cubic polynomial fit

For the surface flaw with length six times its depth, the stress intensity factor expression of Raju and Newman [22, 23] was used. The stress intensity factor K_I (Φ) can be calculated anywhere along the crack front. The point of maximum crack depth is represented by Φ = 0, and this location was also found to be the point of maximum K_I for the cases considered here. The following expression is used for calculating K_I (Φ), where Φ is the angular location around the crack. The units of K_I (Φ) are $ksi\sqrt{in}$.

$$K_I(\Phi) = \left[\frac{\pi a}{Q}\right]^{0.5} \sum_{j=0}^{3} G_j \left(a/c, a/t, t/R, \Phi\right) A_j a^j \tag{6-2}$$

The boundary correction factors G_0 (Φ), G_1 (Φ), G_2 (Φ) and G_3 (Φ) are obtained by the procedure outlined in reference [22, 23]. The dimension "a" is the crack depth, and "c" is the semi crack

length, while "t" is the wall thickness. "R" is the inside radius of the tube, and "Q" is the shape factor.

[

$]^{a,c,e}$

For the prediction of crack growth for a circumferential through-wall flaw in the head penetration along a plane above the attachment weld, an expression first presented by Hiser [25] was used. The stress intensity factor for a circumferential through-wall flaw was developed using finite element modeling by Structural Integrity Associates (SIA), and these results were merged with results obtained by Richard Bass of Oak Ridge National Labs (ORNL), as shown in Figure 6-1. The equation of the stress intensity factor is simply a function of the crack half angle, and is given below:

$$K_1 = 3.476x - 6.619 \times 10^{-2} x^2 + 4.733 \times 10^{-4} x^3 - 1.445 \times 10^{-6} x^4 + 1.790 \times 10^{-9} x^5 \qquad (6-4)$$

In this equation, x is the crack half angle in degrees and K_1 is in ksi$\sqrt{in}$.

[

$]^{a,c,e}$

6.3 AXIAL FLAW PROPAGATION

CRDM Surface Flaws

The results of the calculated growth for inside surface flaws growing through the wall thickness of the CRDM penetration nozzles are shown in Figures 6-2 through 6-7. For outside surface flaws, the results are shown in Figures 6-10 and 6-11. Based on the discussion in MRP-55 report [8], the use of stress intensity factors less than $15\,\text{MPa}\sqrt{m}$ involves assumptions not currently substantiated by actual CGR data for CRDM nozzle materials. Therefore, most of these crack growth curves, excepted as noted, begin at a flaw depth that result in a stress intensity factor of $15\,\text{MPa}\sqrt{m}$, which exceeds the threshold value of $9\,\text{MPa}\sqrt{m}$. This may result in curves with different initial flaw sizes, as seen for example in Figure 6-2. All the crack growth curve results are only provided for the uphill and downhill sides of each penetration nozzle. The stresses for the regions 90 degrees from these locations are in general not limiting. If flaws are found in such a location, the results for either the uphill or downhill location, whichever is closer, can be conservatively used.

Each of these figures allows the future allowable service time to be estimated graphically, as discussed in Section 3. Results are shown for each of the penetration nozzles analyzed in each of these figures. The stresses are much higher near the attachment weld than at 0.5 inch below or above it, so separate figures have been provided for these three regions. For more than 0.5 inch below the weld, the crack growth will eventually come to rest since the stresses are compressive as shown in the hoop stress plots for the CRDM nozzles in Appendix A. Also, the stresses are different on the downhill side of the penetration as opposed to the uphill side, so these two cross sections have also been treated separately.

Example problems are provided in Section 7 for evaluating a range of possible flaw types.

Inspection Coverage of RPV Head Penetration below the Weld

As a result of the First Revised NRC Order EA-03-009 issued in February 2004, most of the power plants in the United States have encountered problems with the required inspection coverage of the head penetrations below the weld. To support the submittal of relaxation request in the event that the required inspection coverage below the weld cannot be achieved, a series of axial through-wall crack growth below the weld charts for the downhill side were prepared for each of the penetrations evaluated. The charts are shown in Figures 6-13 through 6-17.

There is nearly universal agreement that high stresses, on the order of the material yield strength, are necessary to initiate PWSCC. There is no known case of stress corrosion cracking of Alloy 600 below the yield stress [26, 27]. Typical yield strengths for wrought Alloy 600 head penetration nozzles are in the range of 37 ksi to 65 ksi. Weld metal yield strengths are generally higher. The yield strength of the head penetration nozzles for STP varies from 35.5 ksi to 55 ksi [4]. In addition, the stress level of 20 ksi has been determined as a value below which PWSCC initiation is extremely unlikely [27].

In each of the charts, the location of the upper extremity of the postulated through-wall crack is identified on the charts by the distance measured from the bottom of weld. Although the

assumption of any PWSCC crack initiation in the region of the penetration nozzle with a stress level less than 20 ksi is very conservative, nevertheless, the lower extremity of the initial through-wall flaw is conservatively postulated to be located on the penetration nozzle where either the inside or the outside surface hoop stress drops below 0 ksi. The time duration required for the upper extremity of an axial through-wall flaw to reach the bottom of the weld can be determined from these charts as illustrated in Example 5 of Section 7.

Since the charts shown in Figure 6-13 through 6-17 were generated based on postulated axial through-wall flaws, they are suitable to address lack of inspection coverage below the attachment weld of the head penetration. These charts can be used to predict the axial crack growth at the upper crack extremity of any undetected axial flaws in the region below the weld not being able to be inspected.

Head Vent

The only flaw tolerance chart that is necessary for the head vent region is for flaws at and above the weld since no portion of the head vent projects below the weld. Figure 6-8 provides the projected growth of a partial through-wall flaw in the head vent just above the attachment weld.

Gas Vent

The only flaw tolerance chart that is necessary for the gas vent region is for flaws at and above the weld since no portion of the gas vent nozzle projects below the weld. The flaw growth is calculated on both the uphill and downhill sides of the gas vent nozzle. Figure 6-9 provides the projected growth of a partial through-wall flaw in the gas vent just above the attachment weld.

6.4 CIRCUMFERENTIAL FLAW PROPAGATION

Since circumferentially oriented flaws have been found at five plants (Bugey 3, Oconee 2, Crystal River 3, Davis-Besse, and Oconee 3), it is important to consider the possibility of crack extension in the circumferential direction. The first case was discovered as part of the destructive examination of the cracked tube at Bugey 3. The crack was found to have extended to a depth of 0.0886 inch (2.25 mm) in a wall thickness of 0.6299 inch (16 mm). The flaw was found at the outside surface of the penetration (number 54) at the downhill side location, just above the weld.

The circumferential flaws in Oconee Unit 3 were discovered during the process of repairing a number of axial flaws, whereas the circumferential flaw in Oconee Unit 2 and Crystal River Unit 3 were discovered by UT. Experience gained from these findings has enabled the development of UT procedures capable of detecting circumferential flaws reliably.

To investigate this issue completely, a series of crack growth calculations were carried out for a postulated outside surface circumferential flaw located just above the head penetration weld, in a plane parallel to the weld itself. [

]^{a,c,e}

[

]^{a,c,e} The results of this calculation are shown in Figure 6-18. From this figure, it can be seen that the time required for propagation of a circumferential flaw to a point where the integrity of the CRDM penetration nozzle would be affected [   ]^{a,c,e} would be about 49 EFPYs. Due to the conservatism in the calculations, i.e., the time period for a surface flaw to become a through-wall flaw was conservatively ignored and therefore the service life is likely to be even longer. In addition, due to uncertainties in the exact composition of the chemical environment in contact with the nozzle OD, a multiplicative factor of 2.0 is used in the CGR for all circumferential surface flaws on the OD of the head penetration nozzles located above the elevation of the J-groove weld.

6.5   FLAW ACCEPTANCE CRITERIA

Now that the projected crack growth curves have been developed, the question remains as to what flaw size would be acceptable for further service.

Acceptance criteria have been developed for indications found during inspection of reactor vessel upper head penetration as part of an industry program coordinated by NEI (formerly NUMARC). Such criteria are normally found in Section XI of the ASME Code, but Section XI does not require in-service inspection of these regions and therefore acceptance criteria were not available. In developing the enclosed acceptance criteria, the approach used was very similar to that used by Section XI, in that an industry consensus was reached using input from both operating utility

technical staff and each of the three PWR vendors. The criteria developed are applicable to all PWR plant designs.

Since the discovery of the leaks at Oconee and ANO-1, the acceptance criteria have been revised slightly to cover flaws on the outside diameter of the penetration below the attachment weld, and flaws in the attachment weld. These revised criteria are now formally endorsed by the NRC [28], and are used in these evaluations. Portions of the acceptance criteria will be noted below.

The criteria presented herein are limits on flaw sizes which are acceptable. The criteria are to be applied to inspection results. It should be noted that determination of the future service during which the criteria are satisfied is plant-specific and dependent on flaw geometry and loading conditions.

It has been previously demonstrated by each of the owners groups that the penetration nozzles are very tolerant of flaws and there is only a small likelihood of flaw extensions to larger sizes. Therefore, it was concluded that complete fracture of the penetration nozzle is highly unlikely. The approach used here is more conservative than that used in Section XI applications where the acceptable flaw size is calculated by placing a margin on the critical flaw size. For the current application, the critical flaw size would be far too large to allow a practical application of the approach used in Section XI applications, so protection against leakage is the priority.

The acceptance criteria presented herein apply to all the flaw types regardless of orientation and shape. Similar to the approach used in Section XI, flaws are first characterized according to established rules and then compared with acceptance criteria.

Flaw Characterization

Flaws detected must be characterized by the flaw length and preferably flaw depth. The proximity rules of Section XI for considering flaws as separate may be used directly (Section XI, Figure IWA 3400-1). This figure is reproduced here as Figure 6-19.

When a flaw is detected, its projections in both the axial and circumferential directions must be determined. Note that the axial direction is always the same for each penetration, but the circumferential direction will be different depending on the angle of intersection of the penetration nozzle with the vessel head. The "circumferential" direction of interest here is along the top of the attachment weld, as illustrated in Figure 6-20. It is this angle which will change for each penetration nozzle and the top of the attachment weld is also the plane which could cause separation of the penetration nozzle from the vessel head. The location of the flaw relative to both the top and bottom of the partial penetration attachment weld must also be determined since a potential leak path exists when a flaw propagates through the penetration nozzle wall and up the penetration nozzle past the attachment weld. Schematic of typical weld geometry is shown in Figure 6-21.

Flaw Acceptance Criteria

The maximum allowable depth (a_f) for axial flaws on the inside surface of the penetration nozzle, at or above the weld is 75 percent of the penetration wall thickness. The term a_f is defined as the

maximum size to which the detected flaw is calculated to grow in a specified time period. This 75 percent limitation was selected to be consistent with the maximum acceptable flaw depth in Section XI and to provide an additional margin against through wall leakage. There is no concern about separation of the penetration nozzle from the vessel head, unless the flaw is above the attachment weld and oriented circumferentially.

Axial inside surface flaws found below the weld are acceptable regardless of depth as long as their upper extremity does not reach the bottom of the weld during the period of service until the next inspection. Axial flaws that extend above the weld are limited to 75 percent of the wall thickness.

Axial flaws on the outside surface of the penetration nozzle below the attachment weld are acceptable regardless of depth, as long as they do not extend into the attachment weld during the period of service until the next inspection. Outside surface flaws above the attachment weld must be evaluated on a case by case basis, and must be discussed with the regulatory authority.

Circumferential flaws located below the weld are acceptable regardless of their depth, provided the length is less than 75 percent of the penetration nozzle circumference for the period of service until the next inspection. Circumferential flaws detected in this area have no structural significance except that loose parts must be avoided. To this end, intersecting axial and circumferential flaws shall be removed or repaired. Circumferential flaws at and above the weld must be discussed with the regulatory authority on a case by case basis.

Surface flaws located in the attachment welds themselves are not acceptable regardless of their depth. This is because the crack growth rate of the weld material is several times faster than that of the Alloy 600 material, and also because depth sizing capability does not yet exist for indications in the attachment weld.

The flaw acceptance criteria are summarized in Table 6-1. Flaws that exceed these criteria must be repaired unless analytically justified for further service. These criteria have been reviewed and endorsed by the NRC, as documented in references [28, 29, 30] and are also shown in Table IWB-3663-1 in Section XI of the 2004 Edition of the ASME Code [31].

It is expected that the use of these criteria and crack growth curves will provide conservative predictions of the allowable service time.

Table 6-1   Summary of Reactor Vessel Head Penetration Flaw Acceptance Criteria

Location	Axial		Circumferential	
	a_f	ℓ	a_f	ℓ
Below Weld (ID)	t	no limit	t	0.75 circ.
At and Above Weld (ID)	0.75 t	no limit	repair	repair
Below Weld (OD)	t	no limit	t	0.75 circ.
Above Weld (OD)	repair	repair	repair	repair

Notes: Surface flaws of any size in the attachment weld are not acceptable.

a_f =   Flaw Depth
ℓ =   Flaw Length
t =   Wall Thickness

Table 6-2   STP Head Penetration Geometries [1]

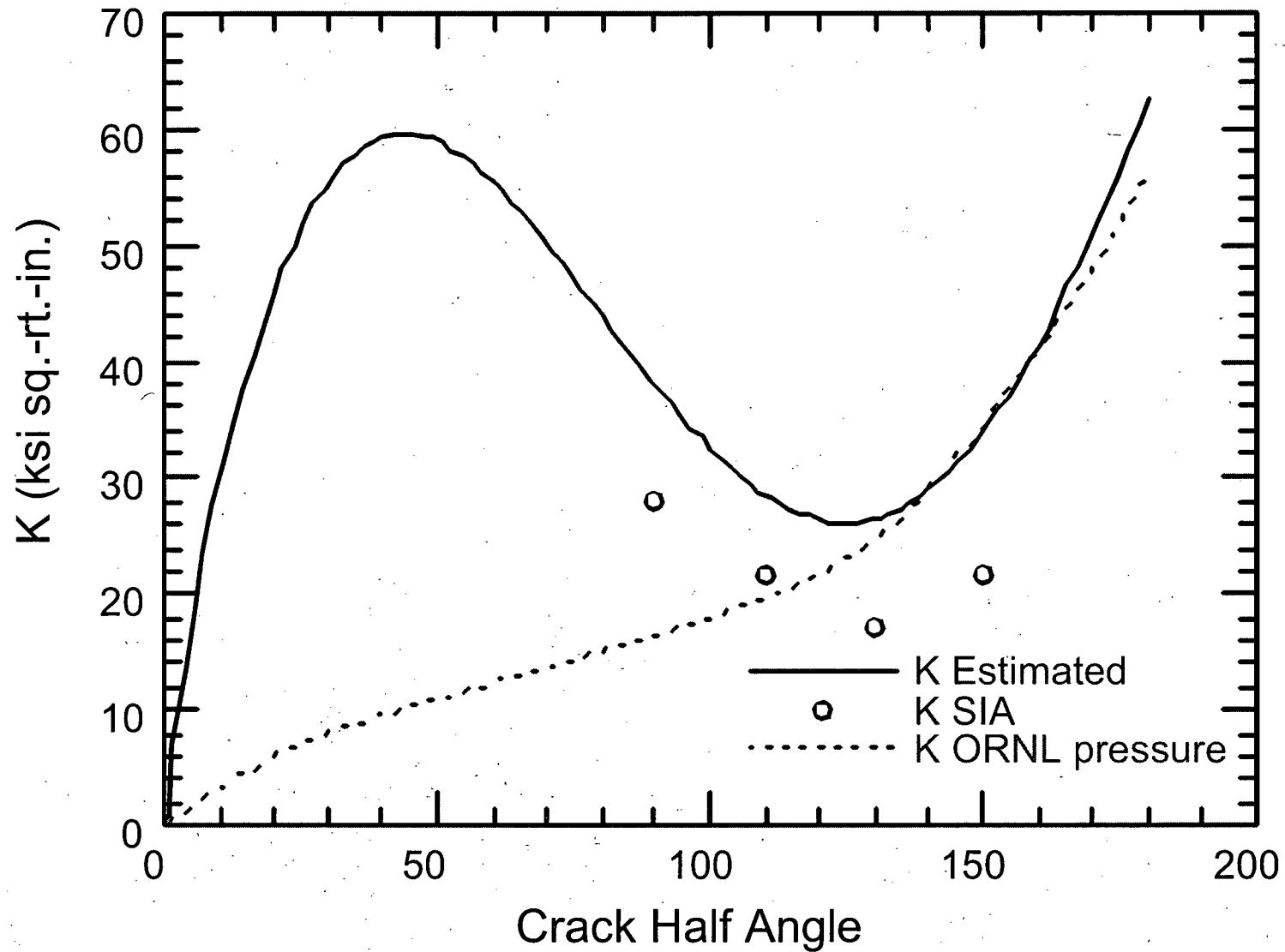| Penetration Type	Wall Thickness (in.)	Penetration OD (in.)
CRDM	0.625	4.000
Head Vent	0.250	1.315
Gas Vent	0.433	3.490

Figure 6-1   Stress Intensity Factor for a Through-Wall Circumferential Flaw in a Head Penetration
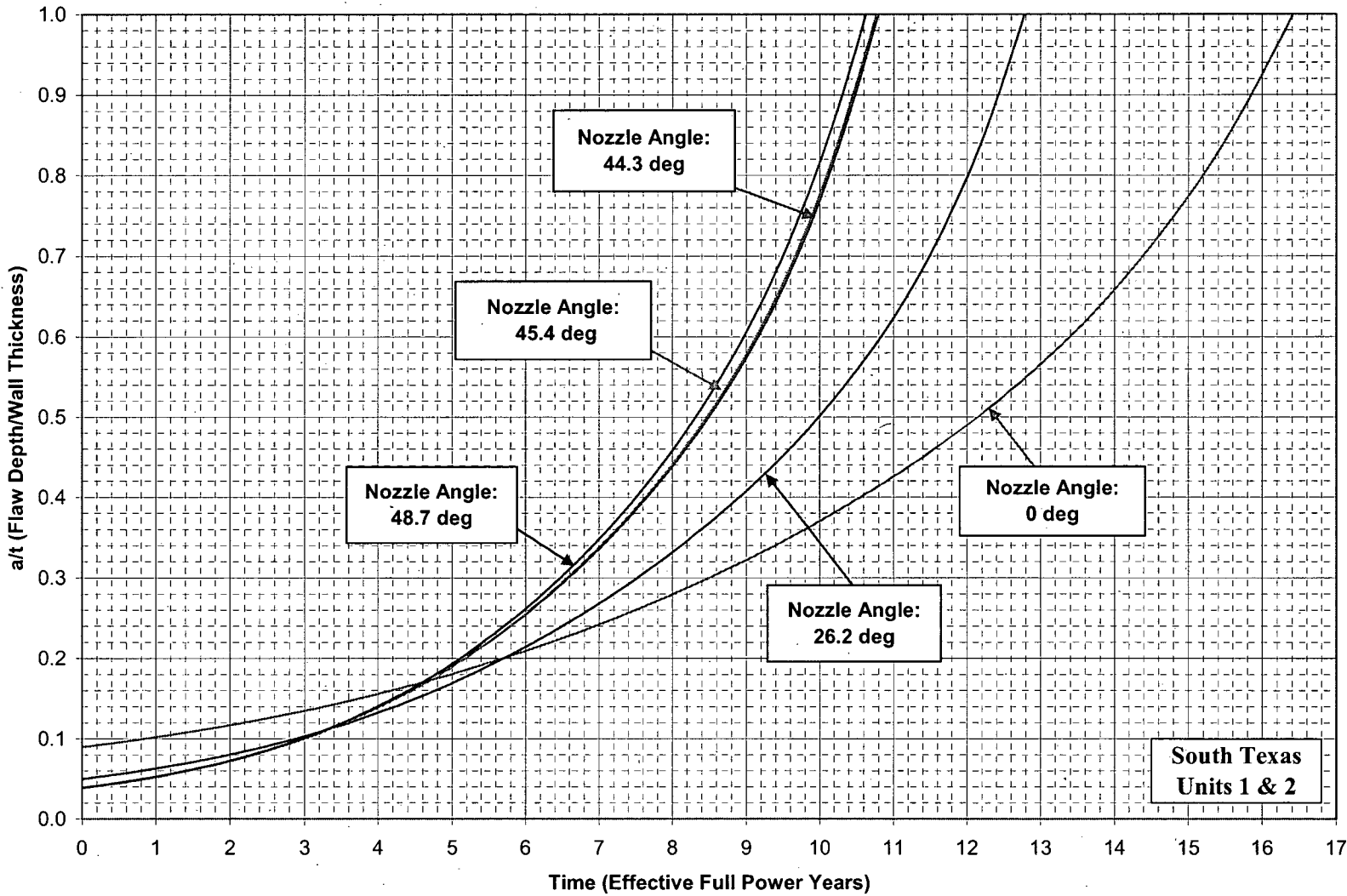
Figure 6-2 Inside, Longitudinal Surface Flaws, 0.5" Below the Attachment Weld, Nozzle Uphill Side - Crack Growth Predictions for STP
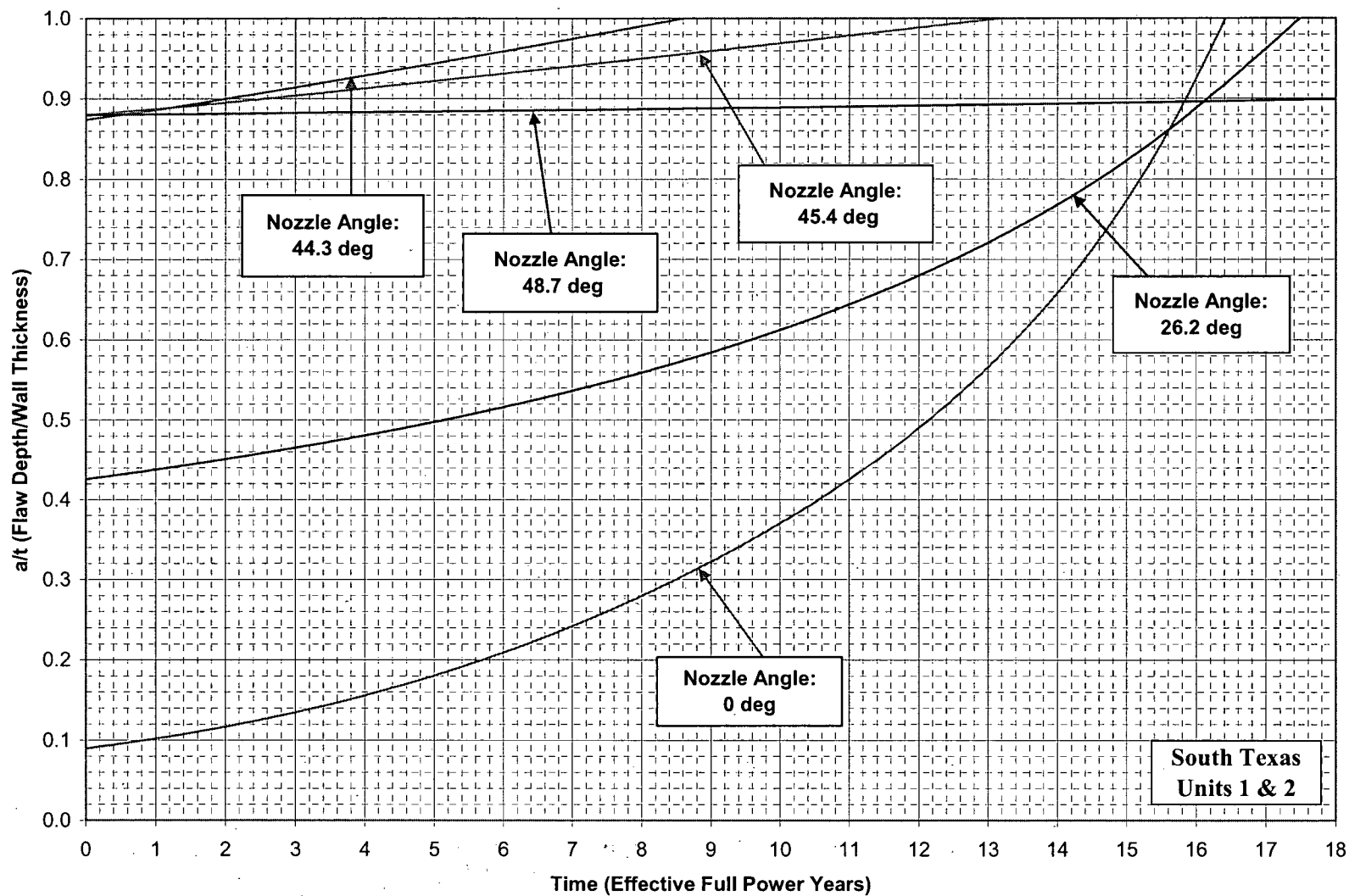
Figure 6-3   Inside, Longitudinal Surface Flaws, 0.5" Below the Attachment Weld, Nozzle Downhill Side - Crack Growth Predictions for STP
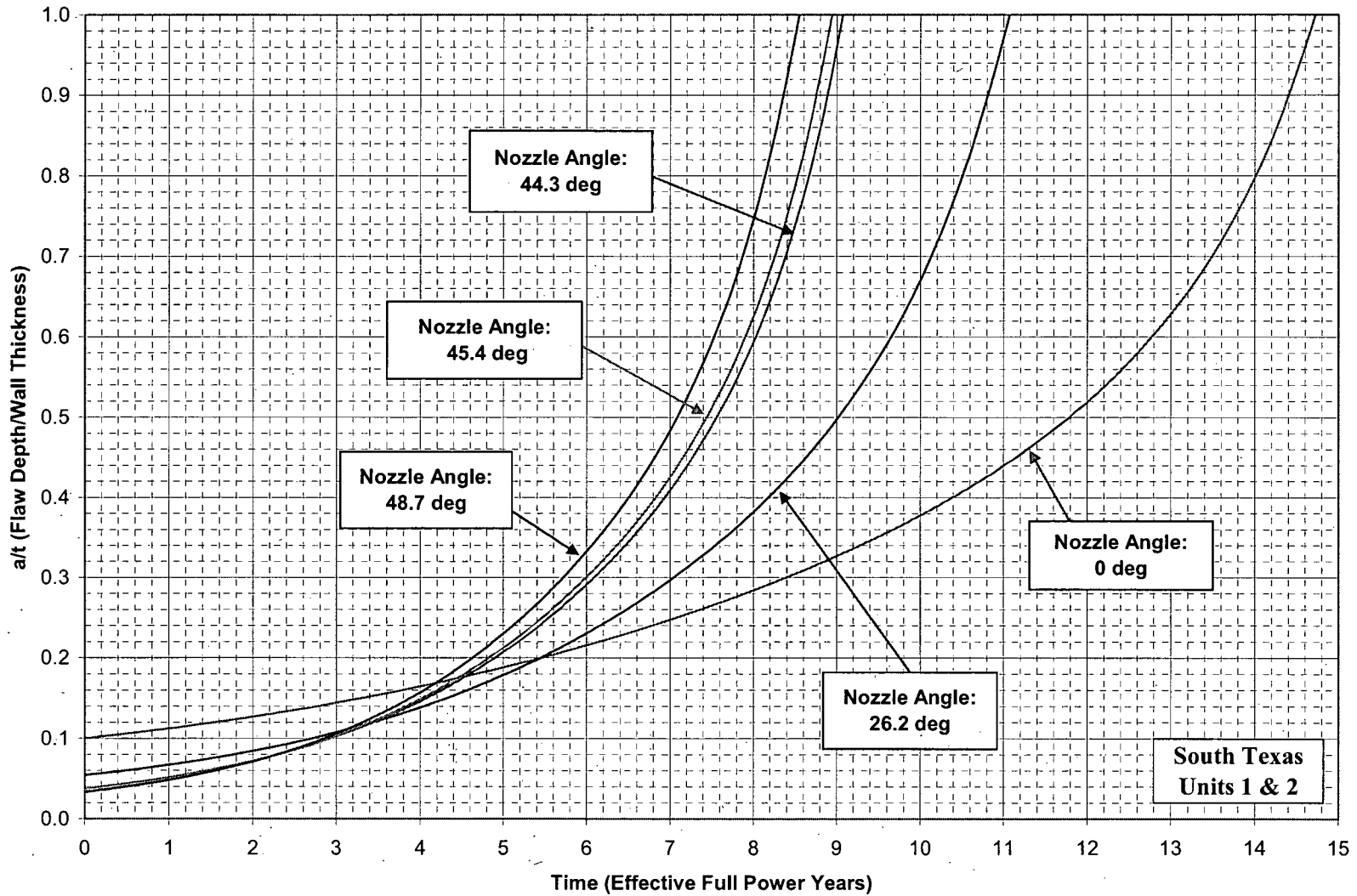
Figure 6-4   **Inside, Longitudinal Surface Flaws, At the Attachment Weld, Nozzle Uphill Side - Crack Growth Predictions for STP**
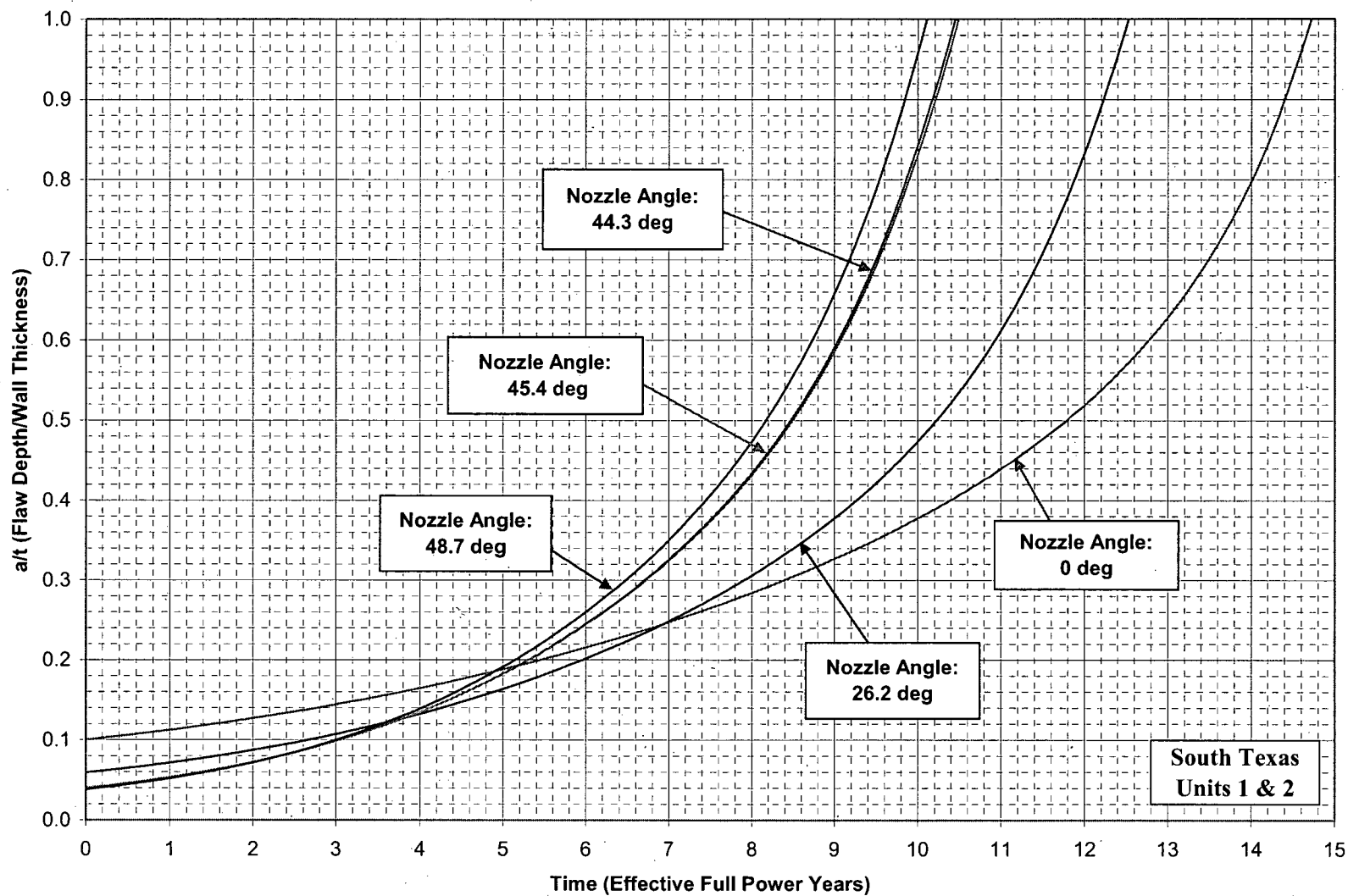
Figure 6-5   Inside, Longitudinal Surface Flaws, At the Attachment Weld, Nozzle Downhill Side - Crack Growth Predictions for STP
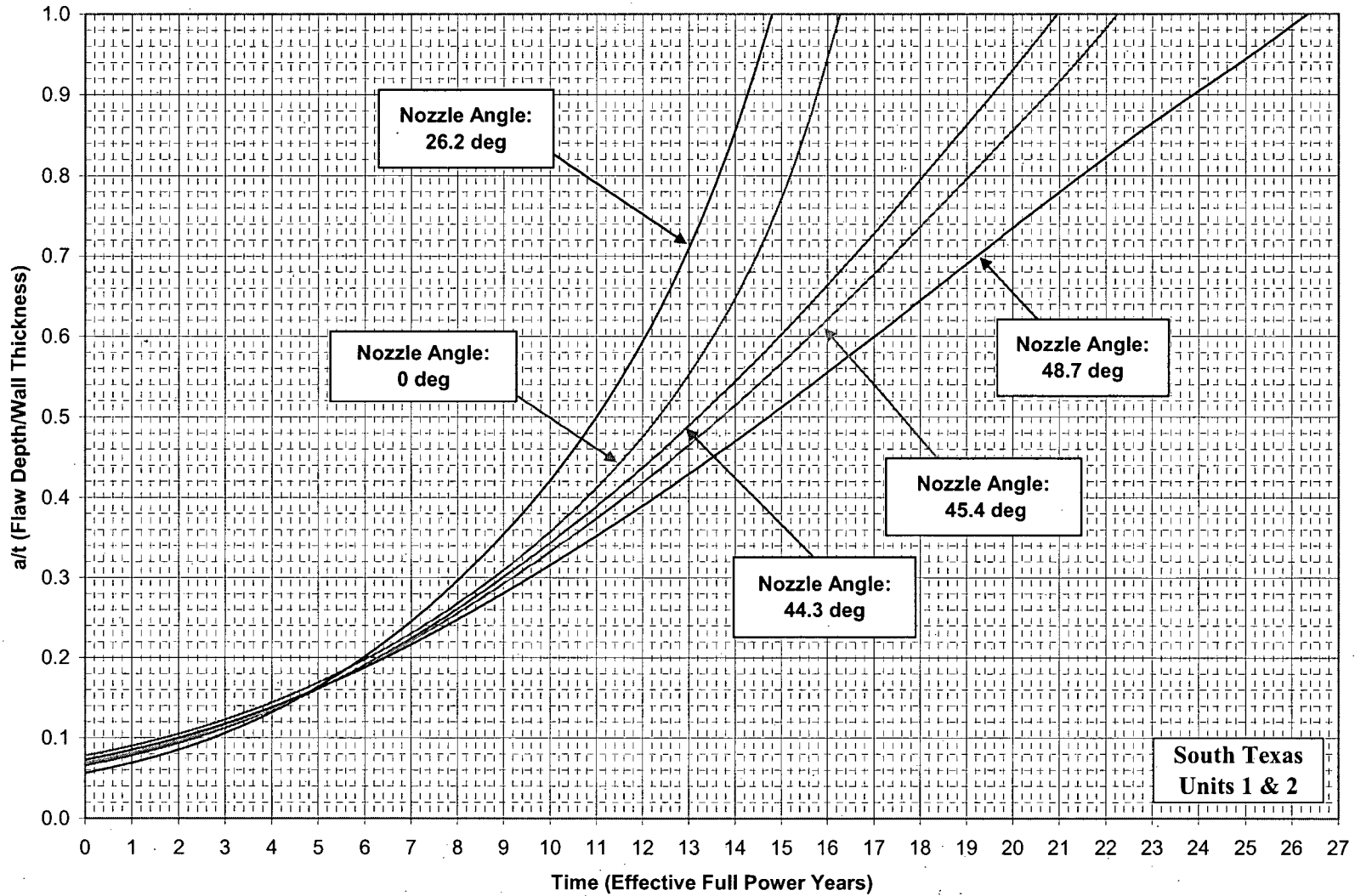
Figure 6-6   Inside, Longitudinal Surface Flaws, 0.5" Above the Attachment Weld, Nozzle Uphill Side - Crack Growth Predictions for STP
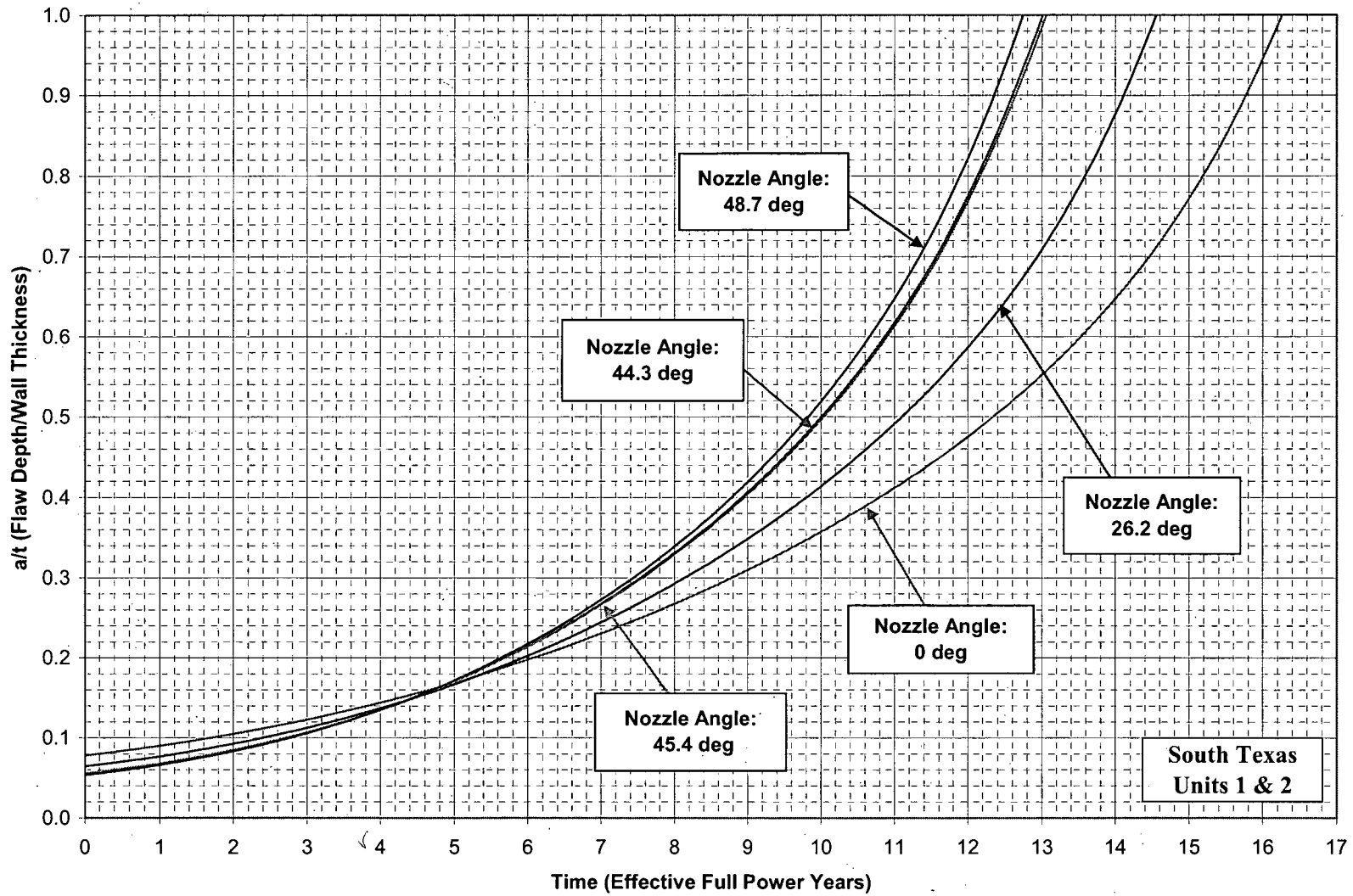
Figure 6-7   Inside, Longitudinal Surface Flaws, 0.5" Above the Attachment Weld, Nozzle Downhill Side - Crack Growth Predictions for STP
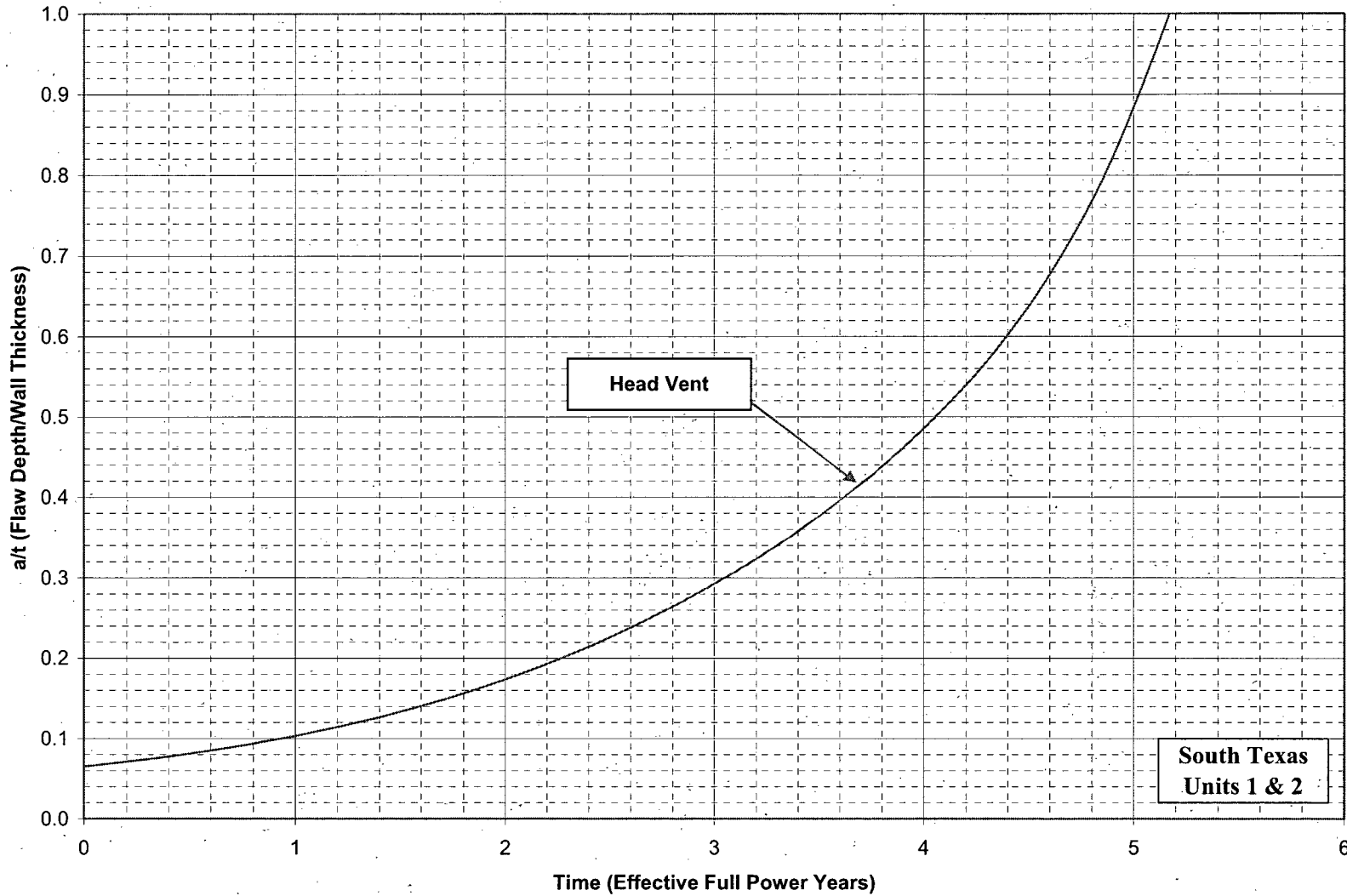
Figure 6-8   Inside, Longitudinal Surface Flaws, At the Attachment Weld, Head Vent- Crack Growth Predictions for STP
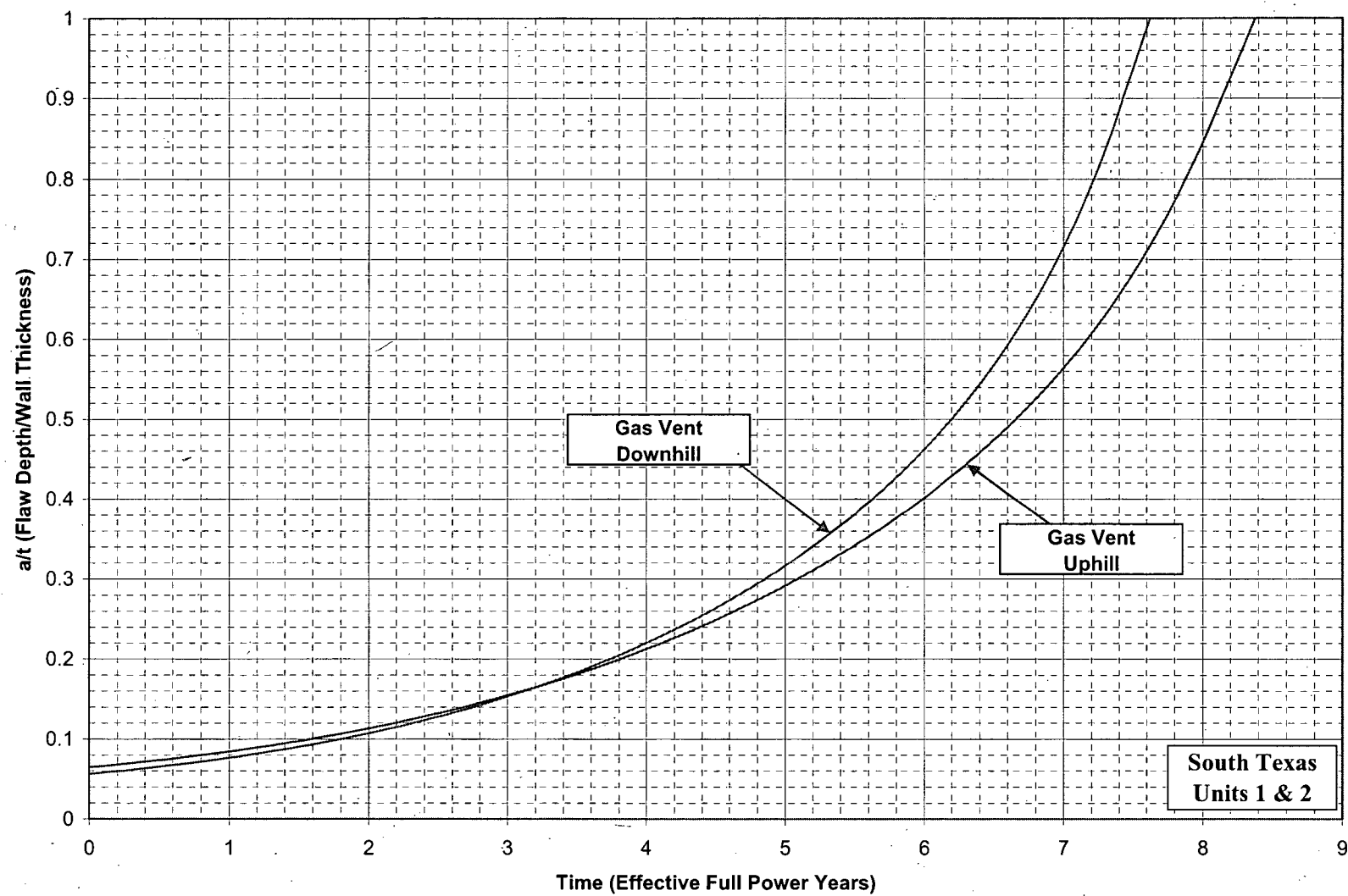
Figure 6-9   Inside, Longitudinal Surface Flaws, At the Attachment Weld, Gas Vent- Crack Growth Predictions for STP

Figure 6-10   Outside, Longitudinal Surface Flaws, Below the Attachment Weld, Nozzle Uphill Side - Crack Growth Predictions for STP
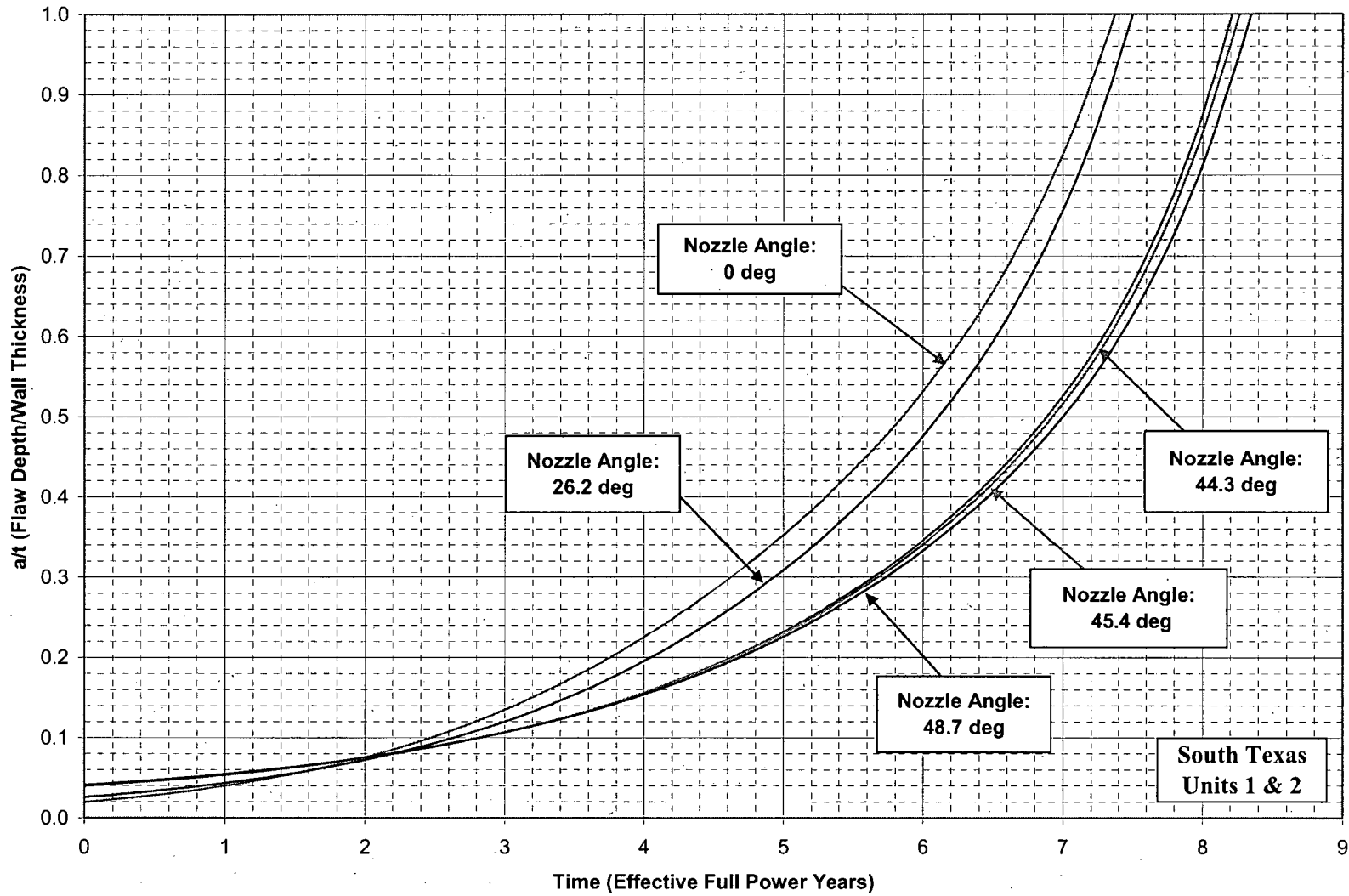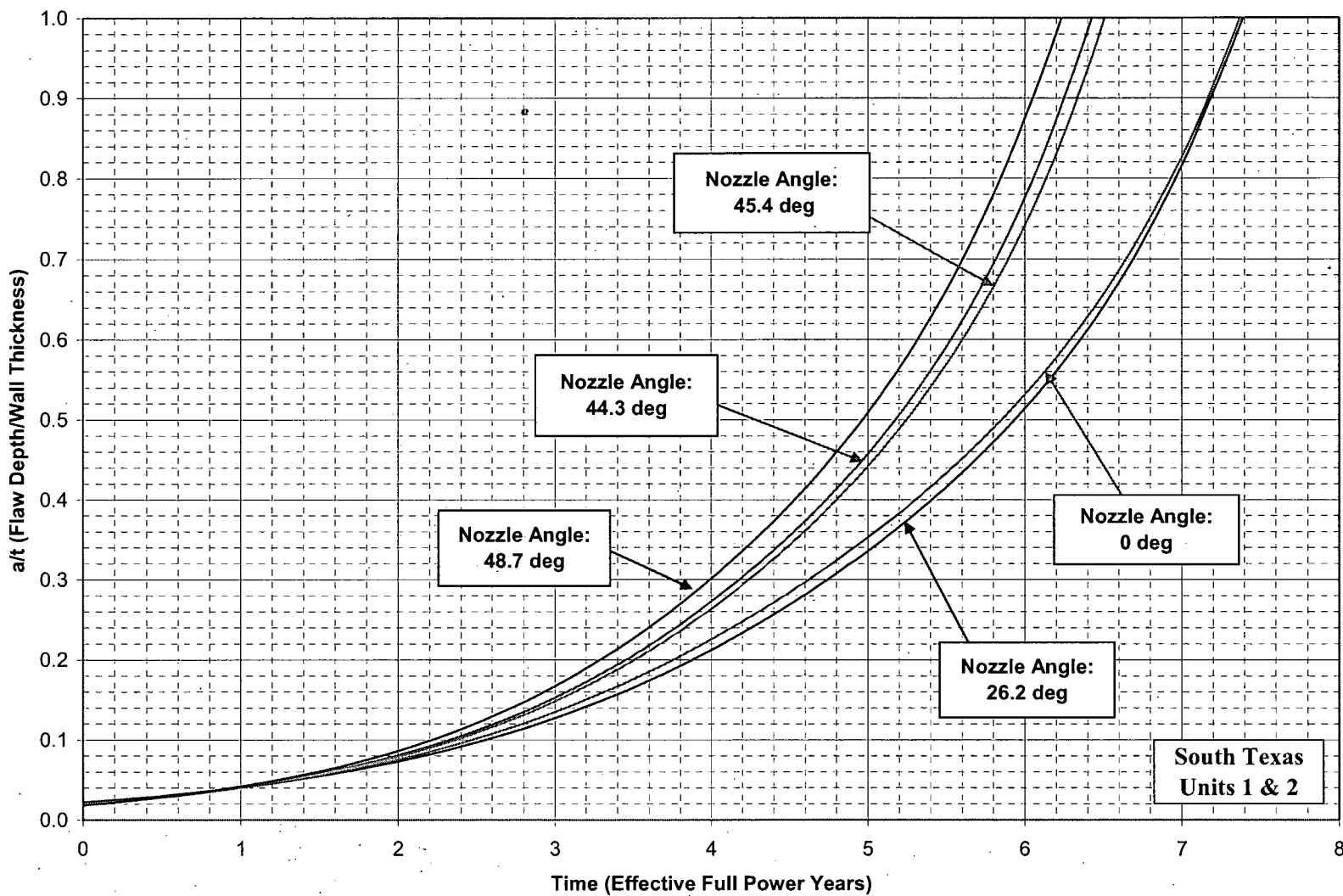
Figure 6-11   Outside, Longitudinal Surface Flaws, Below the Attachment Weld, Nozzle Downhill Side - Crack Growth Predictions for STP
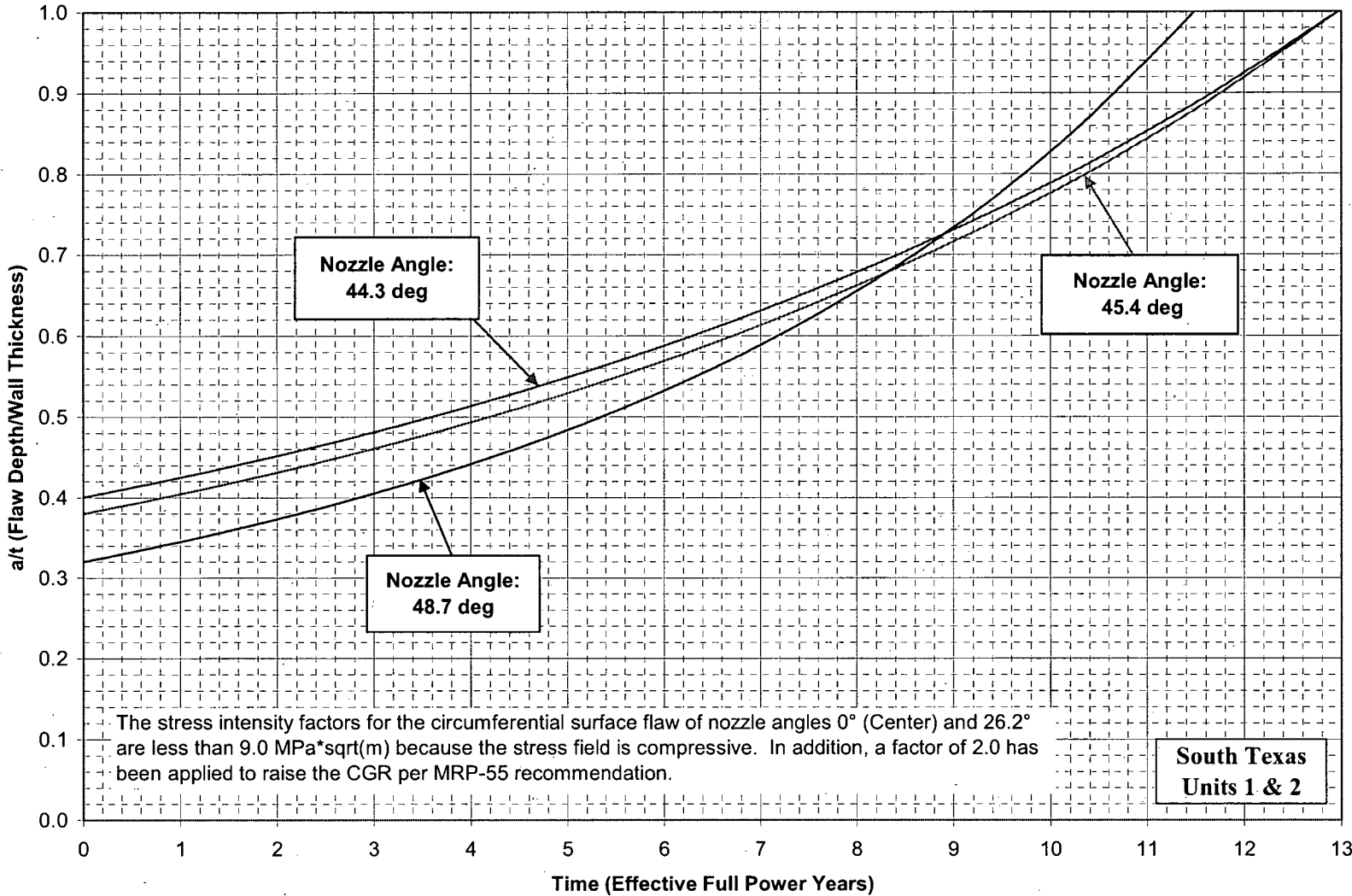
Figure 6-12   **Outside, Circumferential Surface Flaws, Along the Top of the Attachment Weld - Crack Growth Predictions for STP (MRP Factor of 2.0 Included)**
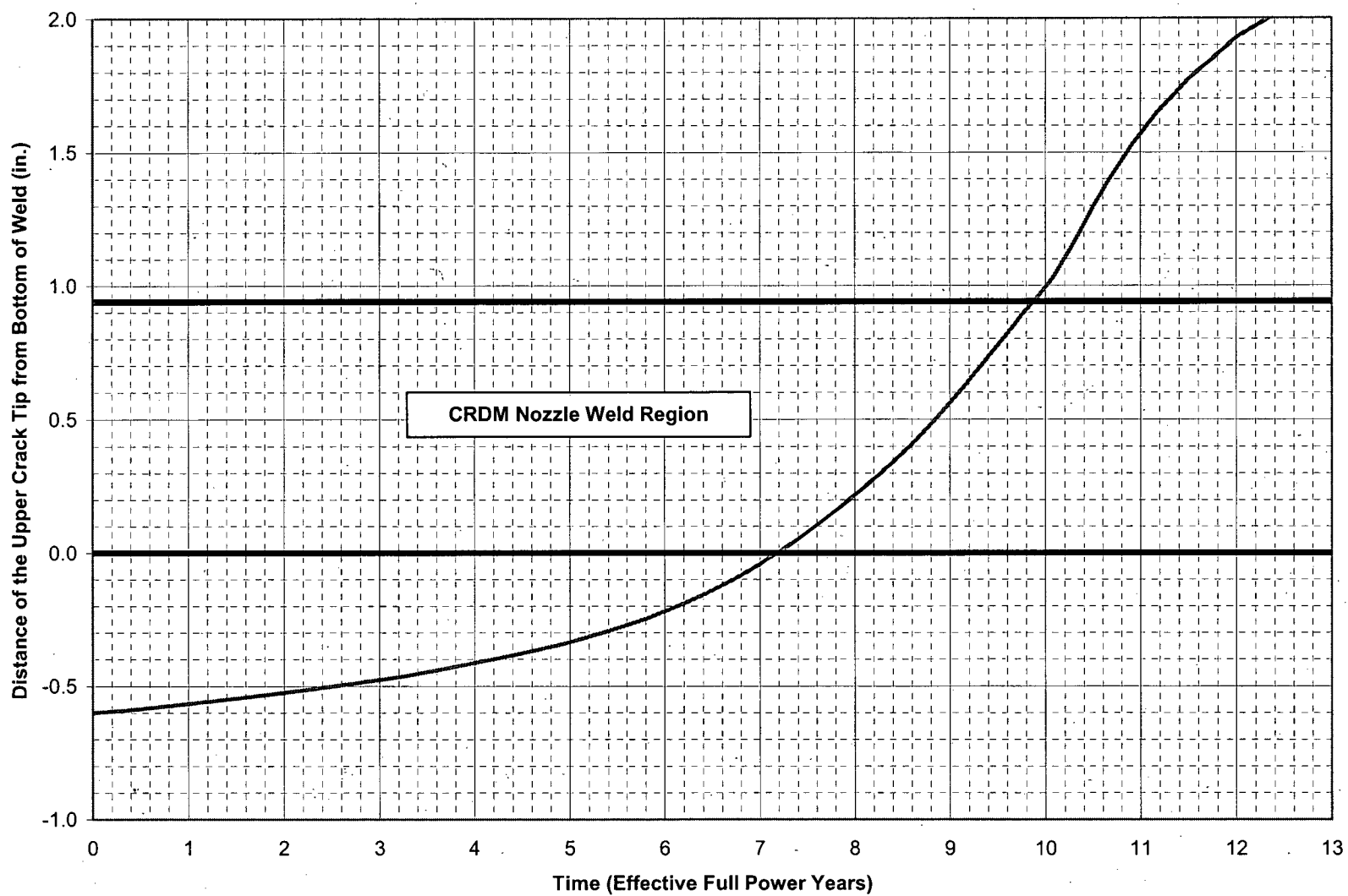
Figure 6-13   Through-Wall Longitudinal Flaws Located in the Center CRDM (0.0 Degrees) Penetration - Crack Growth Predictions for STP
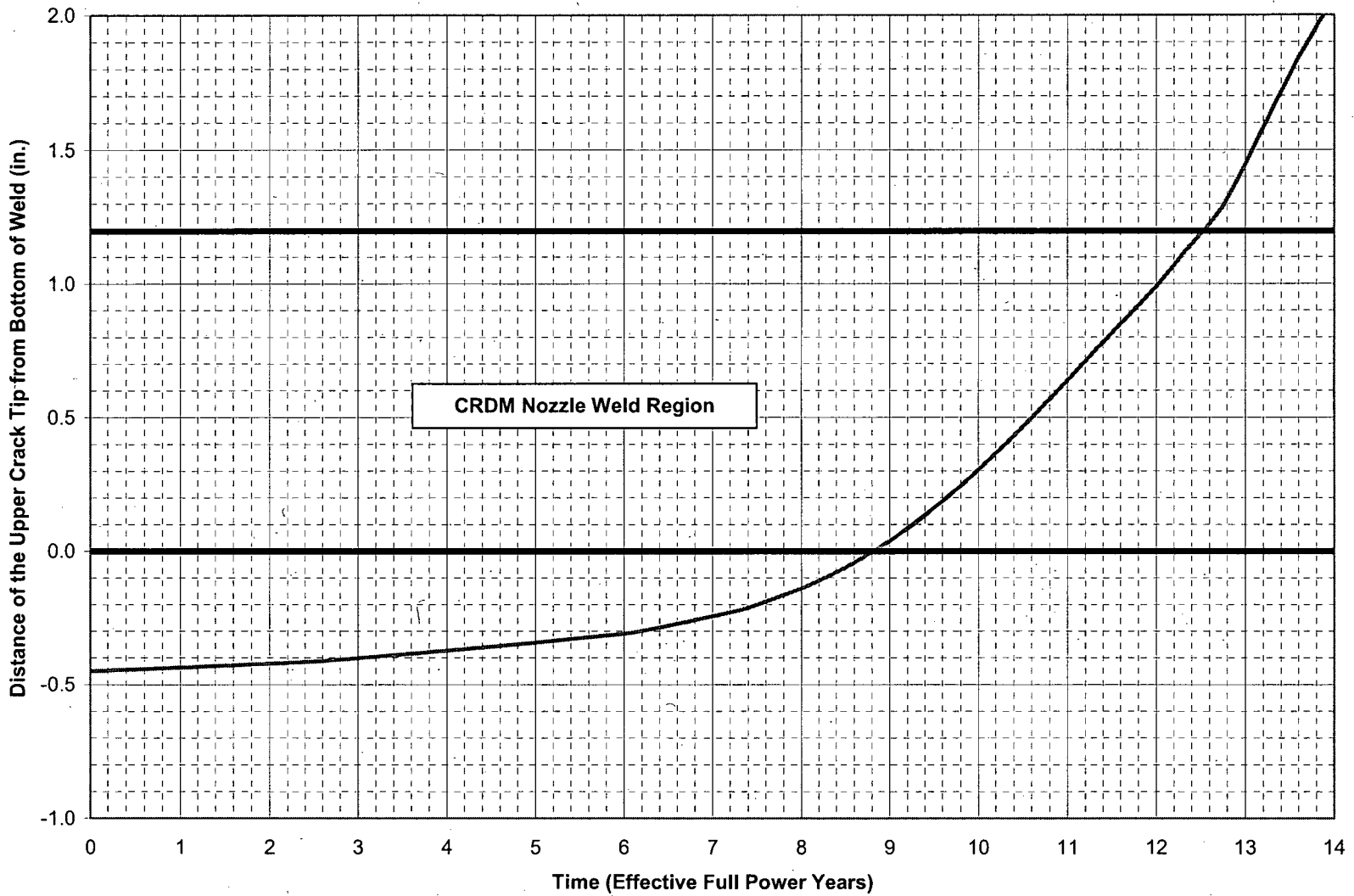
Figure 6-14 Through-Wall Longitudinal Flaws Located in the 26.2 Degrees CRDM Row of Penetrations, Downhill Side - Crack Growth Predictions for STP
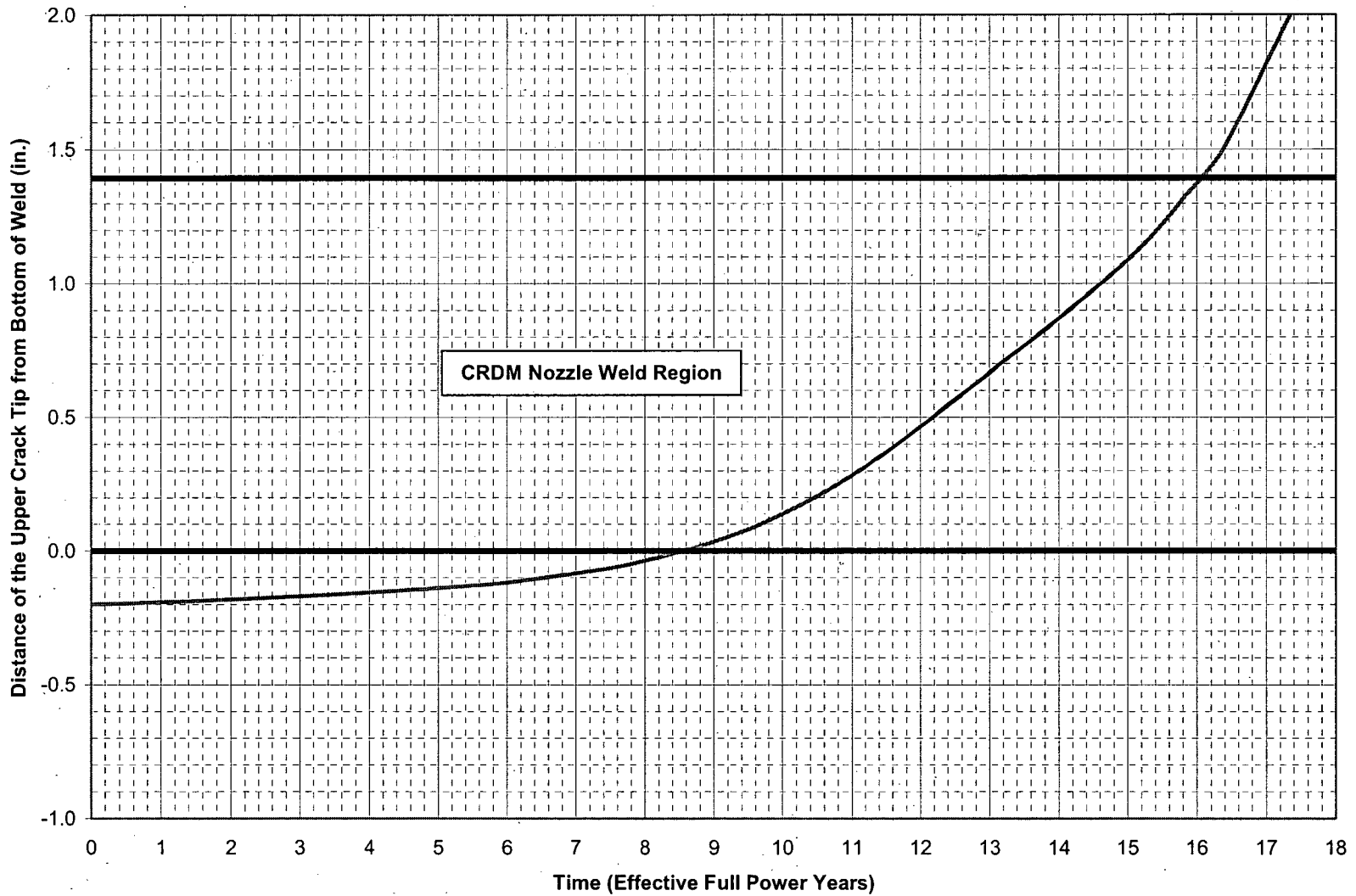
Figure 6-15 **Through-Wall Longitudinal Flaws Located in the 44.3 Degrees CRDM Row of Penetrations, Downhill Side - Crack Growth Predictions for STP**
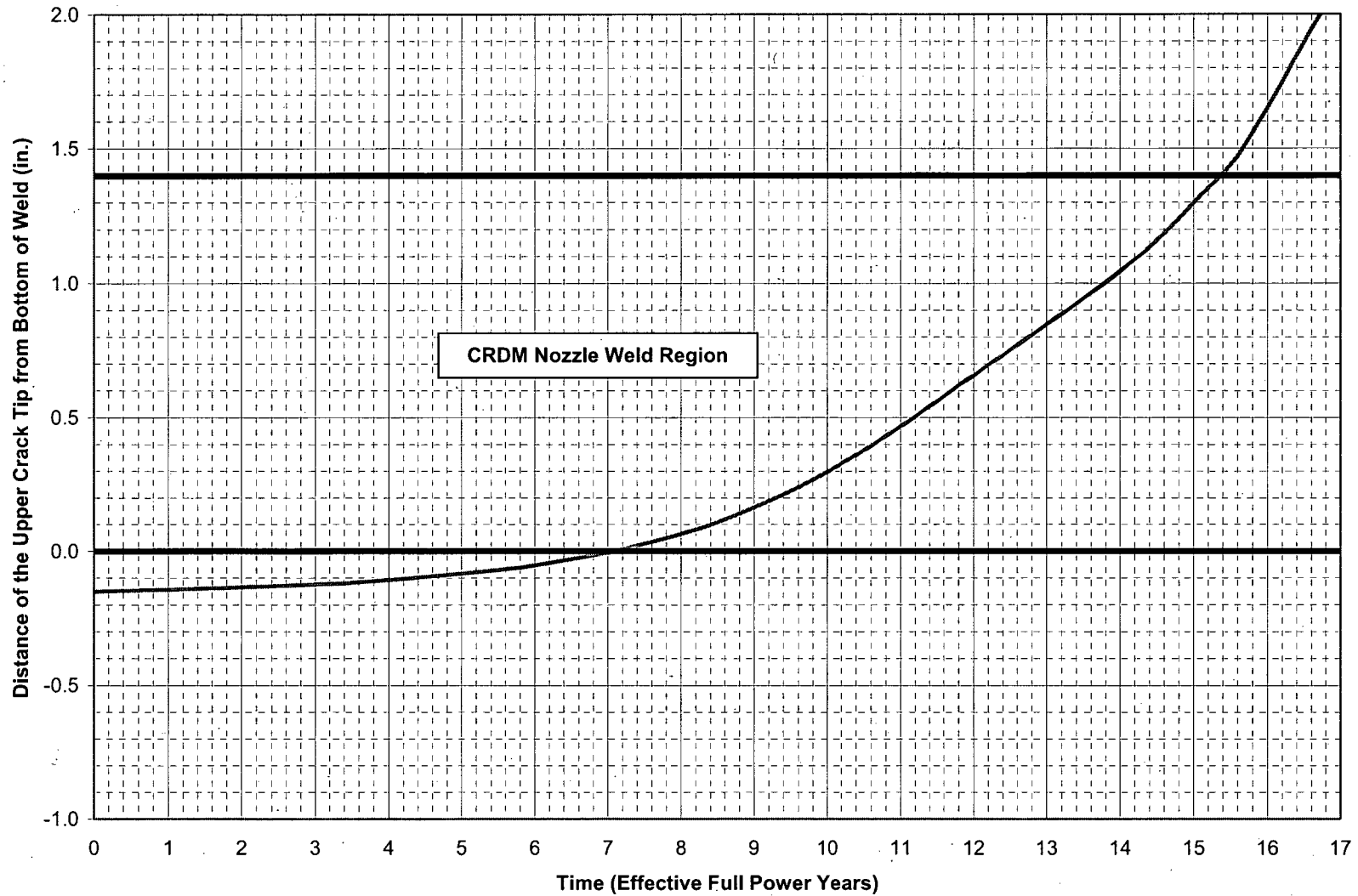
Figure 6-16   Through-Wall Longitudinal Flaws Located in the 45.4 Degrees CRDM Row of Penetrations, Downhill Side - Crack Growth Predictions for STP
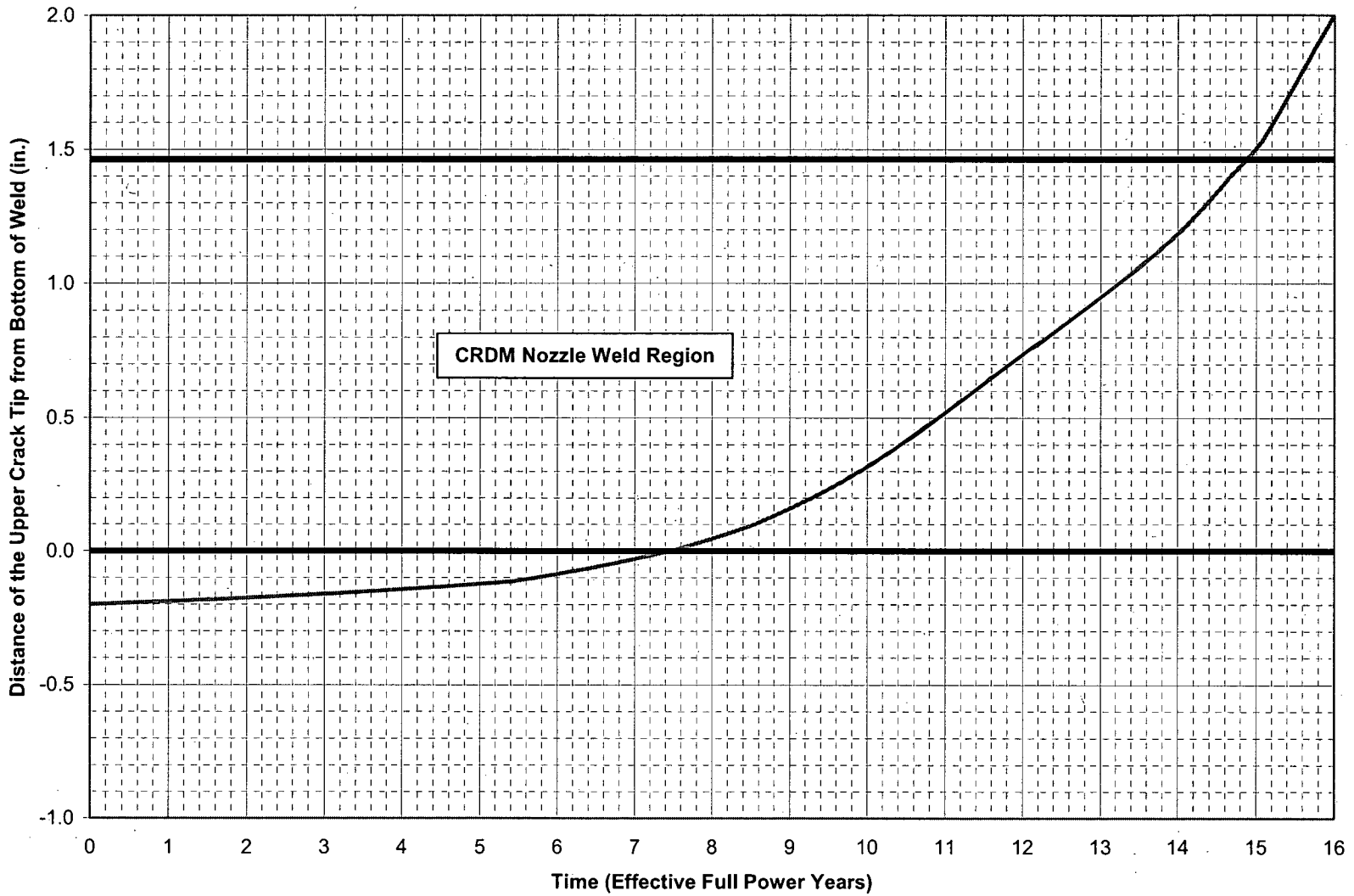
Figure 6-17   **Through-Wall Longitudinal Flaws Located in the 48.7 Degrees CRDM Row of Penetrations, Downhill Side - Crack Growth Predictions for STP**
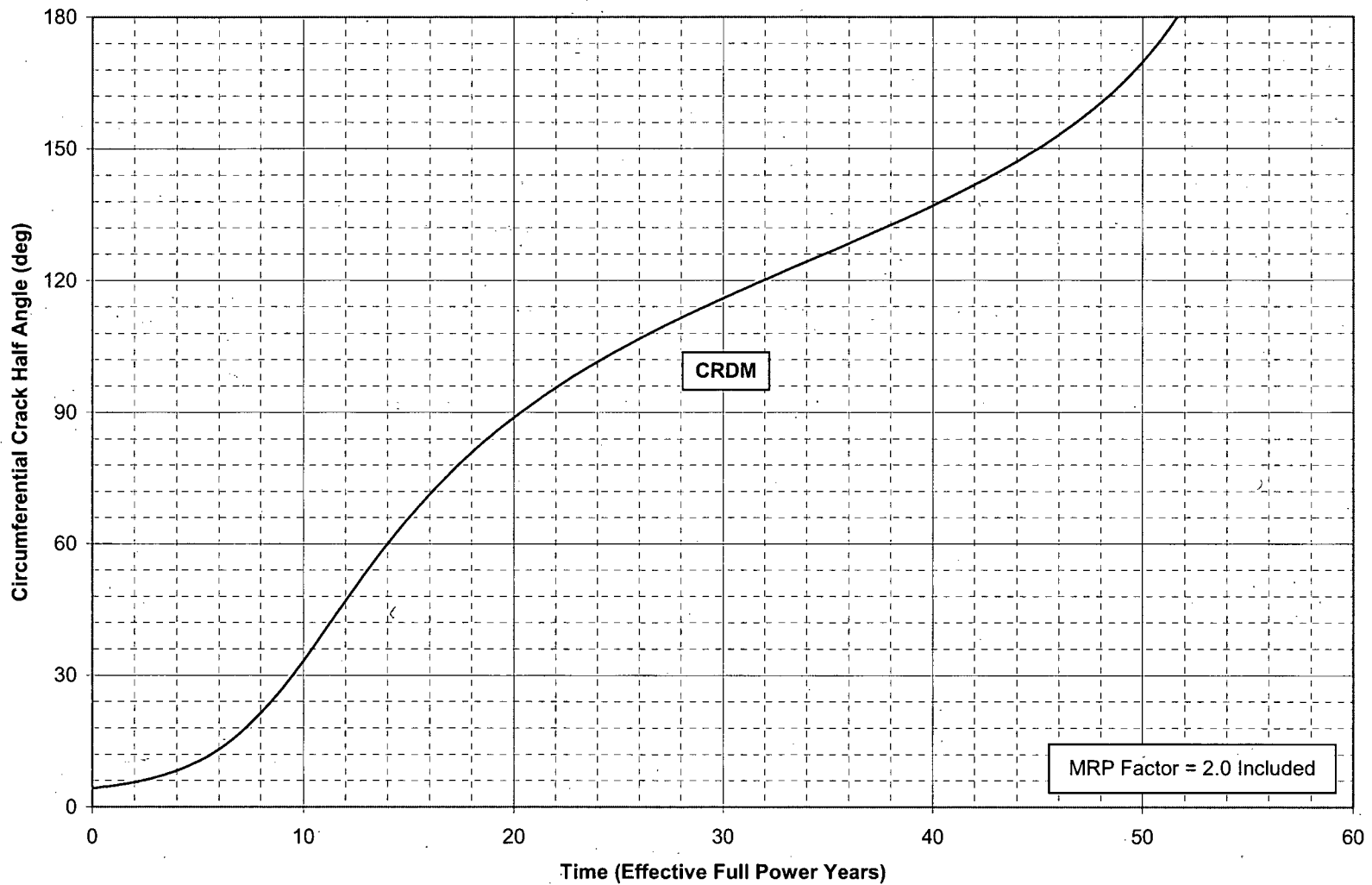
Figure 6-18   Through-Wall Circumferential Flaws Near the Top of the Attachment Weld for CRDM Nozzles - Crack Growth Predictions
for STP (MRP Factor of 2.0 Included)

(a) Single Linear Flaw

(b) Single Curvilinear Flaw

(c) Aligned Linear Flaws
$$\ell_1 \geqslant \ell_2$$

(d) Nonoverlapping Flaws
$$\ell_1 \geqslant \ell_2$$

(e) Overlapping Parallel Flaws

(f) Overlapping Flaws

(g) Nonaligned Parallel Flaws
$$\ell_1 \geqslant \ell_2$$

(h) Multiple Parallel Flaws

Figure 6-19   ASME Section XI Flaw Proximity Rules for Surface Flaws (Figure IWA-3400-1)
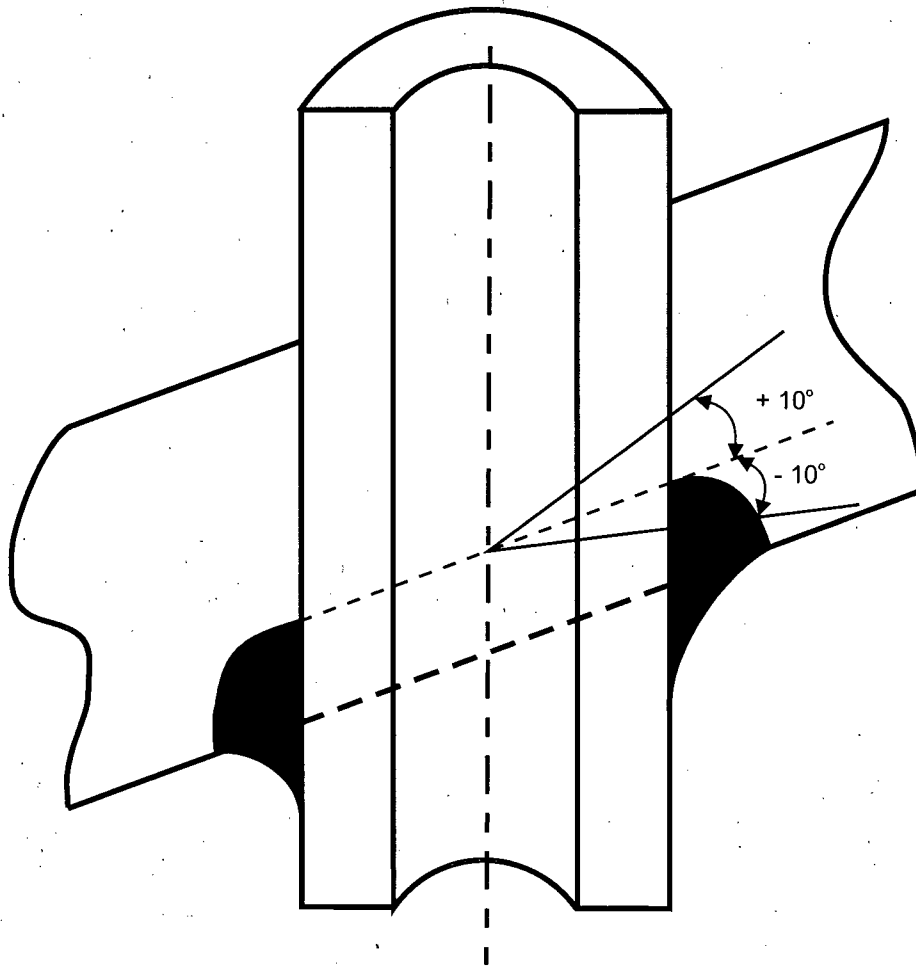
Figure 6-20   Definition of "Circumferential"
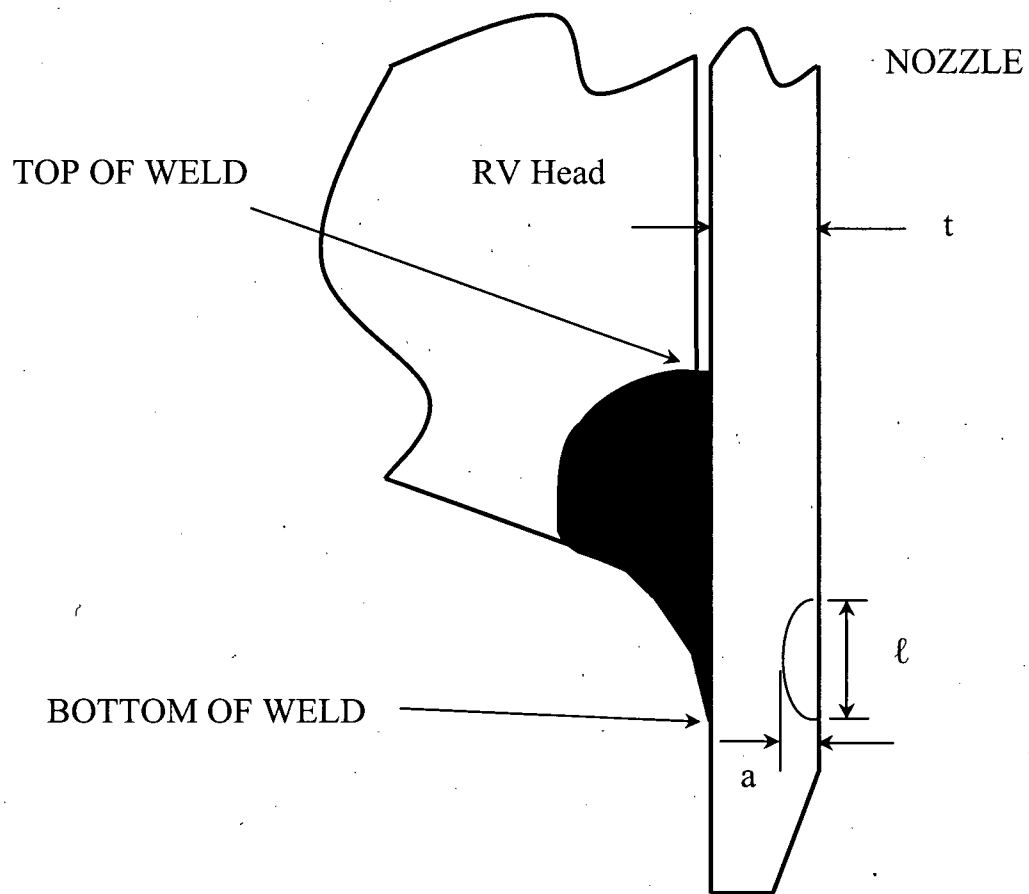
Figure 6-21   Schematic of Head Penetration Geometry

7   SUMMARY AND EXAMPLE PROBLEMS

An extensive evaluation has been carried out to characterize the loadings and stresses, which exist in the STP reactor vessel head penetrations. Three-dimensional finite element models were constructed [3], and all pertinent loadings on the penetrations were analyzed. These loadings included internal pressure and thermal expansion effects typical of steady state operation. In addition, residual stresses due to the welding of the penetrations to the vessel head were considered.

Results of the analyses reported here are consistent with the axial orientation and location of flaws which have been found in service in a number of plants and the largest stress component is the hoop stress, and the maximum stresses were found to exist at the attachment weld. The most important loading conditions were fo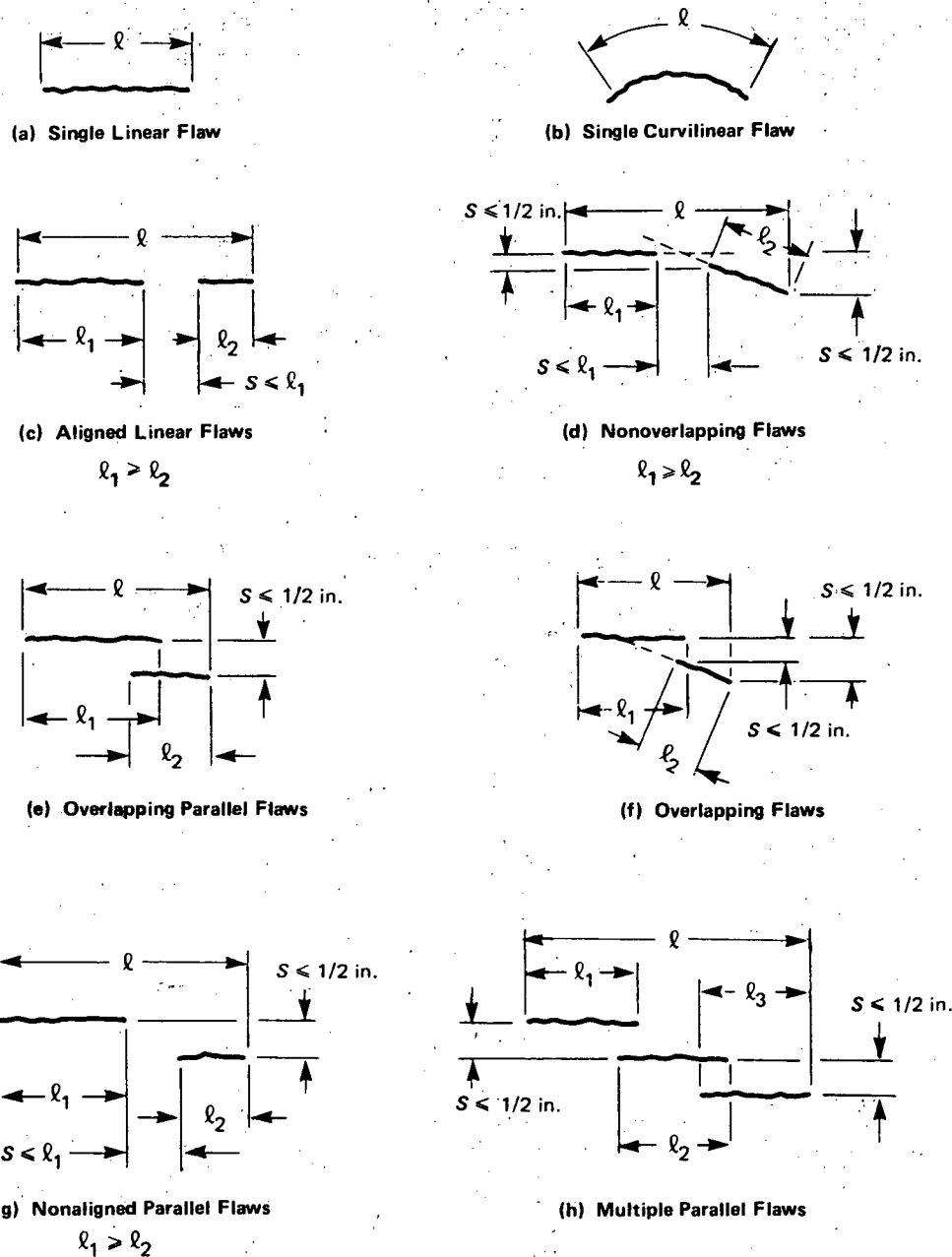und to be those which exist on the penetration for the majority of the time, which are the steady state loading and the residual stresses.

These stresses are important because the cracking observed to date in operating plants has been determined to result from PWSCC. These stresses were used in the fracture calculations to predict the future growth of flaws postulated to exist in the head penetrations. A crack growth rate was calculated specifically for the operating temperature of the reactor vessel head at STP based on the EPRI recommendation, which is consistent with laboratory data as well as crack growth results for operating plants.

The crack growth predictions contained in Section 6 show that the future growth of cracks that might be found in the penetrations will be typically moderate; however, a number of EFPYs would be required for any significant crack extensions. The propagation of circumferential flaws is much slower than that of axial flaws since the stresses responsible for cracking in the circumferential direction (axial stresses) are relatively small in comparison to the hoop stresses responsible for cracking in the axial direction.

7.1   SAFETY ASSESSMENT

It is appropriate to examine the safety consequences of an indication that might be found. The indication, even if it were to propagate through the penetration nozzle wall, would have only minor consequences, since the pressure boundary would not be broken, unless it were to propagate above the weld.

Further propagation of the indication would not change its orientation, since the hoop stresses in the penetration nozzle are much larger than the axial stresses. Therefore, it is extremely unlikely that the head penetration would be severed.

If the indication were to propagate to a position above the weld, a leak could result, but the magnitude of such a leak would be very small, because the crack could not open significantly due to the tight fit between the penetration nozzle and the vessel head. Such a leak would have no immediate impact on the structural integrity of the system, but could lead to wastage in the ferritic steel of the vessel head, as the borated primary water concentrates due to evaporation. Davis-Besse has demonstrated the consequence of ignoring such leaks.   (

Any indication is unlikely to propagate very far up the penetration nozzle above the weld, because the hoop stresses decrease in this direction, and this will cause it to slow down, and to stop before it reaches the outside surface of the head.

The high likelihood that the indication will not propagate up the penetration nozzle beyond the vessel head ensures that no catastrophic failure of the head penetration will occur, since the indication will be enveloped in the vessel head itself, which precludes the opening of the crack and limits leakage.

It should be noted that the objective of the acceptance criteria shown in Table 6-1 is to prevent leakage. Therefore, even though a small leak may have no immediate impact on the structural integrity of the system, it is not acceptable to the NRC and nozzle repair is required.

7.2   EXAMPLE PROBLEMS

The flaw tolerance charts in Figures 6-2 through 6-18 can be used with the acceptance criteria of Section 6.5 to determine the available service life in EFPYs for STP. In this section, a few examples will be presented to illustrate the use of these figures. The example cases are listed in Table 7-1.

Example 1. Determine the service life of an axially oriented inside surface flaw whose upper extremity is located 1.25" below the weld on the uphill side of penetration no. 22. First, the penetration locality angle is obtained from Table 1-1 and, in this case, the locality angle is 26.2 degrees. The initial flaw depth, $a_{initial}$, is 0.078" and the initial flaw length, $2c_{initial}$, is 0.195". Assuming that the initial aspect ratio of 2.5:1 (i.e., 0.195"/0.078") is maintained throughout the time that the inside surface flaw becomes a through-wall flaw, then the final length of the flaw ($2c_{final}$) will be the CRDM wall thickness (t = 0.625") multiplied by the aspect ratio (2.5) = 1.563". The upper extremity of the flaw is now located 1.25" − (1.563" − 0.195") / 2 = 0.566" below the weld and validates the use of a single crack growth curve, which is applicable to flaws located 0.5 inch or more below the attachment weld. The crack growth curve for the 26.2 degrees nozzle angle of Figure 6-2 is applicable and Figure 6-2 has been reproduced as Figure 7-1. The flaw is initially 12.5 percent (0.078"/0.625") of the wall thickness, and a straight line is drawn horizontally at a/t = 0.125 that intersects the crack growth curve. Using the acceptance criteria in Table 6-1, the service life can then be determined as the remaining time for this flaw to grow to the limit of 100 percent of the wall thickness or approximately 9.0 EFPYs (labeled as "Service Life" in Figure 7-1).

Example 2. In this case, the flaw is identical in size to that used in Example 1, but located on the outside surface and on the downhill side of penetration no. 22. This flaw, just as the flaw in Example 1, will not propagate within 0.5 inch below the bottom of the weld region. The applicable curve to use is Figure 6-11. The ratio a/t and initial reference time are likewise found using the same approach as used in Example 1. Using the acceptance criteria in Table 6-1, the determination of service life is illustrated in Figure 7-2, where we can see that the result is approximately 4.4 EFPYs.

Example 3. An axial inside surface flaw is located at the weld and on the downhill/uphill side of penetration no. 1. The initial length of the flaw is 0.250" and the initial depth is 0.05". From Table 1-1, the angle of this penetration nozzle is 0 degrees. The applicable curve is Figure 6-4 or Figure 6-5, and Figure 6-5 is reproduced here as Figure 7-3. In this case, the initial flaw depth is 8.0 percent (0.05"/0.625") of the wall thickness. The initial reference time can be found by drawing a horizontal line at a/t = 0.08. Since the as-found flaw depth is less than the initial flaw depth shown in Figure 6-5, the initial flaw depth shown is conservatively used. As a result, the initial reference time is set at 0 EFPY as shown in Figure 7-3. Using the acceptance criteria in Table 6-1, the allowable service life can then be determined as the time for the flaw to reach a depth of 75 percent of the wall thickness. The final reference time is found through a horizontal line drawn at a/t = 0.75. The service life can be determined through the intersection points of these lines and the crack growth curve. The resulting service life is approximately 13.8 EFPYs, as shown in Figure 7-3.

Example 4. In this case, we have postulated an axial inside surface flaw with an upper extremity located 1.0 inch below the attachment weld on the uphill side of penetration no. 75 (48.7 degrees). The flaw has an initial depth of 0.079" and an initial length of 0.395". Assuming that the initial aspect ratio of 0.395" / 0.079" or 5:1 is maintained as the flaw propagates into the nozzle wall, the final length of a through-wall flaw would be 0.625" x 5 = 3.125" long. The location of the upper extremity of this flaw would have reached within 0.5 inch below the weld as it propagates into the nozzle wall: 1.0" – (3.125" - 0.395") / 2 = -0.365". Therefore the evaluation will require the use of two flaw charts. The first step is to estimate the time required for the initial flaw to grow to within 0.5 inch from the weld. This can be accomplished with the use of Figure 6-2 and is reproduced here as Figure 7-4a. The upper extremity is 1 inch below the weld and is assumed to grow until the extremity is 0.5 inches below the weld. The final half-length of the flaw when it reaches 0.5 inches below the weld will be the sum of the initial half-length and the 0.5 inches it has grown or 0.395" / 2 + 0.5" = 0.698". Multiplying this by two and then dividing by the aspect ratio, 5, gives the flaw depth when the upper extremity is 0.5 inches below the weld: 2 x 0.698" / 5.0 = 0.279". Figure 7-4a can be used to find the time it takes to grow from 12.6% through-wall (a/t = 0.079" / 0.625" = 0.126) to 44.6% through-wall (a/t = 0.279" /0.625" = 0.446). The time is estimated as 4.2 EFPYs. Using the flaw depth calculated previously (a/t = 0.446) as the initial flaw depth, the curves in Figure 6-4 reproduced here as Figure 7-4b for inside surface flaws at the weld can be used to determine the remaining service time. Using the acceptance criteria in Table 6-1, Figure 7-4b shows an additional 1.2 EFPYs of service life for a total of 5.4 EFPYs before the flaw depth reaches the allowable flaw size (a/t = 0.75).

As shown above, flaws whose upper extremities grow within 0.5 inch below the weld require the use of both the "0.5 inch below the attachment weld" and "at the attachment weld" flaw tolerance charts. To avoid the use of these two charts, the "at the attachment weld" chart may solely be used in determining the service life. This shall provide a conservative estimate of the crack growth due to the higher stress field.

Example 5. This case is an axial through-wall flaw with its upper extremity located 0.35 inches below the weld region of penetration no. 22. Similarly, this would be the case where inspection can only be performed from 2 inch above the J-weld to only 0.35 inches below the weld on the downhill side. The objective is to determine the remaining service life for a flaw in the region not

being inspected below the weld to reach the bottom of the J-weld. The angle of the penetration nozzle is 26.2 degrees as shown in Table 1-1. The crack growth curve of Figure 6-14 is applicable and has been reproduced as Figure 7-5. The initial reference time is found by drawing a horizontal line 0.35 inches below the line representing the bottom of the weld, then dropping a vertical line to the horizontal axis. The final reference time is found by drawing a vertical line where the crack growth curve intersects the bottom of the weld horizontal line. If inspection can only be performed from 2 inch above the J-weld to only 0.35 inches below the weld, it would take approximately 4.1 EFPYs for a flaw in the region not being inspected below the weld to reach the weld bottom.

Additional Guidelines

Several additional guidelines are provided below to facilitate the use of these flaw tolerance charts.

1. If a flaw is found in a penetration nozzle for which no specific analysis was performed and there is a uniform trend in the crack growth as a function of penetration nozzle angle, interpolation between penetration nozzles is the best approach.

2. If a flaw is found in a penetration nozzle for which no specific analysis was performed and there is no apparent trend in the crack growth as a function of penetration nozzle angle, the result for the penetration nozzle with the closest angle should be used.

3. If a flaw is found which has a depth smaller than any depth shown for the penetration nozzle angle of interest, the initial flaw depth should be assumed to be the same as the smallest depth analyzed for that particular penetration nozzle.

4. The flaw evaluation charts are applicable for aspect ratio of 6 or less. Consult with Westinghouse if the as-found flaw has an aspect ratio larger than 6.0.

5. All references to service life are in Effective Full Power Years (EFPYs).

6. Results are only provided for the uphill and downhill sides of the selected penetration nozzles. If flaws are found in locations between the uphill and downhill side, use the results for either the uphill or downhill location, whichever is closer.

7. As shown in Example 4, flaws whose upper extremities grow within 0.5 inch below the weld can use both the "0.5 inch below the attachment weld" and "at the attachment weld" flaw tolerance charts. To avoid the use of these two charts, the "at the attachment weld" charts may solely be used in determining the service life. This shall provide a conservative estimate of the crack growth due to a larger stress field.

Table 7-1   Example Problem Inputs: Initial Flaw Sizes and Locations

Example No.	Orientation	Vertical Location	Circumferential Location	Penetration Row	Length (2c)	Depth (a)	Penetration No.	Source Figure
1	Axial - Inside Surface	1.25" Below Weld	Uphill	26.2°	0.195"	0.078"	22	6-2
2	Axial - Outside Surface	1.25" Below Weld	Downhill	26.2°	0.195"	0.078"	22	6-11
3	Axial - Inside Surface	At Weld	Downhill/Uphill	0°	0.250"	0.05"	1	6-5
4	Axial - Inside Surface	1.00" Below Weld	Uphill	48.7°	0.395"	0.079"	75	6-2, 6-4
5	Axial Through-Wall	0.35" Below Weld	Downhill	26.2°	--	--	22	6-14

Example No.	Orientation	Crack Tip Location (d)	Circumferential Location	Penetration Row	Length (2c)	Depth (a)	Wall Thickness	a/t	Penetration No.	Source Figure
1	Axial – Inside Surface	1.25" Below Weld	Uphill	26.2°	0.195"	0.078"	0.625"	0.125	22	6-2

Locality Angle from Table 1-1:

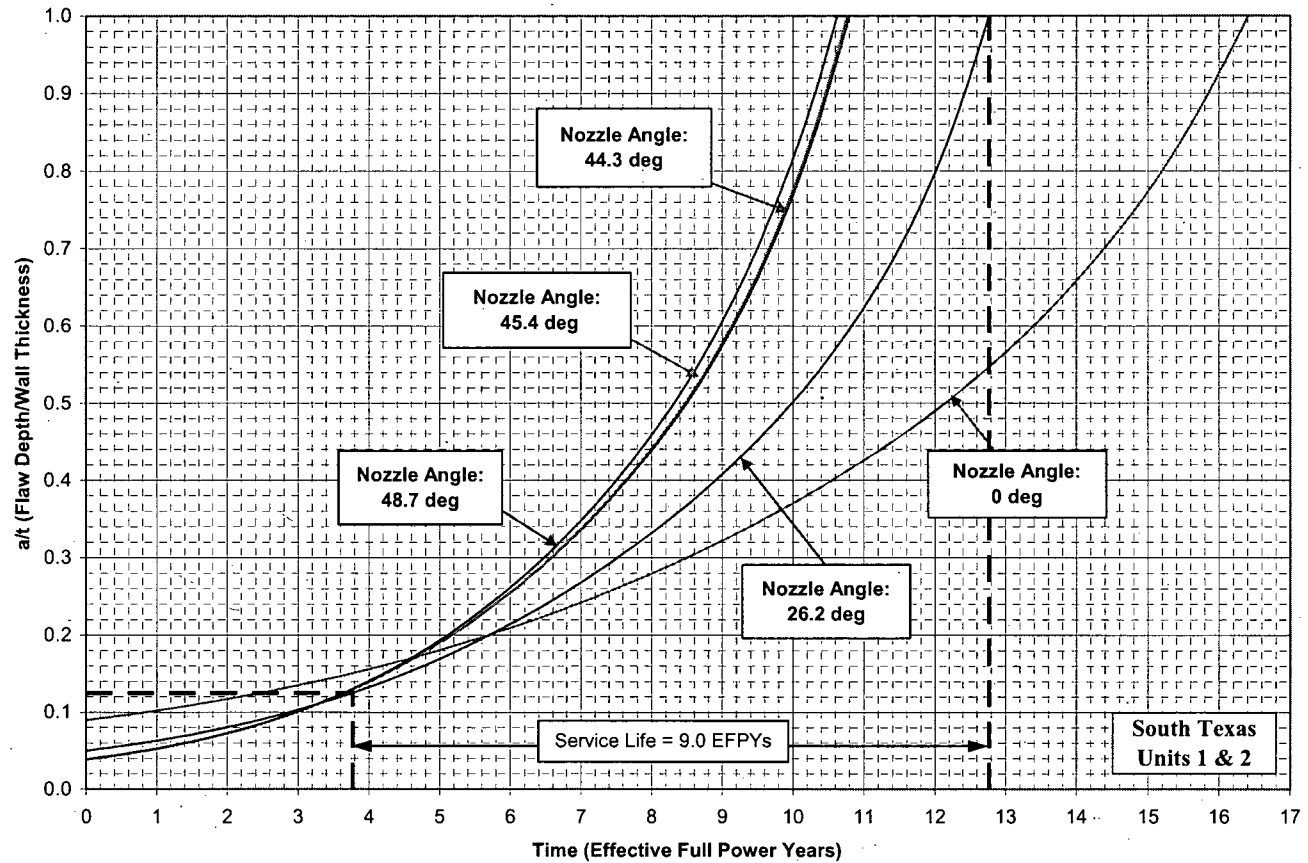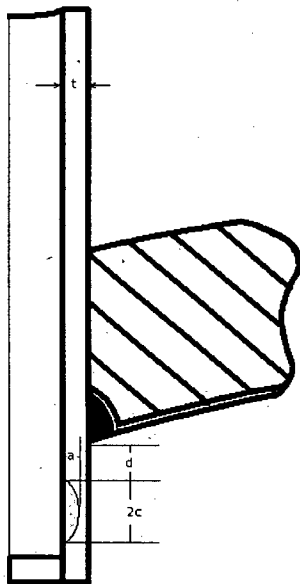| Nozzle No.	Angle
22	26.2°

Figure 7-1   Example Problem 1

Example No.	Orientation	Crack Tip Location (d)	Circumferential Location	Penetration Row	Length (2c)	Depth (a)	Wall Thickness	a/t	Penetration No.	Source Figure
2	Axial – Outside Surface	1.25" Below Weld	Downhill	26.2°	0.195"	0.078"	0.625"	0.125	22	6-11

Locality Angle from Table 1-1:

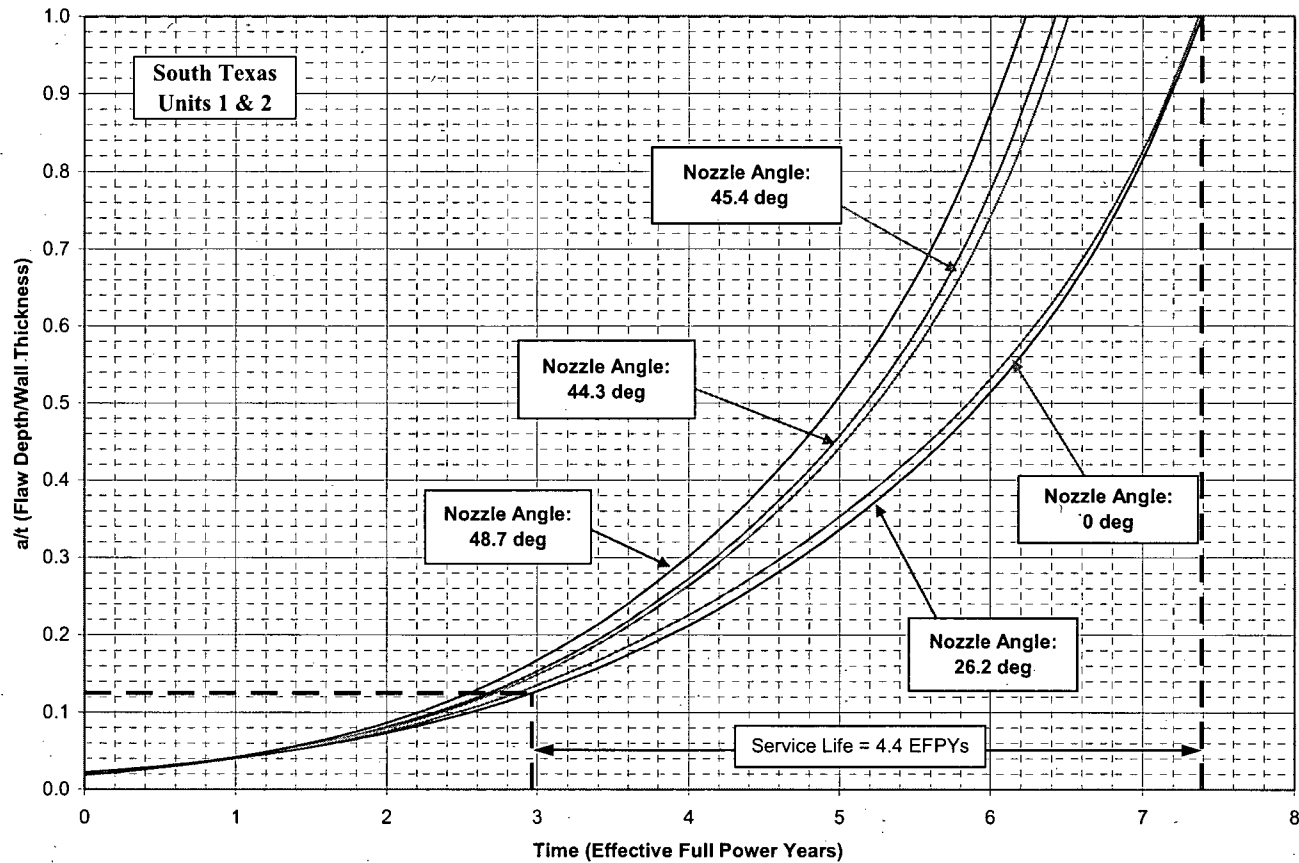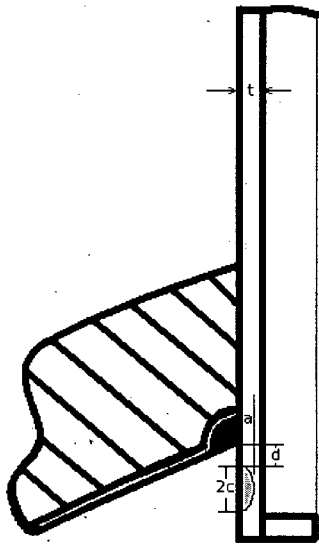| Nozzle No.	Angle
22	26.2°

Figure 7-2   Example Problem 2

Example No.	Orientation	Crack Tip Location (d)	Circumferential Location	Penetration Row	Length (2c)	Depth (a)	Wall Thickness	a/t	Penetration No.	Source Figure
3	Axial – Inside Surface	At Weld	Downhill/Uphill	0°	0.250"	0.05"	0.625"	0.08	1	6-5

Locality Angle from Table 1-1:

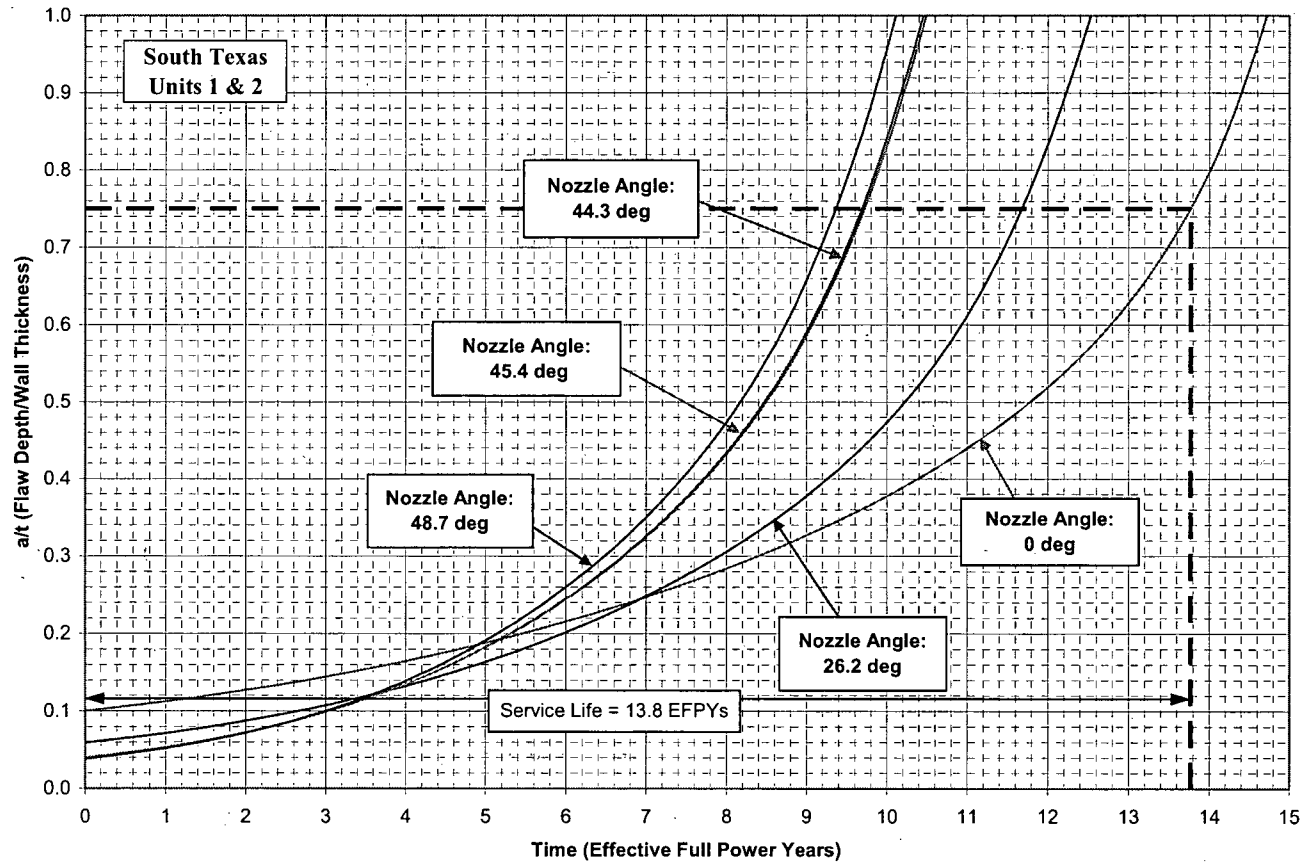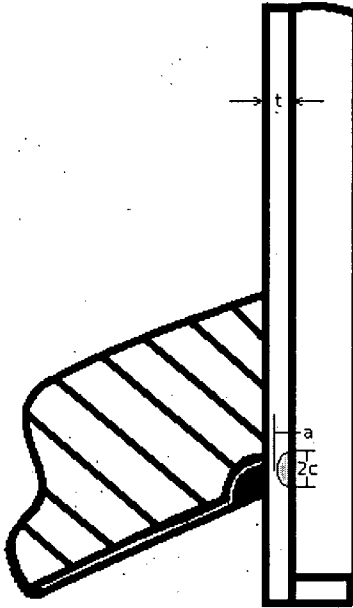| Nozzle No.	Angle
1	0.0°

Figure 7-3   Example Problem 3

Example No.	Orientation	Crack Tip Location (d)	Circumferential Location	Penetration Row	Length (2c)	Depth (a)	Wall Thickness	a$_i$/t	Penetration No.	Source Figure
4	Axial – Inside Surface	1.00" Below Weld	Uphill	48.7°	0.395"	0.079"	0.625"	0.126	75	6-2, 6-4

Locality Angle from Table 1-1:

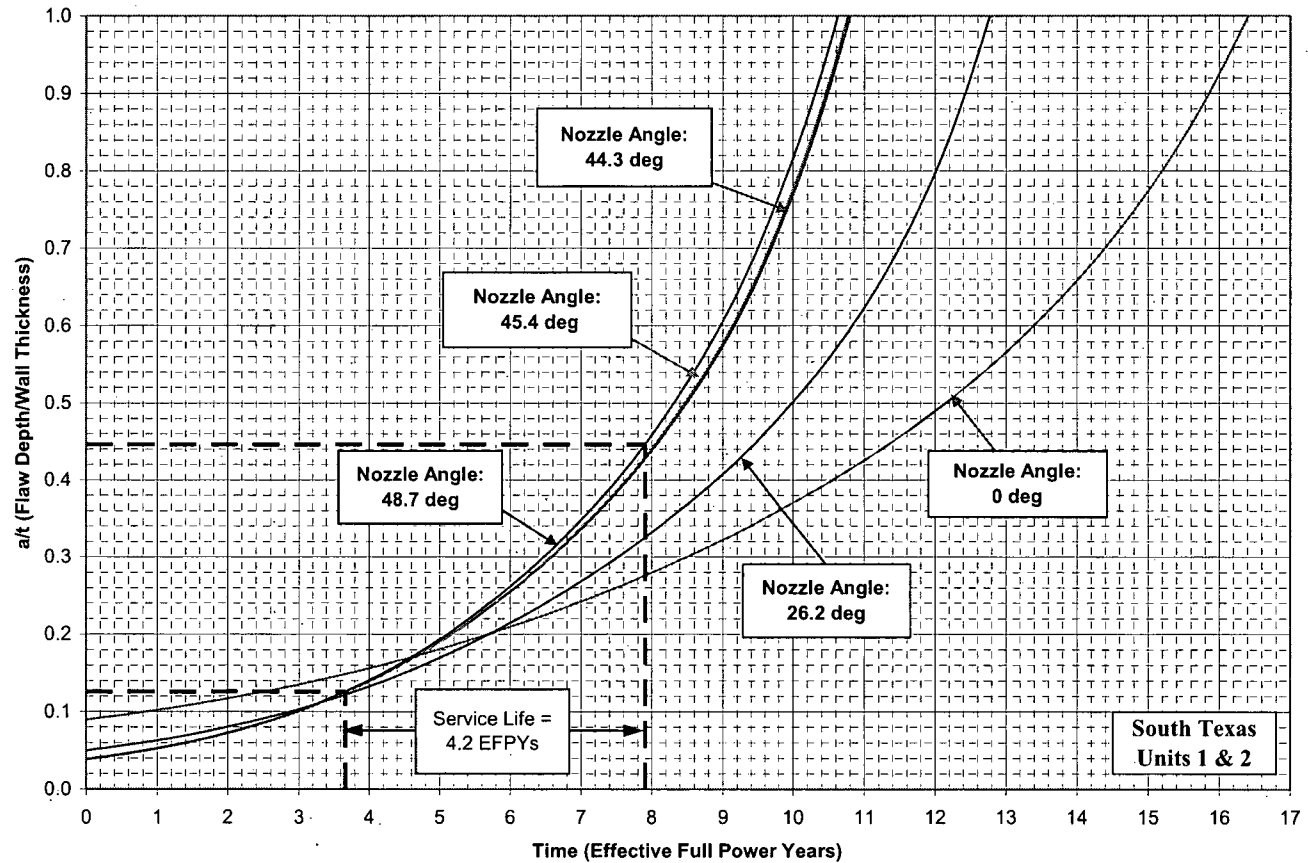| Nozzle No.	Angle
74	48.7°

Figure 7-4a   Example Problem 4 (See also Figure 7-4b)

Example No.	Orientation	Crack Tip Location (d)	Circumferential Location	Penetration Row	Length (2c)	Depth (a)	Wall Thickness	a_i/t	Penetration No.	Source Figure
4	Axial – Inside Surface	1.00" Below Weld	Uphill	48.7°	0.395"	0.079"	0.625"	0.126	75	6-2, 6-4

Locality Angle from Table 1-1:
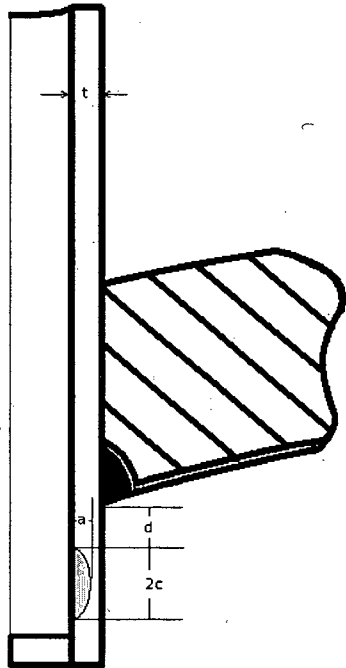
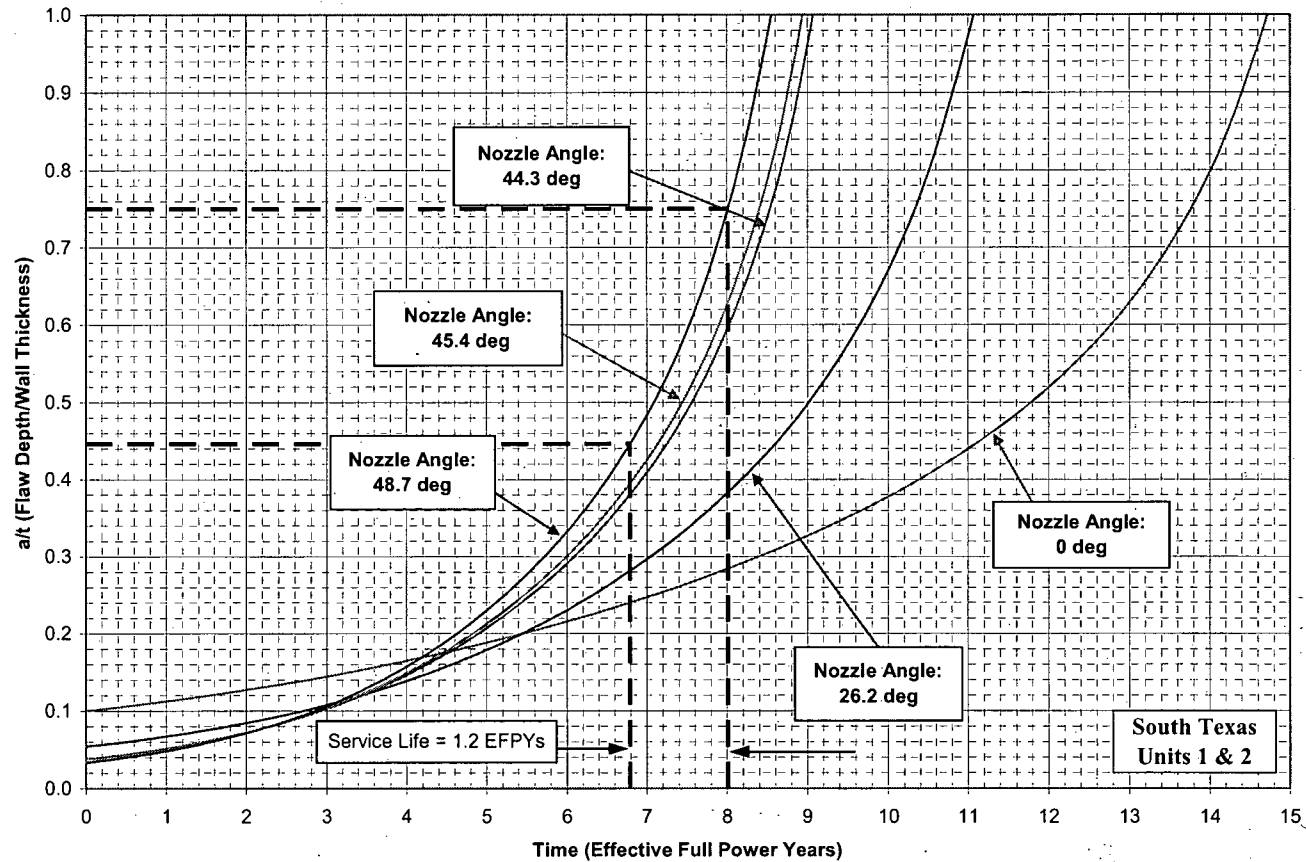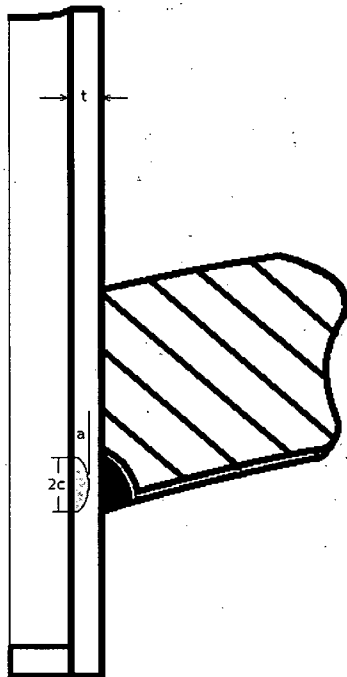| Nozzle No.	Angle
74	48.7°

Figure 7-4b   Example Problem 4 (See also Figure 7-4a)

Example No.	Orientation	Crack Tip Location (d)	Circumferential Location	Penetration Row	Length (2c)	Depth (a)	Wall Thickness	a/t	Penetration No.	Source Figure
5	Axial – Through-Wall	0.35" Below Weld	Downhill	26.2°	N/A	N/A	0.625"	N/A	22	6-14

Locality Angle from Table 1-1:

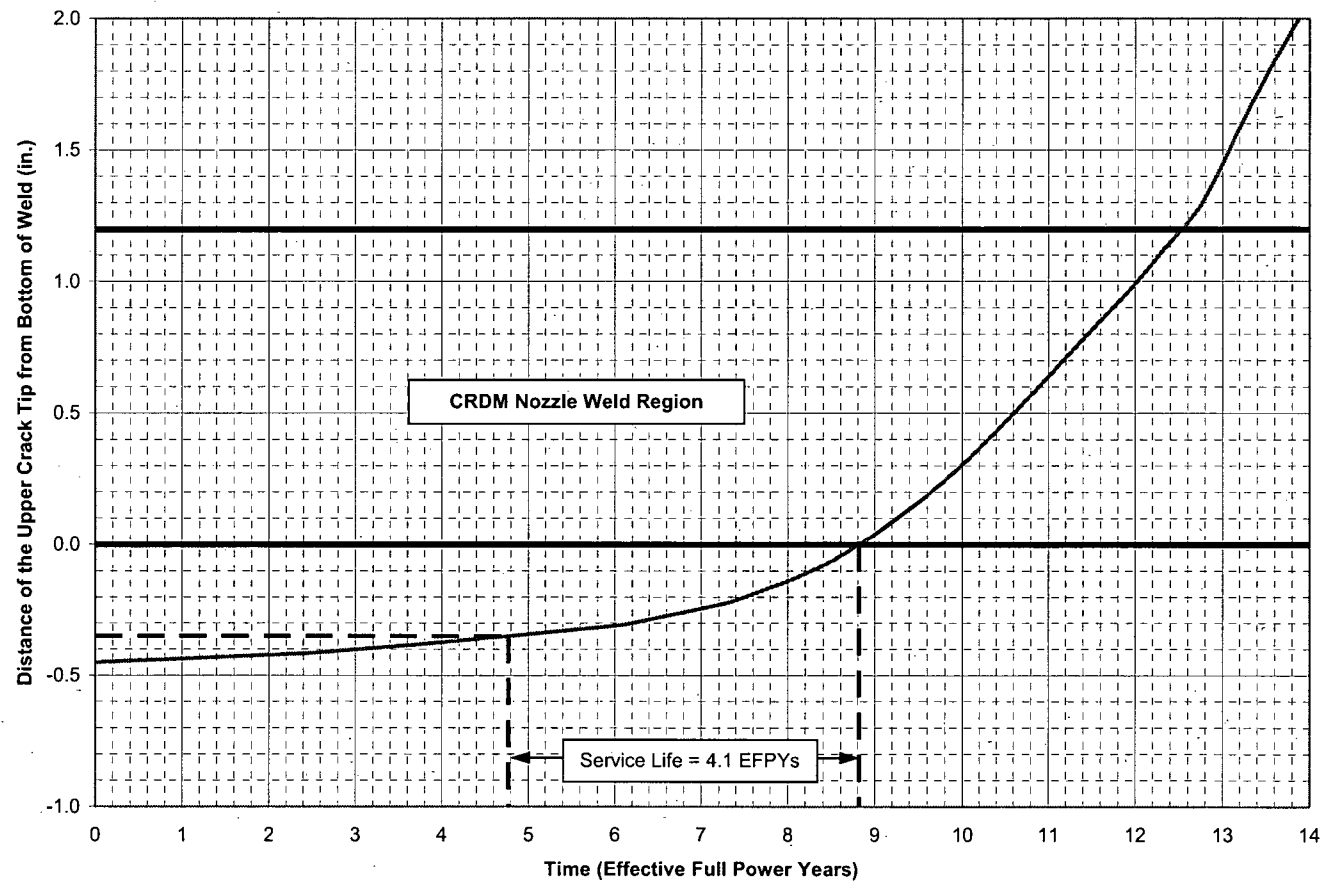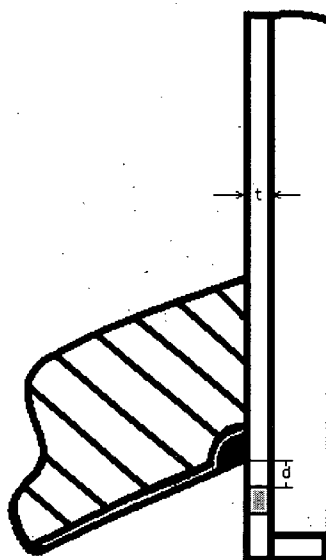| Nozzle No.	Angle
22	26.2°

Figure 7-5   Example Problem 5

8 REFERENCES

1. Combustion Engineering Drawings for STP (Proprietary to Westinghouse):

   A. CE Drawing No. E-11073-101-003, Revision 6, "Closure Head Assembly Westinghouse Electric Corp. 173" I.D. P.W.R.".

   B. CE Drawing No. E-STD11-101-013, Revision 3, "Closure Head Penetrations Final Machining Westinghouse Electric Corp. 173" I.D. P.W.R.".

   C. CE Drawing No. E-11073-101-002, Revision 5, "Closure Head Penetrations Machining & Cladding Westinghouse Electric Corp. 173" I.D. P.W.R.".

   D. CE Drawing No. E-11073-112-003, Revision 1, "Control Rod Mechanism Housing Details Westinghouse Electric Corp. 173" I.D. P.W.R.".

   E. CE Drawing No. D-11073-107-001, Rev. 1, "Vent Pipes Westinghouse Electric Corp. 173" I.D. P.W.R."

2. "PWR Reactor Pressure Vessel (RPV) Upper Head Penetrations Inspection Plan (MRP-75)": Revision 1, EPRI, Palo Alto, CA: 2002. 1007337. (Proprietary to EPRI)

3. Dominion Engineering Inc. Calculation No. C-8736-00-1, Rev 0, "STP CRDM, Head Vent and Gas Vent Nozzle Stress Analysis."

4. Westinghouse Report WCAP-13493, "Reactor Vessel Closure Head Penetration Key Parameters Comparison," September 1992. (Proprietary to Westinghouse)

5. Scott, P. M., "An Analysis of Primary Water Stress Corrosion Cracking in PWR Steam Generators," in Proceedings, Specialists Meeting on Operating Experience With Steam Generators, Brussels Belgium, Sept. 1991, pages 5-6.

6. McIlree, A. R., Rebak, R. B., Smialowska, S., "Relationship of Stress Intensity to Crack Growth Rate of Alloy 600 in Primary Water," Proceedings International Symposium Fontevraud II, Vol, 1, p. 258-267, September 10-14, 1990.

7. Cassagne, T., Gelpi, A., "Measurements of Crack Propagation Rates on Alloy 600 Tubes in PWR Primary Water, in Proceedings of the 5th International Symposium on Environmental Degradation of Materials in Nuclear Power Systems-Water Reactors," August 25-29, 1991, Monterey, California.

8. "Materials Reliability Program (MRP) Crack Growth Rates for Evaluating Primary Water Stress Corrosion Cracking (PWSCC) of Thick Wall Alloy 600 Material (MRP-55) Revision 1," EPRI, Palo Alto, CA: November 2002. 1006695. (Proprietary to EPRI)

9. Crack Growth and Microstructural Characterization of Alloy 600 PWR Vessel Head Penetration Materials, EPRI, Palo Alto, CA. 1997. TR-109136.

10. Vaillant, F. and C. Amzallag. "Crack Growth Rates of Alloy 600 in Primary Water," Presentation to the EPRI-MRP Crack Growth Rate (CGR) Review Team, Lake Tahoe, NV, presented August 10, 2001, and revised October 11, 2001.

11. Vaillant, F. and S. Le Hong. Crack Growth Rate Measurements in Primary Water of Pressure Vessel Penetrations in Alloy 600 and Weld Metal 182, EDF, April 1997. HT-44/96/024/A.

12. Framatome laboratory data provided by C. Amzallag (EDF) to MRP Crack Growth Rate Review Team, October 4, 2001 (Proprietary to EDF).

13. Cassagne, T., D. Caron, J. Daret, and Y. Lefevre. "Stress Corrosion Crack Growth Rate Measurements in Alloys 600 and 182 in Primary Water Loops Under Constant Load," Ninth International Symposium on Environmental Degradation of Materials in Nuclear Power Systems-Water Reactors (Newport Beach, CA, August 1-5, 1999), Edited by F. P. Ford, S. M. Bruemmer, and G. S. Was, The Minerals, Metals & Materials Society (TMS), Warrendale, PA, 1999.

14. Studsvik laboratory data provided by Anders Jenssen (Studsvik) to MRP Crack Growth Rate Review Team, October 3, 2001 (Proprietary to Studsvik).

15. "Crack Growth Rate Tests of Alloy 600 in Primary PWR Conditions," Communication from M. L. Castaño (CIEMAT) to J. Hickling (EPRI), March 25, 2002.

16. Gómez-Briceño, D., J. Lapeña, and F. Blázquez. "Crack Growth Rates in Vessel Head Penetration Materials," Proceedings of the International Symposium Fontevraud III: Contribution of Materials Investigation to the Resolution of Problems Encountered in Pressurized Water Reactors (Chinton, France, September 12-16, 1994), French Nuclear Energy Society, Paris, 1994, pp. 209-214.

17. Gómez-Briceño, D., J. Lapeña. "Crack Growth Rates in Vessel Head Penetration Materials," Proceedings: 1994 EPRI Workshop on PWSCC of Alloy 600 in PWRs (Tampa, FL, November 15-17, 1994), EPRI, Palo Alto, CA, TR-105406, August 1995, pp. E4-1 through E4-15.

18. Gómez-Briceño, D., et al. "Crack Propagation in Inconel 600 Vessel Head Penetrations," Eurocorr 96, Nice, France, September 24-26, 1996.

19. Castaño, M. L., D. Gómez-Briceño, M. Alvarez-de-Lara, F. Blázquez, M. S. Garcia, F. Hernández, and A. Largares. "Effect of Cationic Resin Intrusions on IGA/SCC of Alloy 600 Under Primary Water Conditions," Proceedings of the International Symposium Fontevraud IV: Contribution of Materials Investigation to the Resolution of Problems Encountered in Pressurized Water Reactors (France, September 14-18, 1998), French Nuclear Energy Society, Paris, 1998, Volume 2, pp. 925-937.

20. Bamford, W. H., "D. C. Cook Unit 2 Upper Head Penetration Crack Growth Determined from Inspection Data," Westinghouse Electric Report LTR-SMT-01-72, November 2001. (Proprietary to Westinghouse)

21. South Texas Unit 1 Evaluation January 2006 (projected thru Sep2006), Filenet reference: STI 31975320 and South Texas Unit 2 Evaluation November 2004 (projected thru Oct 2005) Filenet reference: STI 31814859

22. Newman, J. C. and Raju, I. S., "Stress Intensity Factor Influence Coefficients for Internal and External Surface Cracks in Cylindrical Vessels," in Aspects of Fracture Mechanics in Pressure Vessels and Piping, PVP Vol. 58, ASME, 1982, pp. 37-48.

23. Mettu, S. R., Raju, I. S., and Forman, R. G., NASA Lyndon B. Johnson Space Center report no. NASA-TM-111707, "Stress Intensity Factors for Part-though Surface Cracks in Hollow Cylinders," in Structures and Mechanics Division, July 1992.

24. "The Stress Analysis of Cracks Handbook", Hiroshi Tada, 2nd Edition.

25. Hiser, Allen, "Deterministic and Probabilistic Assessments," presentation at NRC/Industry/ACRS meeting, November 8, 2001.

26. "Effect of Strain Rate on SCC in High Temperature Primary Water, Comparison between Alloys 690 and 600", ANS 11th Environmental Degradation Meeting, August 2003, K. M. Boursier, et al (EDF).

27. "Materials Reliability Program: Generic Evaluation of Examination Coverage Requirements for Reactor Pressure Vessel Head Penetration Nozzles (MRP-95)," EPRI, Palo Alto, CA: 2003. 1009129. (Proprietary to EPRI)

28. USNRC Letter, R. Barrett to A. Marion (NEI), "Flaw Evaluation Guidelines," April 11, 2003.

29. USNRC Letter, W. T. Russell to W. Raisin (NUMARC), "Safety Evaluation for Potential Reactor Vessel Head Adapter Tube Cracking," November 19, 1993.

30. USNRC Letter, A. G. Hansen to R. E. Link (Wisconsin Electric Power Company), "Acceptance Criteria for Control Rod Drive Mechanism Penetrations at Point Beach Nuclear Plant, Unit 1," March 9, 1994.

31. ASME Code Section XI 2004 Edition, "Rules for Inservice Inspection of Nuclear Power Plant Components," The American Society of Mechanical Engineers, New York, New York, USA.

APPENDIX A

CRDM HOOP STRESS DISTRIBUTIONS BELOW THE WELD

In this Appendix, the CRDM hoop stress distributions below the weld are plotted for the center penetration (0.0°), 26.2°, 44.3°, 45.4°, and 48.7° penetration rows on both the downhill and uphill sides. The information presented in this Appendix can be used to determine the extent of inspection coverage needed in order to meet the NRC Order EA-03-009 requirements or facilitate the submittal of relaxation requests in the event that the NRC order requirements cannot be met.

The hoop stress distributions on the downhill and uphill sides along the length of the analyzed penetration nozzles below the toe of the J-groove weld are plotted in Figures A-1 to A-9. The stress distributions shown are for the inside and outside surfaces of the reactor vessel upper head penetrations. These stress distributions are typical of those observed in the upper head penetration nozzles for other nuclear power plants. The stresses are highest in the vicinity of the J-groove weld and decrease rapidly as the distance below the toe of the J-groove weld increases.

In accordance with the NRC order, the head penetration shall be inspected from 2 inch above the highest point of the root of the J-groove weld (uphill side) to 1 inch below the lowest point at the toe of the J-groove weld (downhill side) and including the region beyond 1 inch where the operating stress level is higher than 20 ksi. A minimum of 1 inch below the lowest point at the toe of the J-groove weld (downhill side) is required if the stress level for the region beyond 1 inch is less than 20 ksi. For those penetrations where the required inspection coverage can be achieved below the toe of the J-groove weld on the downhill side, no relaxation request is needed for both the uphill and downhill side. This can be demonstrated by reviewing the expected inspection coverage on the uphill side based on the inspection coverage that can be achieved below the toe of the J-groove weld on the downhill side. The inspection coverage on the uphill side is expected to be more due to the elevation differential between the toe of the J-groove weld on the downhill and uphill side, except for the center penetration. Based on this elevation differential and the hoop stress distribution curves, it can be concluded that the hoop stress distribution curve on the downhill side is more limiting in determining the extent of the required inspection coverage. Therefore, no relaxation request is needed for the uphill side if the required inspection coverage below the toe of the J-groove weld on the downhill side can be achieved.

Five rows of penetration nozzles were analyzed in this report. The required inspection coverage for those penetration nozzles not being analyzed can be determined using the bounding results from those analyzed penetrations with bounding nozzle angles.

As shown in Figures A-1 to A-9, the magnitude of the hoop stress at a distance of 1 inch or more below the toe of the downhill side J-groove weld is less than 20 ksi for all the analyzed penetration nozzles. The inspection requirements given in NRC Order EA-03-009 are satisfied provided that a minimum inspection coverage of 1.0 inch can be achieved for all the penetration nozzles.

For those penetrations on the downhill side where inspection coverage does not meet the requirements of the NRC order, the crack growth curves provided for the downhill side in Figures 6-13 to 6-17 of the report can be used to determine the minimum required inspection coverage in order to meet the intent of the requirements in the NRC order. The submittal of a relaxation request to the NRC is required in this case. Based on the through-wall crack growth curves shown in Figures 6-13 to 6-17, the locations of the upper crack tips postulated vary from 0.15 inch to 0.6 inch below the J-groove weld. It should be noted that the locations of the upper crack tips were selected such that the resulting stress intensity factor at the crack tip exceeded the PWSCC stress intensity factor threshold of 9 MPa $\sqrt{m}$. The service life required

for any of the upper crack tips to reach the toe of the J-groove weld all exceeded 6 EFPYs as shown in Figures 6-13 to 6-17. The time duration between inspection cycles is 4 fuel cycles, i.e. 6 years, for STP in accordance with the NRC Order for Low Category plants. As a screening rule, if an inspection coverage of 0.6 inch is achieved below the J-groove weld on the downhill side of all the head penetration nozzles, the upper crack tip of any undetected axial through-wall flaw in the region not being inspected will not reach the toe of the J-groove weld in less than 6 EFPYs. Therefore, the intent of the requirements in the NRC Order is met.

**Figure A-1
Hoop Stress Distribution Uphill and Downhill Side
(0° CRDM Penetration Nozzle)**
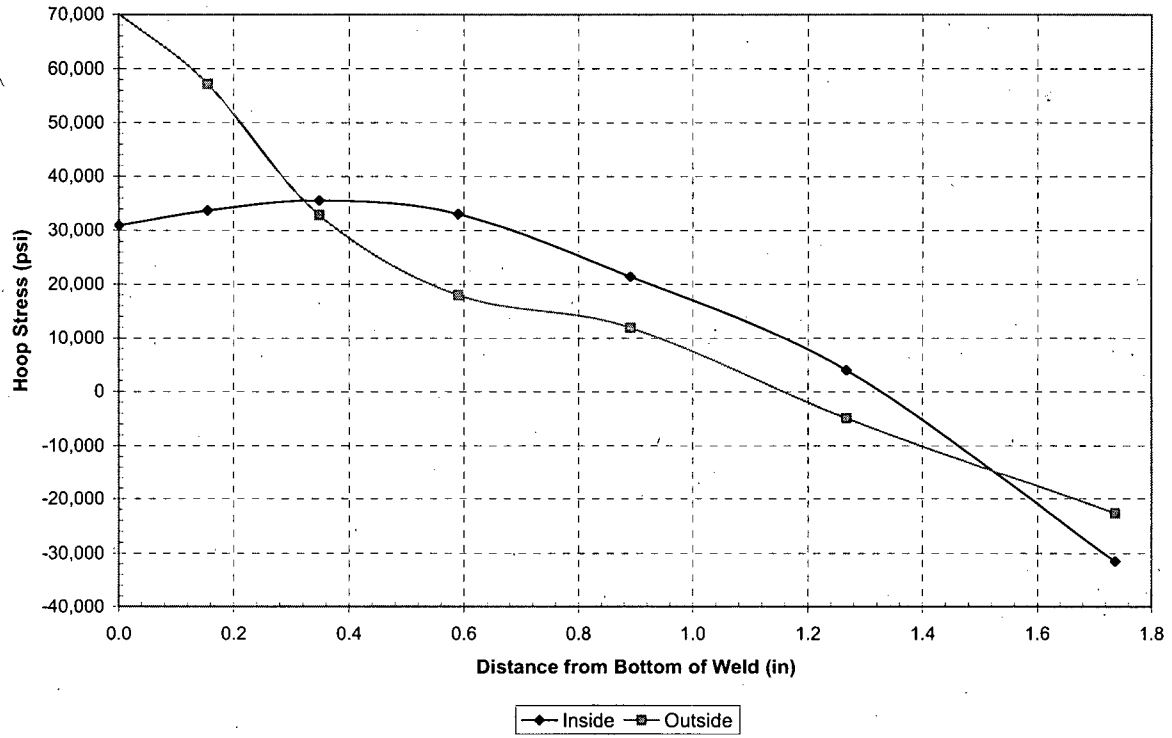
Figure A-2
Hoop Stress Distribution Uphill Side
(26.2° CRDM Penetration Nozzle)
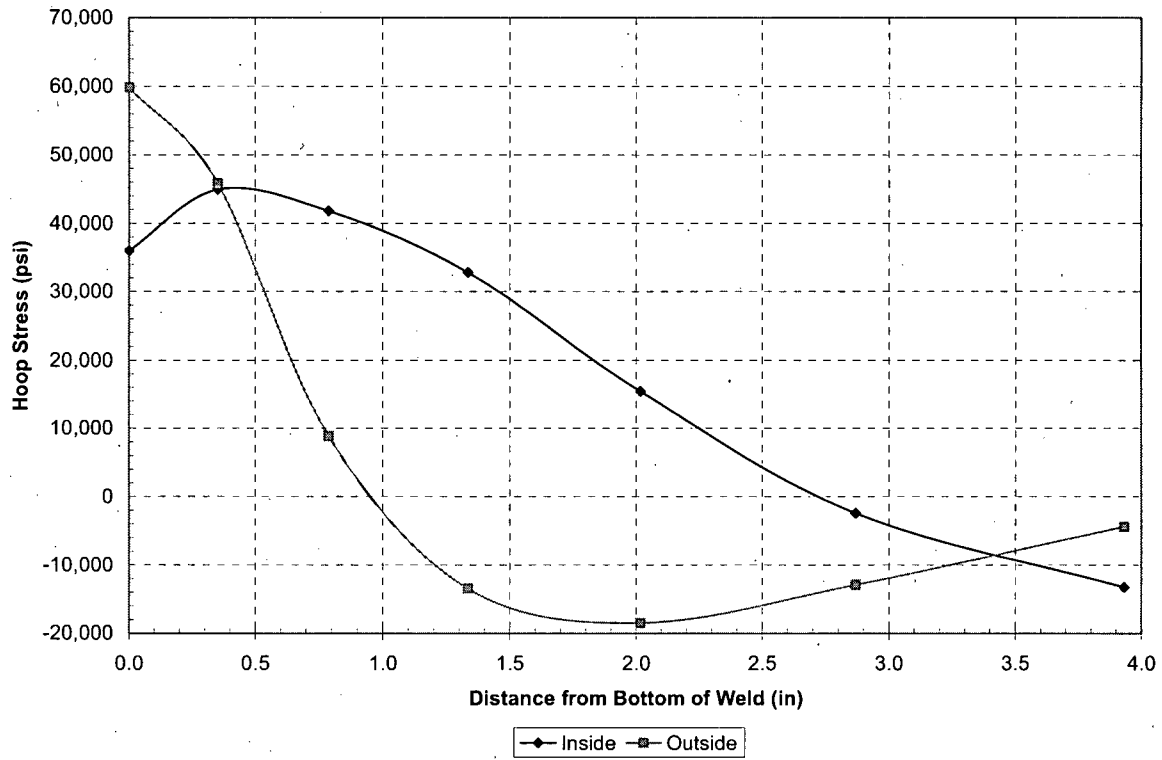
Figure A-3
Hoop Stress Distribution Downhill Side
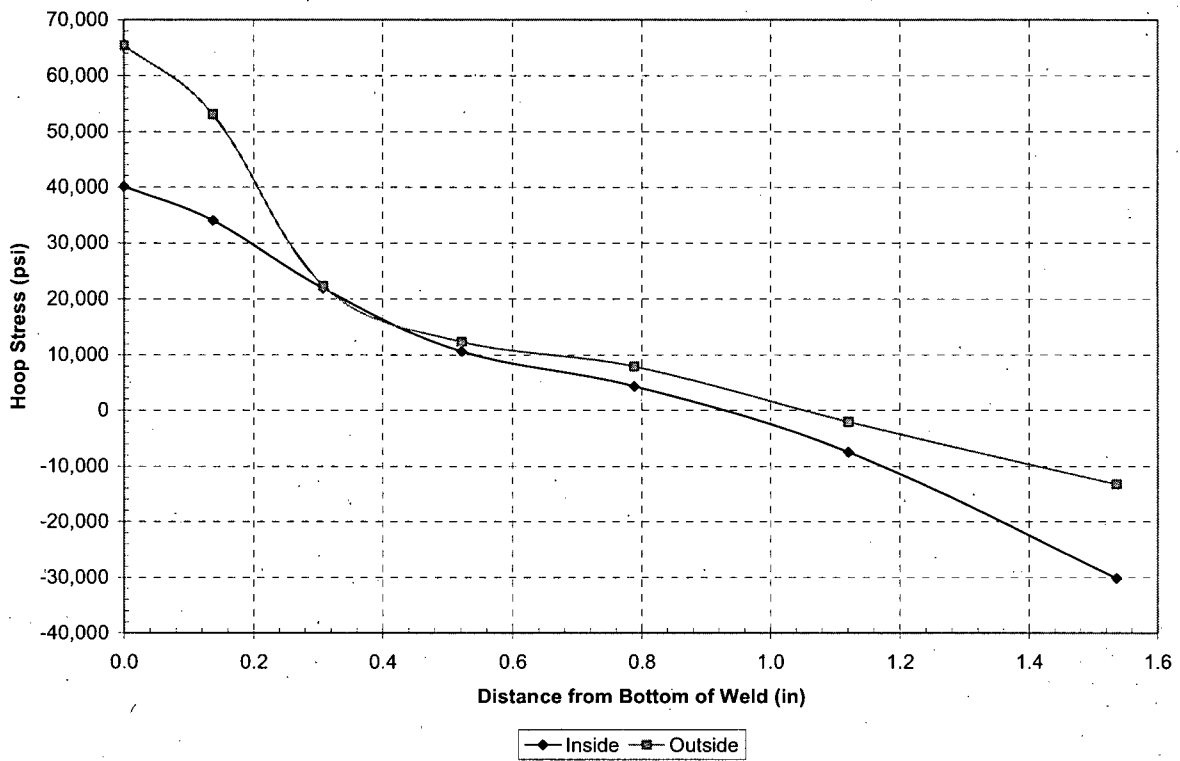**(26.2° CRDM Penetration Nozzle)**

Figure A-4
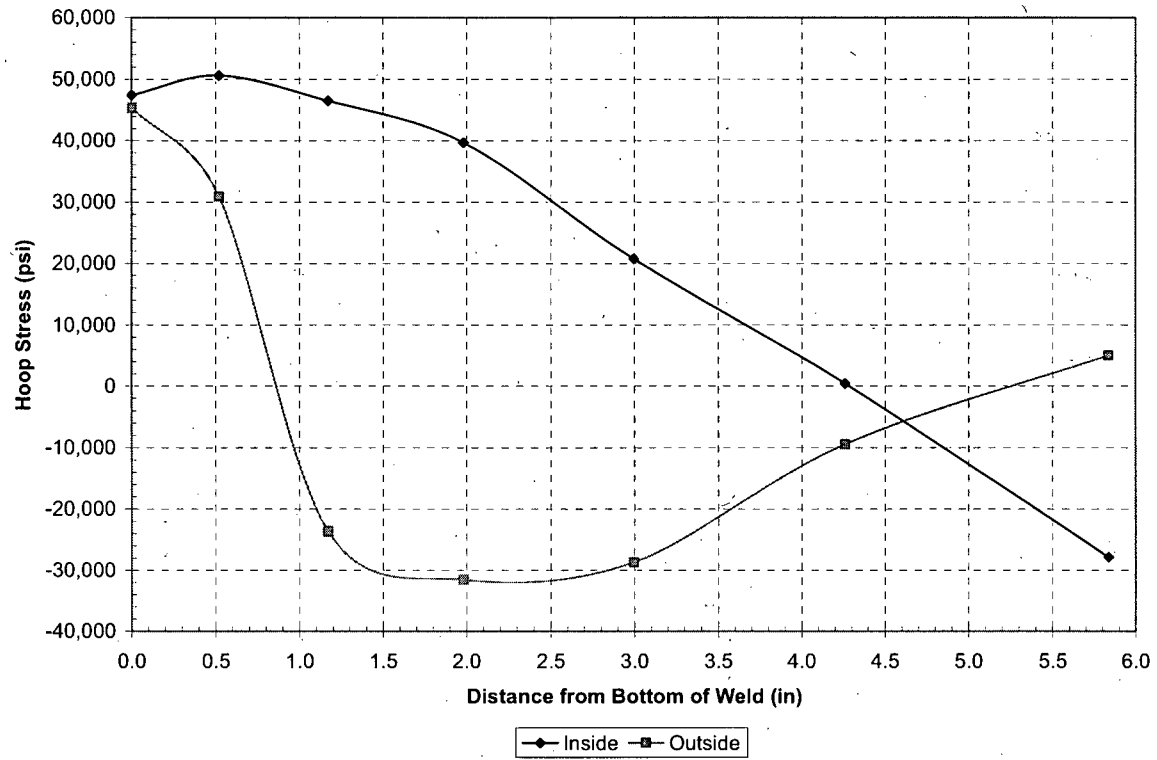**Hoop Stress Distribution Uphill Side**
(44.3° CRDM Penetration Nozzle)

Figure A-5
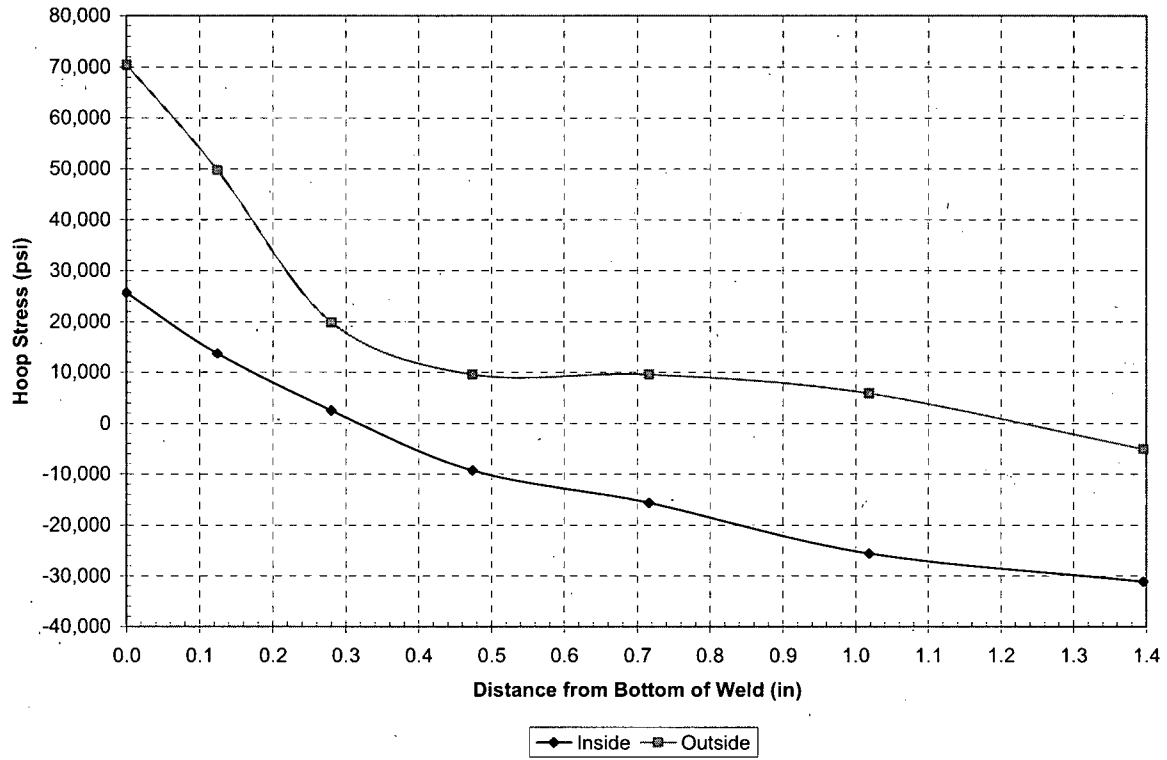**Hoop Stress Distribution Downhill Side**
(44.3° CRDM Penetration Nozzle)

Figure A-6
Hoop Stress Distribution Uphill Side
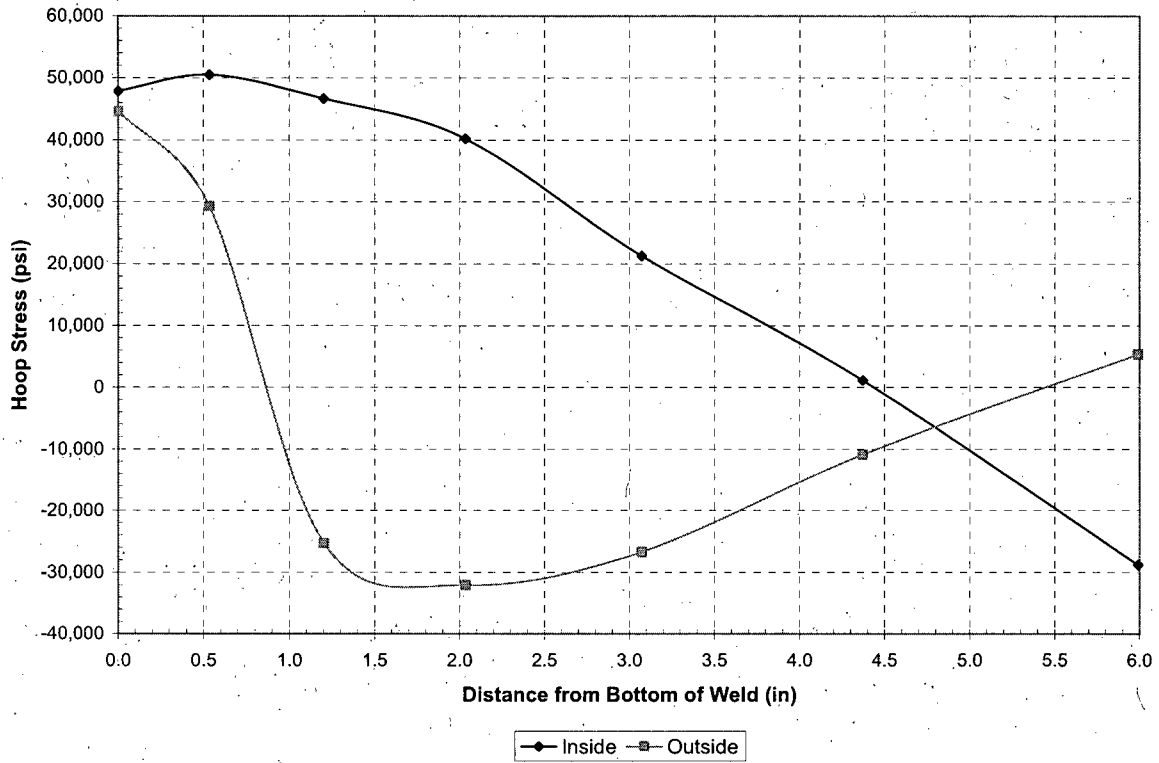**(45.4° CRDM Penetration Nozzle)**

Figure A-7
Hoop Stress Distribution Downhill Side
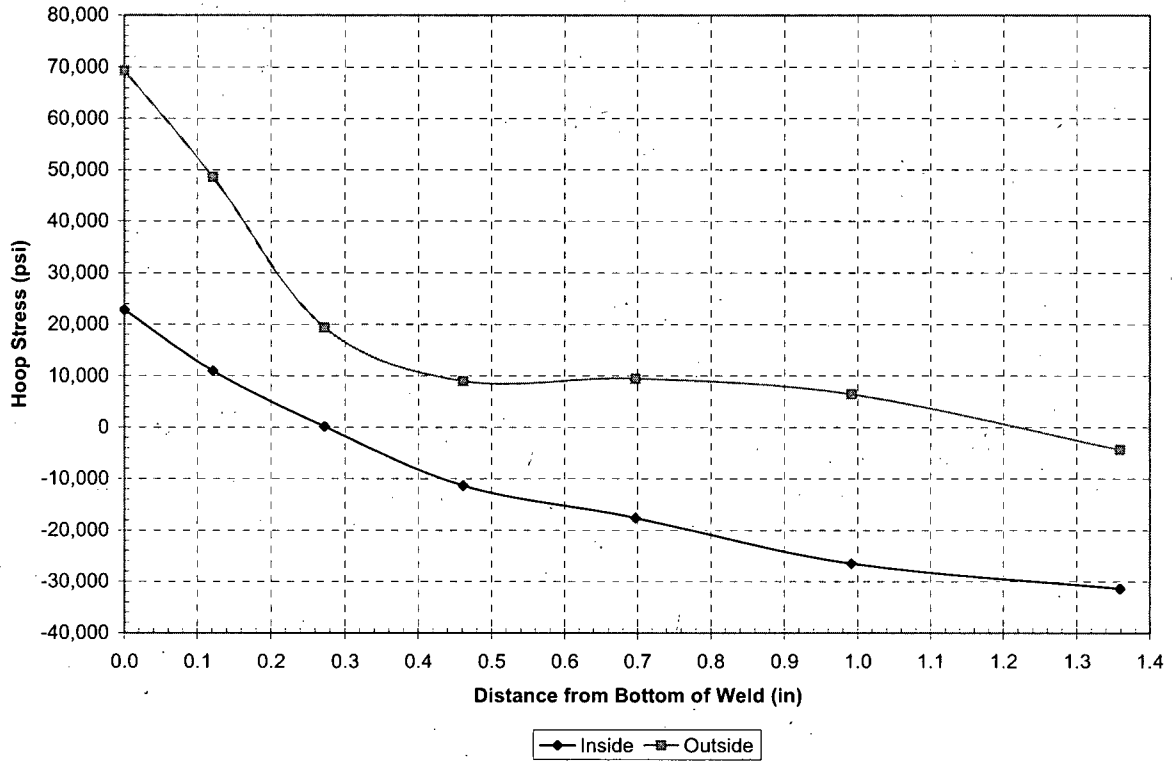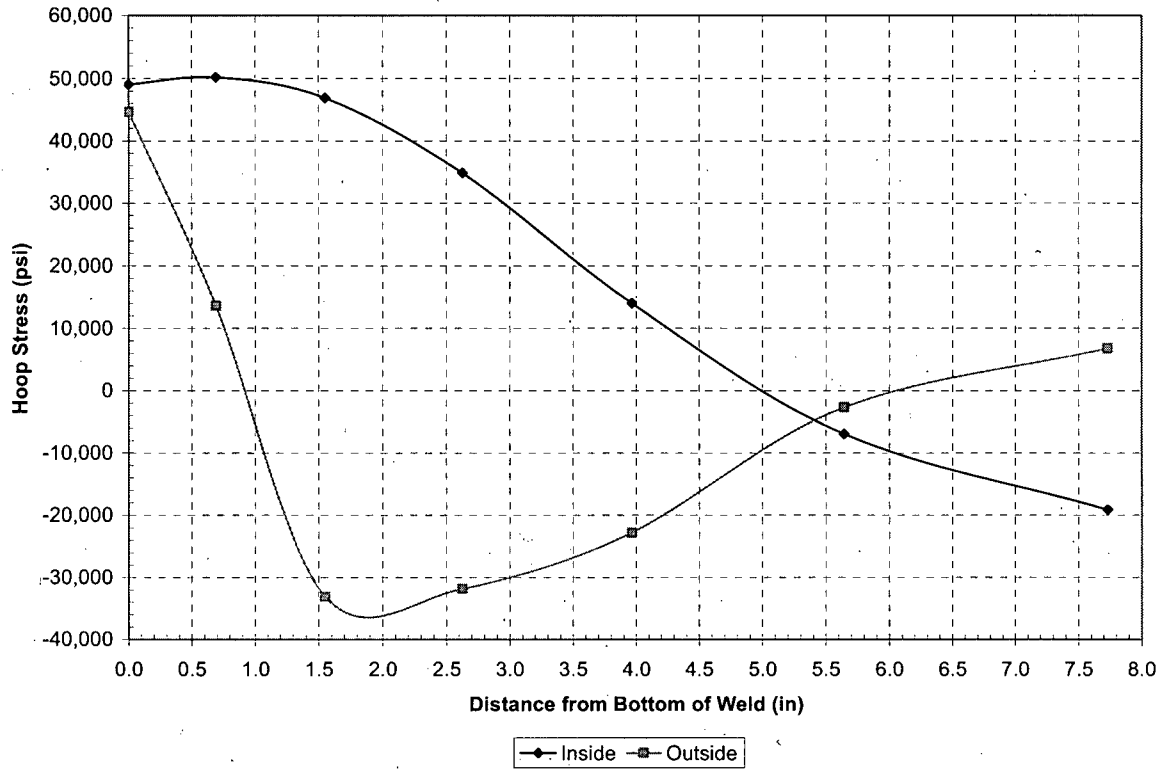**(45.4° CRDM Penetration Nozzle)**

**Figure A-8
Hoop Stress Distribution Uphill Side
(48.7° CRDM Penetration Nozzle)**

Figure A-9
Hoop Stress Distribution Downhill Side
(48.7° CRDM Penetration Nozzle)

Distance from Bottom of Weld (in)

Inside —□— Outside